Micro Wind Energy Systems in Harsh Environments: Failure Analysis of Small Wind Turbines at Remote Sites in Labrador

By

© Jonas Roberts, B.Eng.

A thesis submitted to the School of Graduate Studies

in partial fulfillment of the requirements for the degree of

Master of Engineering

Faculty of Engineering and Applied Science

Memorial University

May 2009

St. John's Newfoundland

Abstract

The operational reliability of small-scale wind turbines in isolated, harsh environments is examined in this thesis. Bell-Aliant operates nearly 40 micro wind turbines (900 W) at hilltop telecommunication tower sites in Labrador, several of which have experienced catastrophic failure, due in part to the extreme meteorological conditions. Consequently, a technological challenge is presented. What are the external forces that caused these failures? Under what circumstances can failure be expected to recur? What, if any, flaws with the machinery may contribute to failure? How may the risk of failure be reduced? This work responds to these questions and in doing so demonstrates a systematic and analytical approach applicable to similar problems. A literature review discusses wind energy technology, applications and the challenges faced when operating in extreme climates. A statistical analysis of site-specific parameters suggests the best indicators of turbine failure potential at a given site were found to be wind speed and turbulence. A forensic mechanical and material analysis of the primary failure mechanism was conducted, highlighting flawed nacelle design. An experimental program whereby turbine response characteristics are analyzed with respect to machine alterations aimed at improving operational reliability showed simple blade modifications are not sufficient to mitigate the primary failure mechanism.

Dedication

For Sue and Eric Roberts

This thesis is dedicated to my parents. Everything that I do is possible because of the love, support and guidance they have given me throughout my life.

Mom, Dad, thank you so much.

Acknowledgments

First and foremost I would like to acknowledge my supervisor and mentor Dr. Stephen Bruneau. He has been helpful in the development of this thesis by providing personal and academic guidance and generous amounts of his own time and resources.

No aspect of this thesis would have been possible without the involvement of Bell-Aliant and their engineers in the building services department. I would especially like to acknowledge Gervase White, Jeff Card, Ian Duffett, and Steve Corbett for their interest and efforts to accommodate my requests. Also, Dan Moody of Solar Winds Energy has been invaluable as a source of operational knowledge and turbine equipment.

There were several other members of Memorial University Faculty and Staff that contributed in a significant way to the successful completion of this thesis. In particular, Dr. Ken Snelgrove has been instrumental in the collection of NARR data and also by providing guidance and funding. Dr. Leonard Lye has helped tremendously by providing guidance for many statistical challenges. Moya Crocker has made life at the university an absolute joy and has assisted with any administrative hurdles I faced.

The technicians in the Faculty of Engineering and Applied science, including Matt Curtis, Craig Mitchell, Greg O'Leary, Shawn Organ, Tom Pike, and Brian Pretty, were

incredibly helpful in many aspects of this research. In particular, I would like to single out Steve Steele for going above and beyond throughout several stages of this work.

I would like to acknowledge NSERC and the provincial government of Newfoundland and Labrador for their significant financial support.

On a personal note I would like to acknowledge Jonathon Bruce for joining me in graduate studies. Finally, I would like to thank Rebecca Hargreaves. Her continued love, patience and support have facilitated this entire process.

Table of Contents

List of Tables

List of Figures

List of Appendices

1. Introduction

1.1. Background Information

This thesis is motivated by a research need expressed by Bell-Aliant, the primary public telecommunications corporation in the province of Newfoundland and Labrador. The challenge is that of periodic failure of micro wind turbines being used for augmenting power at remote hilltop communication sites. The recent introduction of these units for reducing costs and risks associated with diesel generation has been a success in several ways, however, the unexpected and catastrophic failure of some wind generator units has complicated the economic case for continued implementation.

This thesis tackles the problem through a 3-stage investigation that first looks into the site characteristics and meteorological conditions prevailing at the time of failure and during ongoing operations in general. The methods employed meteorological and power production data collection from the client and other far-ranging sources, investigations of the sites and a broad ranging regressional analysis relating various parameters to operational outcomes. The second phase was an investigation of the specific mechanical failure of the turbines. All units were the same model from one manufacturer and most failures were mechanically similar and furling-related. Thus, the scope of the forensic work was focused on the applied stresses and material state in a discrete part of each unit. The third stage of the investigation was to determine experimentally the complex furling

characteristics of the units, not found in the literature, and in doing so propose and test some mitigative measures. The conclusion of the work describes the conditions under which failures may, or can be expected to, occur; defines the mechanism of the failure, and investigates ways to reduce the likelihood of this failure in the future.

The first section of the thesis introduces the reader to the meteorological and mechanical sciences relevant to this study of micro wind energy conversion systems.

1.2. Introduction to Small Wind Turbines

In recent years there has been an increase in the manufacture and use of small and micro wind turbines (SWTs). The most common use for turbines of this scale are private off-grid applications such as providing electricity for a cabin or sailboat, providing impressed-current cathodic protection for underground pipelines, powering remote monitoring equipment, and augmenting the diesel power supply for isolated telecommunications installations.

It is for the latter application that this thesis explores the performance of a specific unit in extreme conditions. Figure 1.1 places this field of research in perspective to the ever-broadening field of renewable energy studies.

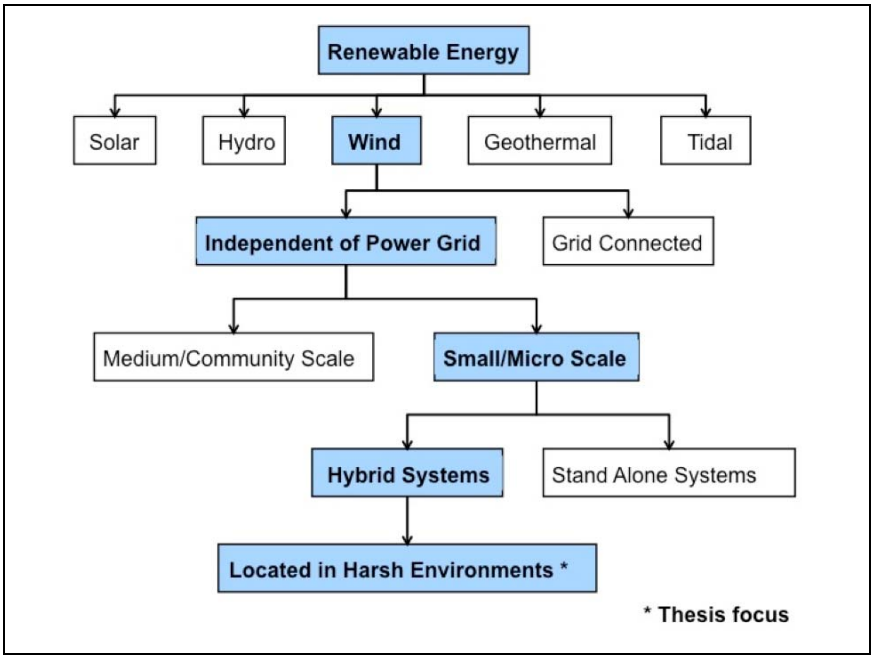

Figure 1.1 – Flowchart of research field

The bulk of this work was completed in cooperation with engineers at Bell-Aliant who provided operational and anecdotal data along with several critical pieces of equipment, including failed turbines. Bell-Aliant has approximately 30 microwave relay stations at remote hilltop locations in Labrador, of which six use SWTs as part of a hybrid power system. Beginning in 2003, Bell-Aliant initiated a wind power program using Southwest Windpower's Whisper 100 (WH100) shown in Figure 1.2 as the primary turbines. The WH100 is a three-bladed, upwind machine, rated at 900 W. It is 2.1 m in diameter and uses an angled furling mechanism for overspeed protection. The turbines are mounted on 30 foot guyed towers and are used in conjunction with photovoltaic cells as well as diesel generators to charge the battery banks that provide the power for each site.

Whisper 100 Technical Specifications
Provided by: [Southwest Windpower 2008]

Rotor Diameter – 2.1 m
Weight - 21 kg
Start-Up Wind Speed - 3.4 m/s
Voltage - 12, 24, 36, 48 VDC
Rated Power - 900 watts at 12.5 m/s
Body - Cast aluminum
Blades - 3-Carbon reinforced fiberglass
Overspeed Protection - Side-furling
Survival Wind Speed - (55 m/s)

Figure 1.2 – Picture and technical specifications of the Whisper 100 wind turbine

Influenced by the Labrador Current to the east and westerly winds from Hudson Bay, coastal Labrador experiences extremely harsh weather, particularly in the winter months. This extreme weather is exacerbated at hilltop locations, due to the adiabatic drop in temperature at higher elevations, wind speed up effects, rime icing and the lack of protection. This environment subjects SWTs to conditions often beyond the normal limits of the operation and, predictably, several units have failed [Roberts *et al* 2007].

1.3. Thesis Structure

This thesis explores two opportunities that are of potential benefit to Bell-Aliant in trying to increase the survivability of the turbines. The first opportunity is to forecast which

locations and resulting situations to avoid in order to reduce failures. The second opportunity discussed is how specific catastrophic failures occur and how best to mitigate them.

A literature review of topics relating to the operation of small-scale wind turbines in harsh environments is provided in Chapter 2. As a measure of introduction to the reader, it includes a look at the current state of wind energy technology and the global industry, comparison of large and small wind turbines, and harsh environment mitigations.

Chapter 3 presents a statistical analysis of turbine failures at Bell-Aliant's hilltop sites in Labrador. A correlation and regression analysis, consisting first of seven months of data and then updated with seven additional months, explores the relationship between the number of failures experienced and the operational variables, including geographical and meteorological characteristics.

A forensic analysis of the most common catastrophic failure experienced by the WH100 is conducted in Chapter 4. This failure includes the severing of one portion of the nacelle into two pieces, causing the rotor and generator to fall to the ground. The forensic analysis explores the type of failure and failure mechanisms, possible situations in which the failure likely occurred and recommends potential solutions.

Chapter 5 details an experimental program undertaken to investigate feasible solutions for the mitigation of the catastrophic failure explored in Chapter 4. The field program involved controlled velocity trials through the development and use of a trailer mounted turbine and anemometer apparatus. Once qualitative and quantitative observations of the unaltered unit in operation were complete, modification of the blade geometry and limiting the furling capability were undertaken to determine the resulting effects of the turbine's operational characteristics.

This thesis concludes with a brief summary of the results from each of the chapters and a preliminary operational guideline for Bell-Aliant. A proposal for an 'ideal' robust small wind turbine is also presented along with recommendations for future research.

2. Literature Review

Solar irradiation causes uneven heating on the surface of the earth, creating density and pressure differentials that drive the planet's atmospheric circulation system. The Coriolis Effect, land formations, and oceanic circulations further contribute to the strength and direction of wind at a given location. Strong winds have power densities an order of magnitude higher than solar irradiance. Although a gentle breeze of 5 m/s only has about 0.075 kW/m^2, a violent storm can have up to 10 kW/m^2 of energy in the wind, while solar power only has a maximum power density of 1 kW/m^2 [Quaschning 2005]. This concentration of energy found in strong winds worldwide is the reason why wind energy conversion systems are an attractive technology, now vying as an alternative to non-renewable sources.

2.1. Introduction to the Wind

Presently, all known wind turbines operate within the earth's atmospheric boundary layer (ABL). The ABL is the part of the troposphere that is directly influenced by the presence of the earth's surface and responds to surface forcings with a time scale of about an hour or less [Stull 1988]. Within this area of the atmosphere there is a great deal of turbulent mixing of the air, primarily driven by the changing heat released from the sun-heated ground throughout the cycle of the day as illustrated in Figure 2.1. There is a general wind velocity distribution within the surface layer of the ABL, shown in Figure 2.2,

where the wind speed gradually increases with its distance from the earth's surface. The Power Law presented in Equation 2.1 can describe this velocity distribution, in which the exponent α depends on the roughness of the terrain over which the wind travels, with typical values ranging from 1/10 for coastal areas to 1/3 for urban areas. Empirical data is often used to determine the value of α for a specific region. Above the ABL, in the 'free atmosphere' the winds are primarily geostrophic and relatively uninfluenced by the surface of the earth.

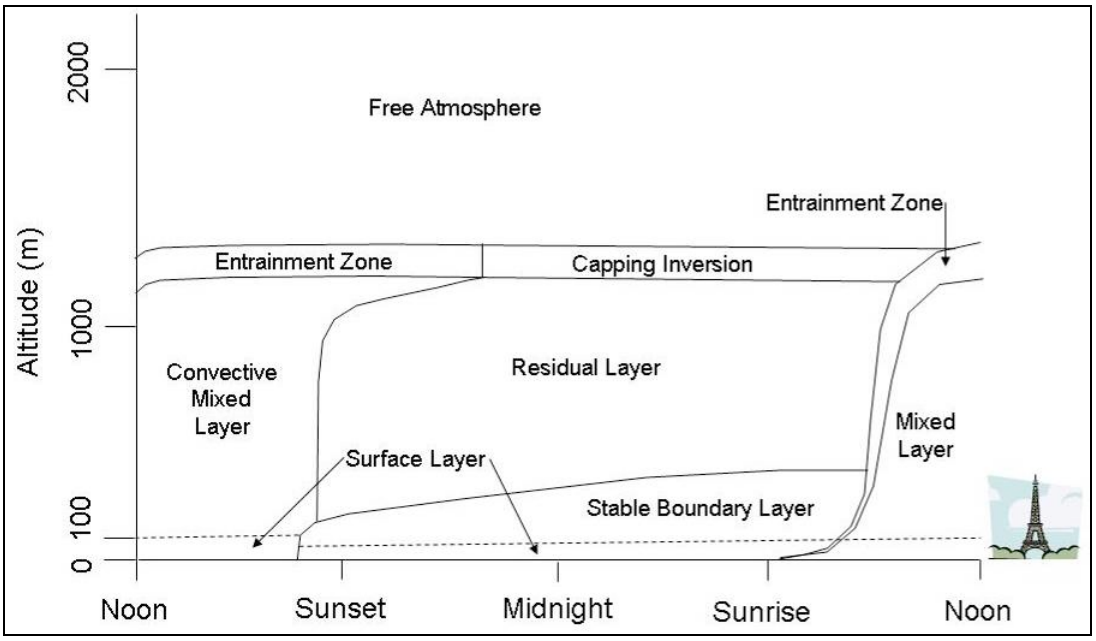

Figure 2.1 – The atmospheric boundary layer over land

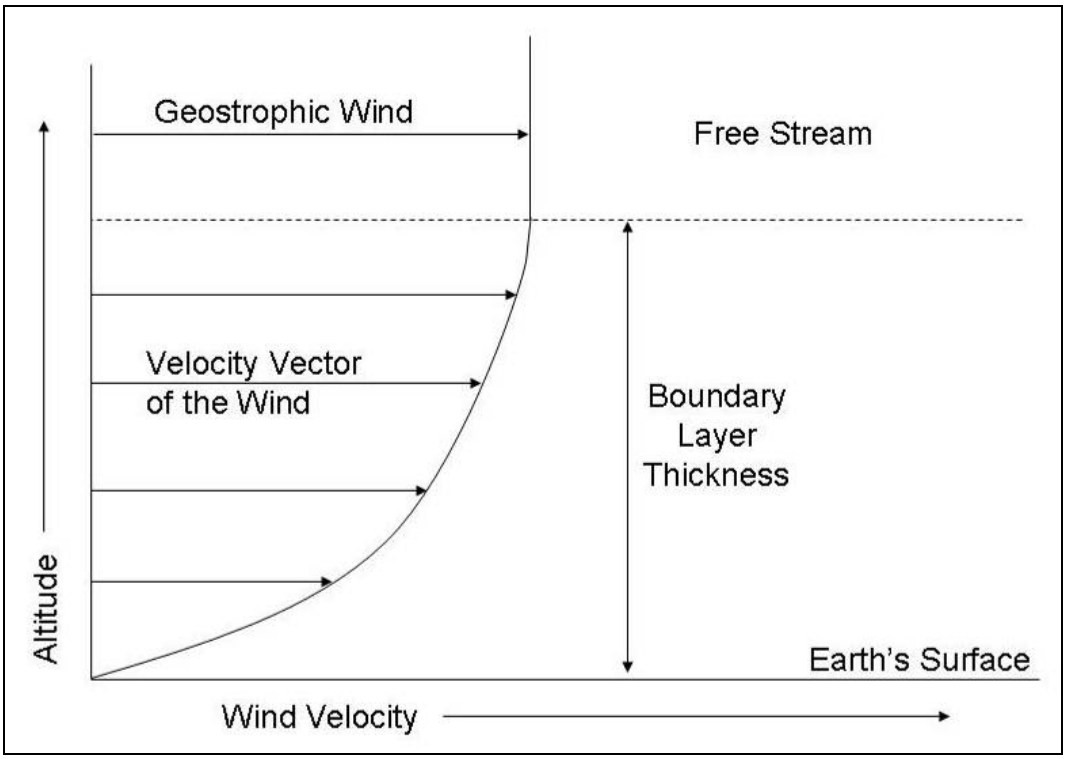

Figure 2.2 – Boundary layer wind velocity distribution

$$U_Z = U_{10}\left(\frac{Z}{10}\right)^{\alpha} \qquad [2.1]$$

where,

U_Z = wind speed at height Z in meters

U_{10} = wind speed at height 10 meters (determined empirically)

α = exponent based on terrain surface roughness

Elevation changes can greatly affect the speed of the wind within the distance of a few hundred meters. On the luff, or windy, side of a hill or mountain, the wind speed can nearly double its uninfluenced value, as illustrated in Figure 2.3, due to the ground rising

up to higher altitudes where the wind has a greater velocity and compression of the ground level air as it travels up the hill. On the other hand, wind speed is greatly reduced on the lee side [Quaschning 2005]. Obstacles near the site, such as trees, buildings and other turbines can slow down the wind and, as a general rule of thumb, the hub height should be at least three times higher than a single obstacle or placed 35 times the height of the obstacle away. Wind speed increases with height as the effects of ground roughness are lessened and becomes increasingly less dependent of height at altitudes greater than 100 m [Quaschning 2005].

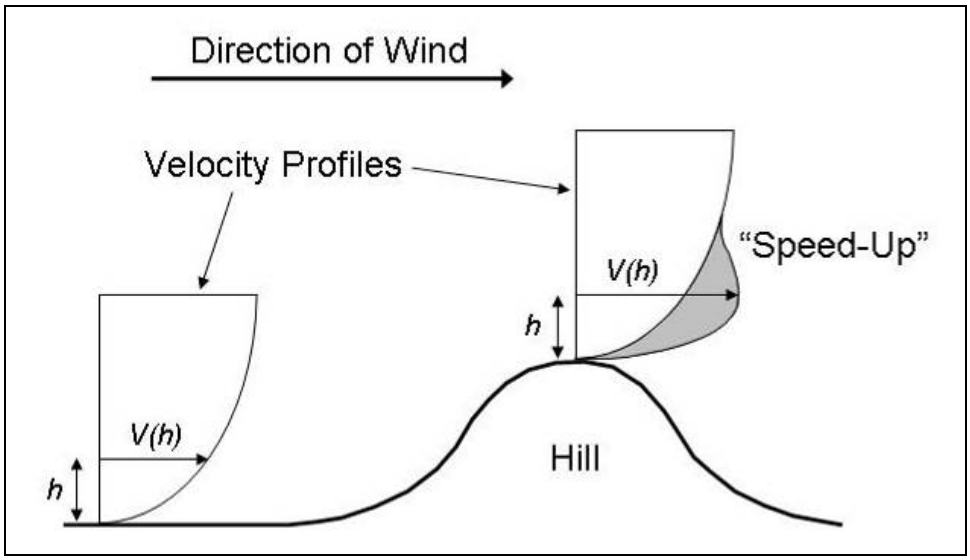

Figure 2.3 – Wind speed-up effect over a hill

2.1.1. Power in the Wind

Power in the wind is defined as the amount of kinetic energy available with respect to a unit time. Thus it is found by multiplying the dynamic pressure over the wind's projected

frontal area to get the force. Then multiplying this force by distance covered to get the energy and subsequently dividing this energy by the unit time over which it is measured. This process is outlined in Equations 2.1 to 2.4.

Dynamic Pressure:

$$p = 0.5 * \rho * V^2 \quad [2.1]$$

Force:

$$F = p * A = 0.5 * \rho * V^2 * A \quad [2.2]$$

Energy:

$$E = F * \Delta L \quad [2.3]$$

Power:

$$P = \frac{E}{\Delta t} = F * \frac{\Delta L}{\Delta t} = F * V = 0.5 * \rho * V^3 * A$$

$$P = 0.5 * \rho * A * V^3 \quad [2.4]$$

where,

p = dynamic pressure

ρ = density of the air

V = wind speed

F = force

E = energy

P = power

A = cross-sectional area of the wind

ΔL = unit distance

Δt = unit time

While it is obvious that wind speed is variable, the density of air can change up to 30% in extreme cases, influenced primarily by temperature, pressure and elevation. As the air temperature drops the density increases while the opposite is true of elevation. As such an ideal location for maximum energy capture form the wind would be close to sea level in a colder climate.

The theoretical maximum amount of power that can be extracted from the wind using a lift driven device, the Betz Limit, was first determined theoretically by Albert Betz and is equal to 16/27 (59.3%). In practice the maximum efficiency achieved is usually between 40% and 50%. Similarly, it has been calculated that the theoretical maximum power that can be derived from a drag driven device is 4/27 or 14.8%.

The Betz limit is reached when the rotor reduces the wind speed by one third. To come close to this theoretical maximum the turbine needs high rotor speeds with low torque, as high torque produces greater wake losses [Gipe 1999]. Power is a product of torque and rotational velocity so it is beneficial to decrease the rotor torque as long as the rotational velocity is proportionally increased.

As described by Equation 2.4, the power in the wind varies with the cube of the wind speed and has the resulting consequences: i) strong steady winds becomes very important for site selection, ii) a turbine's design speed is usually twice the average wind speed, iii) turbines may not turn in low winds and iv) a rapid increase in wind speed can quickly bring a wind turbine to its maximum rated value of power generation resulting in the need for controlling actions [Twidell 1998].

2.1.2. History

The power in the wind has been harvested throughout human history, the Egyptians employed it for navigation on the Nile River over 5000 years ago. Windmills have been in use for nearly 3000 years, with their earliest applications used to facilitate irrigation. The common practice of grain milling began in Afghanistan in the 7th century, while Europe widely adopted the technology around the 12th century. The Netherlands employed tens of thousands of autonomous wind-tracking windmills for land drainage in the 17th and 18th centuries, while North America adapted the technology for their water pumping needs in the 19th century.

Shortly after the invention of the electric generator, near the end of the industrial revolution, the first electricity generating wind turbines were produced in Europe [Manwell et al 2006] and the technology was quickly adapted in the rural United States. However once the rural electrification of the Unites States began in the 1930's, negating

the need for self-sufficient power sources, the wind power industry came to a grinding halt. That was until the oil crisis of the 1970's brought about the realization that diversification of energy sources was important and wind turbine research and manufacturing once again returned to mainstream industry.

Germany was leading the industry in technical development up until the 1990's, while Denmark has the most wind energy per capita, with 20% of the nation's electrical energy coming from wind turbines. The global industry has approximately doubled in size every three years for the past decade and continues to be the fastest growing industry in electrical power generation [WWEA 2008].

2.1.3. Current Global State

The current global capacity is over 95 GW, of which 19.7 GW were added in 2007 [WWEA 2008]. While the large-scale wind turbines (LWTs)[1], typically in the megawatt range produce the most electricity, small wind turbines (SWTs)[1] are the most numerous. Even though SWTs are small in absolute terms they make a big difference in the lives of people in remote areas around the globe. There are more than 50 manufacturers of SWTs, creating a total of over 100 available models [Gipe 1999]. In the 1980's and 1990's over

[1] To simplify discussion within this thesis, SWTs will refer to those machines with a generation capacity less than 20 kW while LWTs will refer to everything above. If mentioned specifically, micro scale wind turbines refer to machines smaller than 1 kW, but discussion of SWTs will generally include micro scale machines.

60 000 SWTs were built in western countries along with tens of thousands more in China. Micro wind, in particular gained prominence in the 1990's as their applications spread from marine to more terrestrial prominence [Gipe 1999].

2.2. Wind Turbine Technical Basics

There are two basic types of wind turbine: those whose blades rotate about a vertical axis (VAWT) and those whose blades rotate about a horizontal axis (HAWT). VAWTs were among the first wind conversion systems but the HAWTs dominate today's industry.

2.2.1. Vertical Axis Wind Turbines

Three of the most widely used VAWTs include the Savonius, Darrieus and H-rotor. The fundamental Savonius rotor design is similar to a cup anemometer and is primarily a drag device. The Darrieus rotor, commonly referred to as the 'eggbeater', has two or three near-parabolic blades. Even though they apply the principle of lift, in practice Darrieus rotors only have about 75% the efficiency of modern HAWTs [Quaschning 2005]. Another drawback to the Darrieus design is that they are not self-starting, unless wind conditions are ideal, resulting in the need of a starter motor. The H-rotor is another VAWT, which uses three straight, airfoil blades attached vertically to the axis of rotation. Simplifications of these VAWT designs can be seen in Figure 2.4

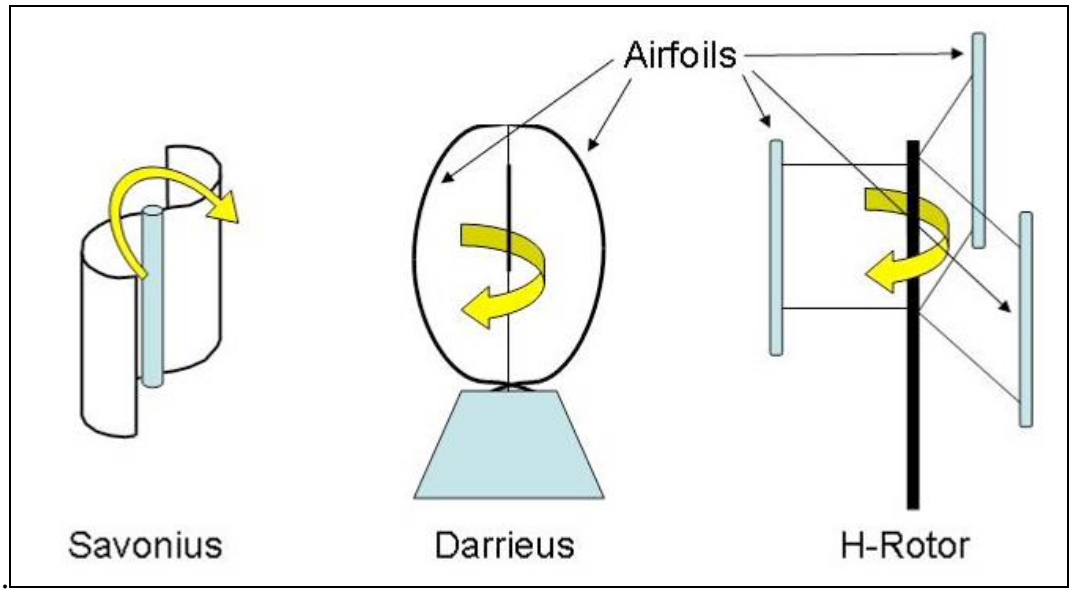

Figure 2.4 – Widely used VAWT designs

While not as common as HAWTs, VAWTs do offer certain advantages. Their structure and assembly are fairly simple and the generator and gears can be placed at ground level allowing easy access for maintenance. Also, VAWTs don't need to be oriented into the wind, which could be of particular importance in locations where the wind direction changes frequently. The disadvantages, however, often out-weigh any advantage offered by a VAWT. The two main deficiencies found in most commercially available VAWTs is the large amount of material required for their construction and their typically lower efficiencies. Also, VAWTs do not operate high in the air as they are generally mounted close to the ground and are unable to capitalize on the increased wind speeds in higher altitudes.

Another issue with all lift based VAWT is that the lift forces reverse direction on every rotation. The centrifugal forces in the H-rotor induce severe bending stress in the blades at the point of attachment. The Darrieus design was developed to overcome this challenge. Darrieus turbines are lighter for their overall strength and they can operate at higher speeds than their straight predecessors. A Darrieus turbine can extract up to forty percent of power from the wind under ideal conditions, however, the H-rotor captures more wind than a similar sized Darrieus rotor [Gipe 2004]

2.2.2. Horizontal Axis Wind Turbines

The higher efficiency and lower material costs of HAWTs appeals to a wide base within industry and are predictably the primary focus of manufacturers, despite some inherent challenges, discussed further in this section.

The basic components of nearly all modern HAWTs include rotor blades, rotor hub, electrical generator, vaning or yaw mechanism, nacelle, tower, foundation and controls. Components usually on larger turbines, but not smaller turbines, include a pitch mechanism, gearbox and yaw drive. A simplified schematic of a typical small HAWT is shown in Figure 2.5.

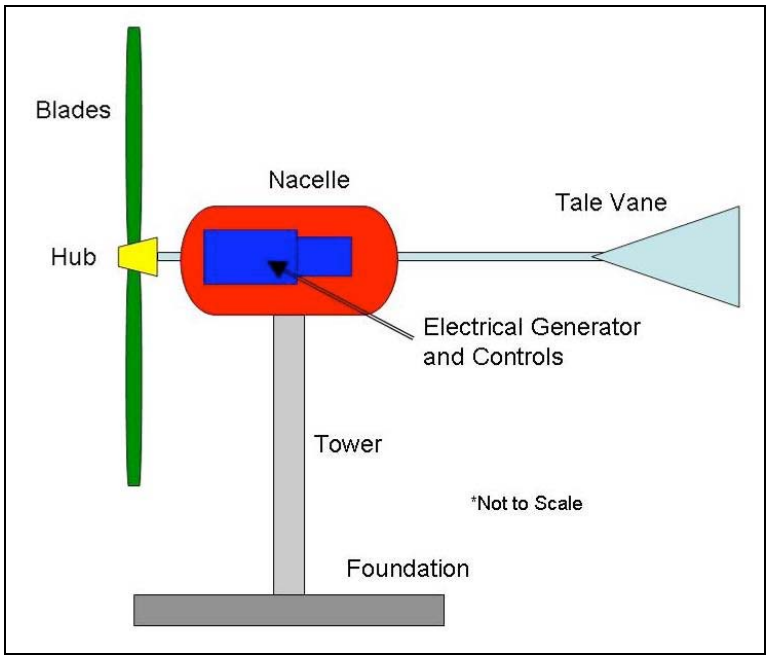

Figure 2.5 – Simplified schematic of a HAWT

Structural design details of HAWTs are dominated by the following: i) forces in the wind vary with the square of the wind speed, ii) the rotational frequency and its harmonics cause unwanted, but predictable, vibrations (designers need to avoid vibrational frequencies near to the fundamental resonant rotor frequency and its harmonics), iii) unpredictable turbulence in wind causes persistent, rapid and frequently violent oscillations, iv) gravity stress cycles are at least 100 times greater on turbine blades than on equivalent fatigue cycles on comparably sized aircraft wings [Twidell 1998].

One disadvantage of the HAWT is that the additional degree of freedom demands that slip rings and further bearings are introduced, thus complicating the turbine. Another drawback is that most of the heavy equipment is placed up high on top of the tower and requires additional maintenance efforts.

2.2.2.1. Blades and Solidity

The wing profile of an HAWT's blades makes air flow in smooth laminar fashion more rapidly over the top of the blade than the bottom, using Bernoulli's principle to introduce lift in the direction of blade rotation. As such, a rotating blade moves into a space previously occupied by another blade. The limit to rotational velocity occurs when air in this space is too strongly perturbed by the previous blade and no lift can be created to sustain the rotation. Therefore, fast turning rotors should have fewer blades. A three-bladed design is common due to its steady motion and is considered to be visually most acceptable [Twidell 1998].

While turbines with two blades are in production, three-bladed machines are the industry norm. Their improved power production quality and optically smoother operation often beat out the lower material cost of two blades. Also, turbines with two blades have trouble yawing because when the rotor orientation is vertical there is very little resistance force to induce yawing, while when the rotor is horizontal this force is at a maximum. This alternating minimum and maximum resistance causes uneven yawing and can increase the likelihood of fatigue.

As the speed of rotation increases the rotor will appear more solid to the wind, forcing the air to become more turbulent and reducing rotor efficiency. Conversely, as the rotational speed decreases, air is allowed to pass through the rotor unperturbed, which also

decreases efficiency. Modern turbines are designed to operate at some middle value that produces the optimum efficiency [Twidell 1998].

Wind turbine performance is usually characterized by its power coefficient, which is inversely proportional to the square of the tip speed ratio, presented in Equation 2.5. Rotors with the fewest blades have the highest power coefficients [Twidell 1998] and the fewer blades there are the greater the loading and rotational velocity will be [Gipe 2004].

$$\lambda = \frac{R * \Omega}{V} \qquad [2.5]$$

where,

λ = tip speed ratio

R = rotor radius

Ω = rotor rotational speed

V = wind speed

Solidity is the ratio of blade area to swept area [Manwell *et al* 2006]. As solidity increases so does torque and high solidity wind energy conversion systems, such as the American farm windmill, operate best in low winds and are material intensive. They typically extract about 15% of the power from the wind [Gipe 2004] when operating but have a much wider window of operational time than those with lower solidity.

2.2.2.2. Operating Ranges and Overspeed Control

Wind turbine operation typically falls into the ranges listed in Table 2.1 below [Quaschning 2005].

Table 2.1 – Wind Turbine Operation Ranges

Operation	Wind Speed Range (m/s)	Description
Cut-in	2.5 – 4.5	Rotor turns and generator begins producing electricity
Design	6 – 10	Defined by the tip speed ratio
Nominal	10 – 16	Generates the rated power, ideal wind speed
Cut-out	20 – 30	Rotor stops to protect system integrity
Survival	50 – 70	The upper threshold wind speed of the system

To maintain the nominal power production from the generator at speeds above the nominal speed HAWTs can employ a variety of overspeed protection devices. This is where the most significant differences between wind turbines occur. Larger turbines are often equipped with stall (passive or active) or pitch control and electrical or mechanical brakes, while smaller turbines often employ furling or even blade flutter. A further discussion of SWT overspeed protection systems takes place in *Section 2.6.3*.

2.2.2.3. Rotor Orientation

The rotor can be placed upwind of the tower or downwind, as illustrated in Figure 2.6. The advantage of a downwind orientation is that there is no need for a tail vane or yaw

mechanism. The main disadvantage would be the cyclic strains induced as each blade passes the tower wind shadow.

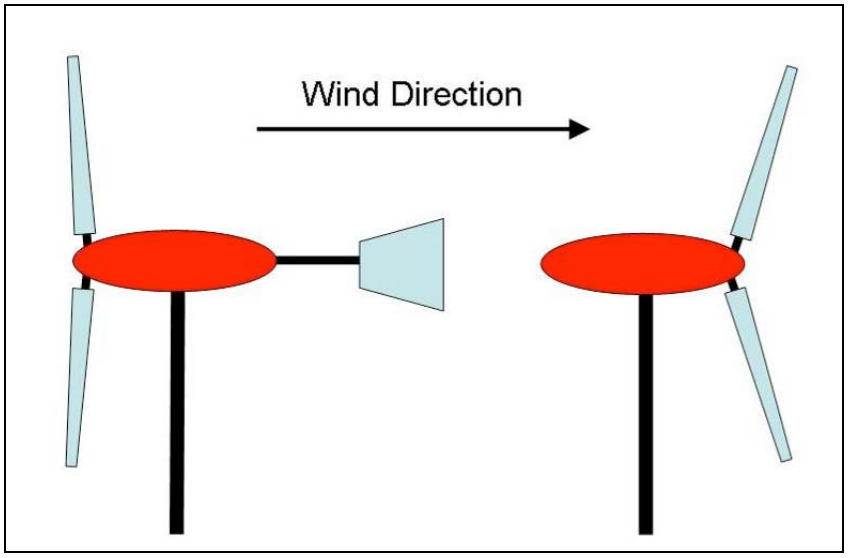

Figure 2.6 – Upwind (left) and downwind (right) rotor orientation

2.3. Economic Viability of Small Wind Turbines

Under normal operating conditions SWT profitability is most sensitive to a change of average wind speed as well as changes in predicted maintenance and operating costs. [Leuven 1984] and the energy used to make the wind turbine is often recovered within a year [Gipe 2004]. With present day technology, cost effectiveness is linearly proportional to machine size.

According to [Gipe 1999], there are three methods for calculating the gross amount of energy SWTs may capture: i) rotor swept area, ii) manufacturer's advertised power curve

and iii) manufacturer's published estimates. While manufacturer's performance data will often be overly optimistic, the rotor swept area is a fairly consistent indicator of production potential.

2.4. Applications of Small Wind Turbines

Three quarters of all SWTs are destined for stand alone power systems at remote sites [Gipe 2004] and are most frequently used in hybrid systems, which can include diesel, photovoltaics and batteries [Clausen and Wood 2000]. Stand-alone hybrid systems are beneficial in the mid latitudes of the northern hemisphere, where winds are stronger in the winter and solar irradiation is stronger in the summer. In most stand alone applications the high value that a wind turbine adds to a hybrid wind-solar system warrant its use, often regardless of the wind resource, with some exceptions [Gipe 1999]. Some manufacturers estimate that up to 80% of their wind turbines are used in hybrid systems along side photovoltaic modules.

There are three aspects to each stand-alone system: i) generation, ii) storage and iii) loads. These systems need batteries to ensure a reliable supply of electricity to the end user but not much more than 50% of the energy stored in a battery can be withdrawn without sulfating the plates and significantly decreasing their effectiveness and life. If an alternating current load is required then inverters must be installed downstream of the battery [Gipe 1999].

Telecommunications is one of the small wind turbine's earliest applications. There are many of these sites situated on isolated mountaintops were a regular supply of diesel is difficult and expensive. The first use of SWTs for telecommunications applications was by *Australian PTT* when they installed over 150 wind turbines at telephone repeater sites in the 1950's and 1960's [Norton 1982]. A photograph of one of Bell-Aliant's telecommunication sites (Mulligan, Labrador) that employs wind turbines as part of a hybrid power generation system can be found in Figure 2.7. Wind turbines are in the background, photovoltaic cells in the foreground, while the structures housing the diesel generators and battery bank are in the middle with the communication tower itself.

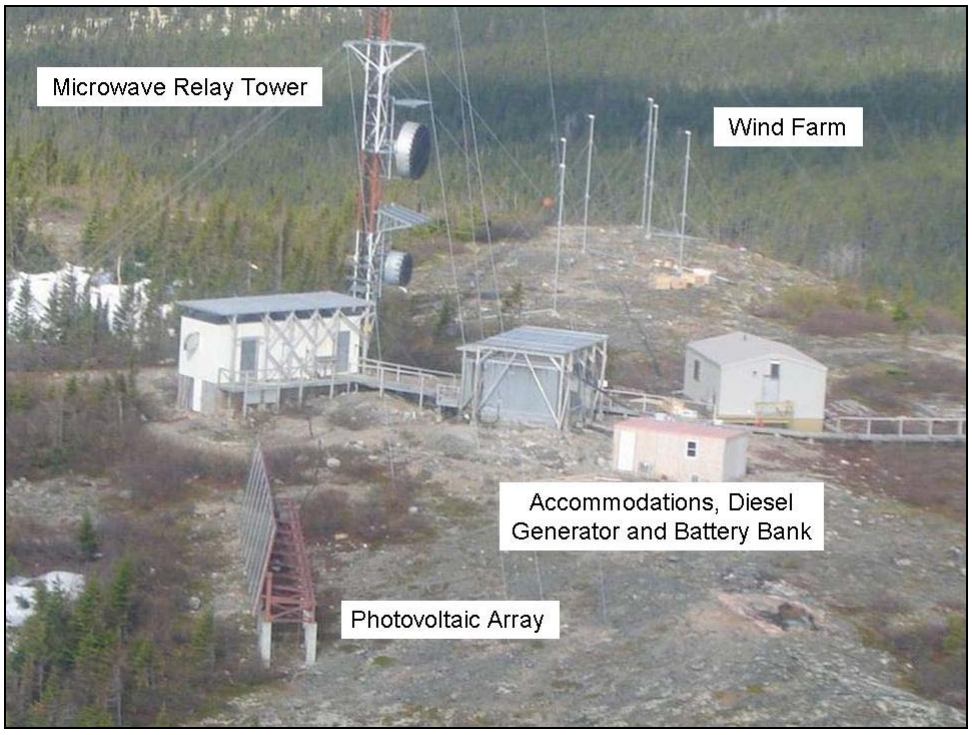

Figure 2.7 – Telecommunications site employing a hybrid power system

Wind turbines used to power isolated telecommunication towers are required to operate in more extreme weather, run more often (sometimes in excess of 7500 hours per year) and function unattended for longer periods of time than typical SWTs. Only robust wind machines using fully integrated direct drive designs perform satisfactorily. Northern Power System's HR3 was designed specifically for these demanding conditions, while the Bergey Excel has seen similar success [Gipe 2004].

Small wind turbines interconnected to the grid proved to be a commercial failure in the United States for regulatory and political reasons. Europe, in particular Denmark, Germany and the Netherlands, was much more receptive, where a grassroots effort spawned a one billion dollar industry [Gipe 2000]. In North America, the recent expansion of the SWT industry has been due in large part to battery charging systems in off-grid applications.

Not all SWTs are a part of a hybrid system or connected to a large electrical grid. Some turbines are used by themselves to provide impressed-current cathodic protection for pipelines. Cathodic protection counteracts galvanic corrosion in highly reactive soils and does not require a constant load. The variable, but repeated, load provided by a micro wind turbine is ideal for such an application.

It is interesting to note that there are more than one million water-pumping windmills still in use worldwide.

2.5. Comparison of Large and Small Wind Turbines

SWTs haven't received the same level of engineering or scientific attention as LWTs. They are generally manufactured by smaller companies with limited capital and government influence. As a result, the technical sophistication of SWTs is considerably below LWTs [Clausen and Wood 2000]. While many of their basic technological principles remain the same, there are some very distinct differences between LWTs and SWTs.

2.5.1. Site Selection and Energy Capture

Large-scale wind installations often require at least a year of local wind measurements to ensure economic viability. Small, especially micro, scale wind on the other hand is more likely added to a pre-determined site and doesn't often have the luxury of site selection. The site is usually already selected for some other purpose and wind turbines are chosen as a potential energy source. Finding the optimal wind location is impractical for most SWT users as a SWT can be installed for a similar cost to recording anemometer. As such, SWTs are often purchased and installed to determine the viability of a location for wind power [Gipe 1999]. Meteorological data can be effectively correlated with short term testing as an alternative to long term wind monitoring [Watson 1981].

LWTs are sited properly for ideal wind situations, such as the farm in Figure 2.8 that is located on a relatively flat and open piece of land, near transmission lines, while SWTs are sited close to the load they provide. This can result in lower wind speed conditions and as such, SWTs are often designed to extract power effectively at low wind speeds. The starting torque is primarily dependent on the number of blades, chord length and the rotational inertia of the blades (if blade inertia dominates that of other components). Minimizing blade weight or increasing the number of blades improves the starting torque but may complicate yaw behaviour and over speed production as the rotor would be more sensitive to changes in wind direction and velocity. The smaller the wind turbine, the lower the starting torque. Starting is also affected by the general absence of pitch control (due to cost) on SWTs [Clausen and Wood 2000].

Figure 2.8 – LWT wind farm in California
(source: http://en.wikipedia.org/wiki/Wind_farm)

SWTs are typically designed to perform best in low-wind regimes (e.g. with an average annual wind speed of 4-5 m/s). As such, when the annual wind speed increases the efficiency of the turbine actually decreases even though there is a lot more energy in the wind [Gipe 1999]. Aerodynamic efficiencies of the rotor are of great importance in larger scale turbines while the efficiency of SWTs depends on the entire system [Watson 1981].

Some of the best SWT rotors currently available can capture up to 40% of the energy in the wind, while their generators seldom convert more than 90% of the energy delivered to them (higher for LWTs). These efficiency levels combined with additional losses lead to an overall conversion efficiency of around 30% in ideal conditions. If looked at on an annual basis the efficiency will likely be closer to 20% [Gipe 1999].

2.5.2. Mechanical Drives

SWTs are too small to economically accommodate most mechanical drives common in LWTs. Some notable cases are yaw drives, variable pitch and gearboxes. A common finding is that the reliability of SWTs and minimal maintenance is paramount [Walker 1999] and can be facilitated by ensuring a simple system with few moving parts.

Yaw drives can be replaced with tail vanes or a downwind orientation. SWTs are generally fixed pitch and the preferred pitch can only be set during the initial attaching of the blades to the hub. It is possible on some machines to manually change the pitch

depending on the season [Gipe 2004]. Also, as the relative wind speed seen by the tip and the hub is quite different, blades are often twisted and tapered with the extremes occurring at the hub and tip respectively. Alternatively, some SWTs use pultrusion as a manufacturing technique, which results in a constant cross section [Gipe 2004]. The basic aerodynamics of blades is independent of size [Clausen and Wood 2000].

SWT rotor technology differs importantly from LWT. For rotors less than one meter in diameter a lack of controls may be acceptable under certain conditions, such as a multi-bladed rugged turbine with relatively low rotor velocity. Southwest Windpower uses electronics and blade flutter to protect its lightweight Air series micro turbines. Most manufacturers, however, try to avoid blade flutter as it can cause damage to the blades and the turbine. Furling is the simplest and most foolproof method for SWT rotor control. Furling decreases the frontal area of the turbine intercepting the wind. It is typically vertical or horizontal and would use gravity or a spring respectively to return the rotor to its normal position [Gipe 2004].

Overspeed protection for LWTs is usually a combination of more than one method, redundancy in the interest of safety. Mechanical or electrical braking systems are almost always accompanied by variable pitch, passive stall, blade tip brakes (shown in Figure 2.9) or other types of aerodynamic brake. The combination of these two separate techniques ensures that if one system fails the other will still be able to protect the integrity of the turbine in high winds.

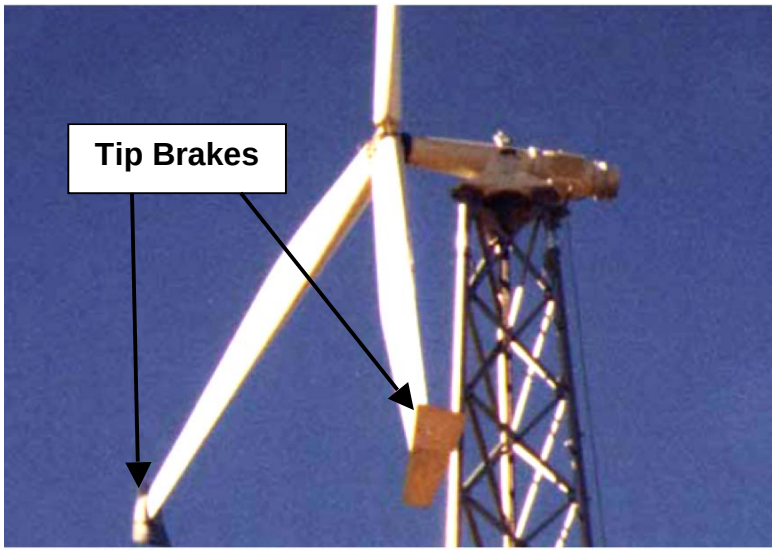

Figure 2.9 – 50 kW wind turbine with blade tip brakes (source: http://www.nrel.gov/wind/pdfs/34382.pdf)

Some machines can increase or decrease the pitch to a stall or feather position in order to control the amount of lift produced by the blade. Pitching to feather is more complex but will result in a more robust system. SWTs have a poor survival record when using stall pitch control [Gipe 2004] and mechanical governors have proven too costly and unreliable for many manufacturers. Pitching can maintain near constant peak power in high winds where furling can result in a sharp output drop. Pitching governors have substantially more moving parts than furling governors. Passive pitching methods with no mechanical governors do exist but have faired poorly over time [Gipe 2004].

Aerodynamic stall is used but not wholly relied upon for SWTs while mechanical brakes aren't generally used on SWTs, but would be coupled with some other control device in case of failure. Aerodynamic tip brakes are sometimes used on larger SWTs. Coning has been used in downwind and H-rotor VAWTs.

One of the inherent challenges with SWTs is that rotor speed increases with decreased size, which increases the importance of centrifugal forces and fatigue loads. Another inherent problem is the difficulty of manufacturing accurate blades when the tip chord is only a few centimeters in length [Clausen and Wood 2000].

Nearly all SWT are variable speed, which simplifies controls and increases aerodynamic performance [Gipe 2004]. Variable speed operation gives more energy than the fixed speed wind turbines [Arifujjaman *et al* 2008].

2.6. Small Scale Wind Turbine Technology

2.6.1. Blades and Rotor Orientation

Most SWTs are upwind HAWTs with three blades, as they run smoother than two and generally last longer as a result. SWTs typically use composite materials, such as fiberglass or carbon fiber, for rotor blades, while a few SWTs still employ wood blades, either timber or laminate. Aluminum, however, is no longer used due to the effects of metal fatigue [Gipe 1999]. Wood laminates are among the toughest and lightest composite materials available [Twidell 1998].

In a downwind orientation the blades are swept slightly downwind to form the shape of a shallow cone with the rotor hub as the apex. Heavy blades will experience a cone angle

of one to two degrees while light blades experience a coning of eight to ten degrees. A major disadvantage of downwind turbines is their tendency to get caught upwind, especially during light, variable winds and they have been known to even hunt the wind, whereby they 'walk' around the tower. Another disadvantage is that downwind machines are unable to furl in high winds unless they have a mechanically controlled yaw system [Gipe 2004].

2.6.2. Production and General Operation

SWTs are notorious for defying manufacturer's expectations, especially in battery charging systems, as no international standard for measuring SWT performance exists. However, this is difficult to measure as the system may be 'spilling' energy if the battery is fully charged. As there are no standards for rating SWTs, [Gipe 1999] suggests comparing the rotor diameter if you are trying to decide which turbine would have the best power generation capacity. Even a small difference in rotor diameter can have a large impact on electricity generation.

SWT experts Mick Sagrillo and Hugh Piggot state in [Gipe 2004] that the durability of SWTs is inversely proportional to the tip speed ratio and a tip speed ratio of $\lambda = 5$ is aerodynamically optimal for SWTs. As the tip speed ratio increases so does the noise and associated tip losses caused by vortex shedding.

Typical operating parameters of SWTs can be found in [Clausen and Wood 2000]. Blade Radius, R, affects many performance parameters. Figure 2.10 outlines the dependence of important parameters on blade radius, for geometrically similar blades of constant density, operating at the same tip speed ratio.

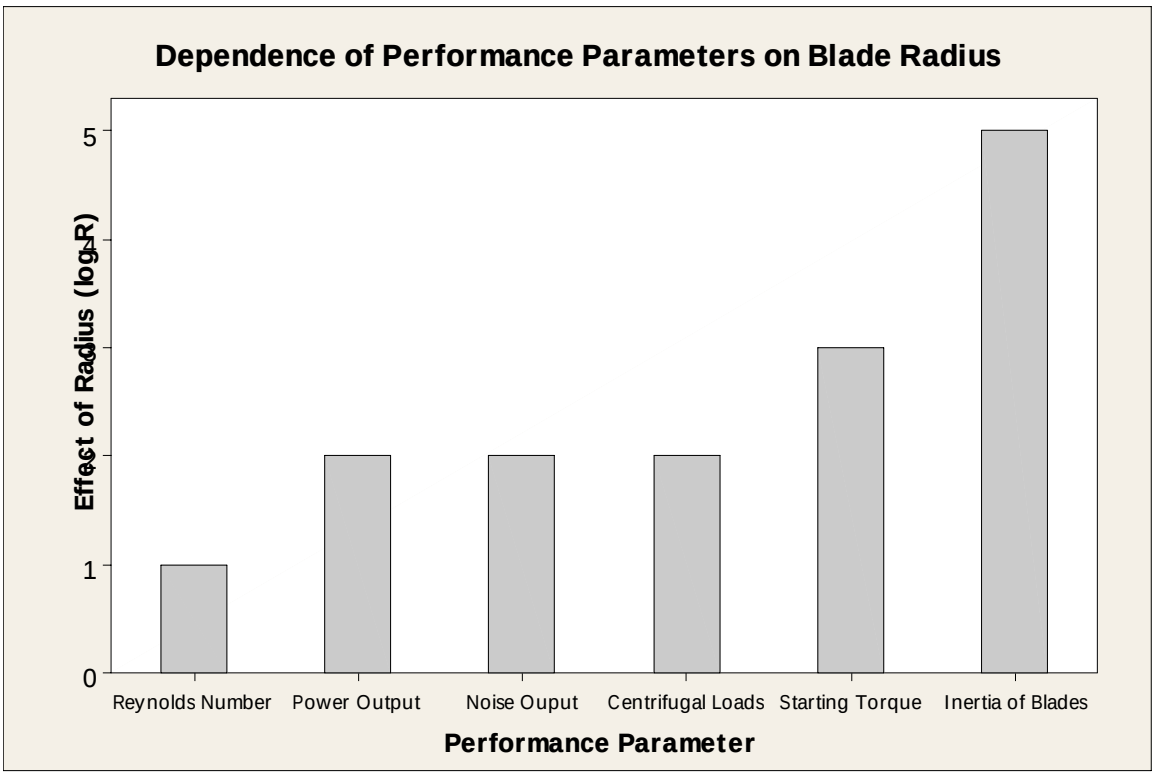

Figure 2.10 – Dependence of performance parameters on blade radius

[Giguere and Selig 1997] say adverse effects of low Reynolds' Numbers usually occur below Re = 500 000 (an approximation depending on aerofoil), which is within the SWT operating range. For an increased lift:drag ratio at low Reynold's Numbers, thin airfoils are required to decrease acceleration over the upper surface. At very low Reynold's Numbers the optimum blade thickness approaches zero. Increasing blade thickness

toward the root should be avoided for small blades as the hub region often gives most of the starting torque (rather than rated torque) [Clausen and Wood 2000]. A uniquely important aspect of SWTs, their starting behaviour, is a complex combination of unsteadiness, low Reynold's Number operation and high angles of attack. [Clausen and Wood 2000].

Power loss occurs from poor yaw performance and blade loads increase significantly during yaw, as tail fins have low damping ratios [Ebert and Wood 1995]. Yaw behaviour improves when the turbine is extracting power, presumably due to the stabilizing effect of blades coning slightly under load [Bechly *et al* 2006] and the stabilizing effects of the rotor's angular momentum. A long tail boom with a small fin can minimize yaw rate [Kentfield 1996].

2.6.3. Overspeed Control

Overspeed control is one of the most widely varied aspects in SWTs. Most micro-scale machines furl (fold about a hinge), as demonstrated in Figure 2.11 so that the rotor swings toward the tail vane and out of the wind. Often there is a mechanism, such as a spring or shock absorber, to dampen the rate at which the rotor returns to its full running position. Furling action typically reaches steady state within 10 seconds in high wind speeds [Arifujjaman *et al* 2008]. Several machines in the order of 10 to 20 kW employ variable pitched blades as a means of overspeed protection.

Figure 2.11 – Whisper 100 SWT while furling

2.6.4. Electrical Power Generation

Most small and micro sized wind turbines use permanent magnet alternators, which tend to be the simplest and most robust generator configuration, however there is a level of diversity in 10 to 20 kW wind turbines. Attaching the magnets to the casing rather than the shaft is more robust as the centrifugal forces on the shaft would tend to 'throw' the magnets loose from their specific positions. In light winds permanent magnet generators may suffer from cogging where the shaft sticks when the magnets align with the coils. Simply skewing the magnet slots in the laminations of the armature reduces cogging [Gipe 1999]. Normal power production is not strongly influenced by generator characteristics other than efficiency [Clausen and Wood 2000].

SWTs typically use a direct drive transmission even though industry flirted with gear driven machines in the 1970's and early 1980's. Some machines have used belts or chains but have proved to be unreliable in practice. As wind turbine size decreases the rotor speed increases and the need for a gearbox decreases [Gipe 2004].

Turbines that are designed for longer life and decreased maintenance are usually fitted with more costly low-speed generators. Many manufacturers build special purpose, direct-drive, slow-speed alternators for use in isolated harsh environments. Alternators, which produce alternating current, cost less that direct current generators for a given output and as such they tend to dominate the market. Most SWTs generate variable frequency, three-phase alternating current (as the rotor velocity increases so does the output frequency). Battery charging wind turbines often rectify AC to DC either at the generator or at some distance from the generator [Gipe 2004].

Microprocessor based control systems combined with field excited generators have improved SWT operation in a few ways. Off-grid SWTs are not required to generate at grid-synchronous frequency and can be maintained at optimum tip speed ratio over a wide range of wind speeds by sensing the blade rotational speed (as output current, which is cheaper to measure than wind speed for SWTs) and using it to adjust the field current in field excited generators. Field excited generators can be used for over speed protection by sensing power output [Bechly et al 1996].

2.6.5. Towers

There are several tower options when erecting a small wind turbine, some of which include free standing lattice, free standing tubular or guyed mast, shown in Figure 2.12. The guyed mast is generally considered the cheapest and easiest to install for SWT systems.

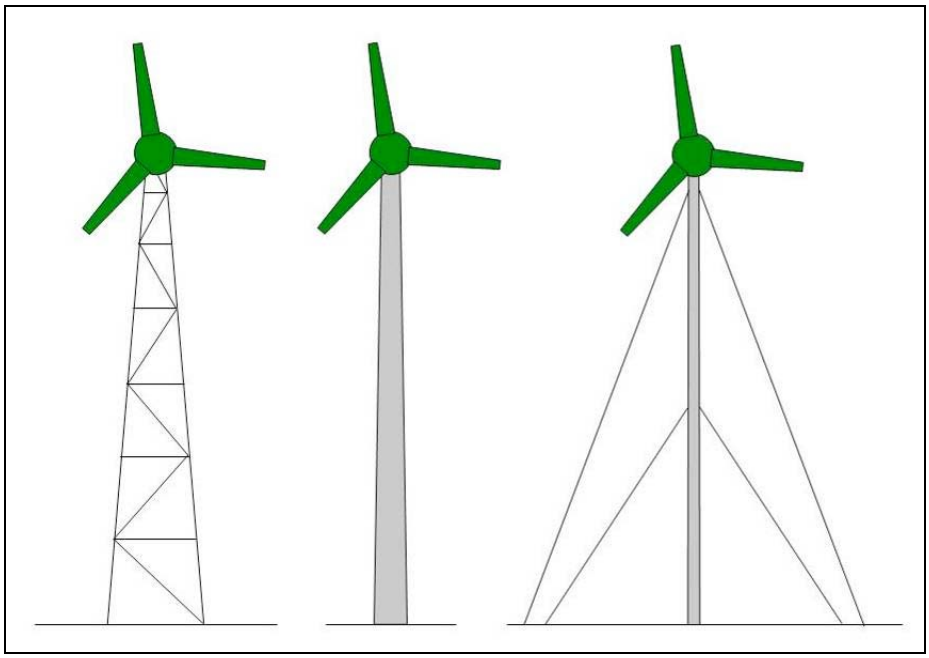

Figure 2.12 – Common tower types: lattice (left), tubular (center), guyed mast (right)

2.6.6. Rotors

The blades on the rotor are generally the part most prone to catastrophic failure. Solid timber, glass-fiber laminated composites, carbon-fiber laminated composites are common

SWT blade materials. Blades experience a high number of flexing cycles and will likely have a lower life than LWT blades. Timber is good because of its long fatigue life and reasonable price [Sagrillo 1995], unfortunately it is difficult to use for complex shapes [Clausen and Wood 2000]. With careful design a blade with low mass has a low rotational inertia leading to easier starting. Composite materials have a higher capital cost for molds and development of one of their many possible manufacturing techniques. Scaling up a blade design is likely to be more successful than scaling down because of the inevitable increase in Reynolds' Number [Clausen and Wood 2000].

Wood is readily available, easy to work with, cheap and has good fatigue characteristics. Polyurethane tape, as used on helicopter blades, is used in conjunction with wooden blades to protect the blades from wind erosion and hail damage [Gipe 2004]. Solid planks work well for blades up to 2.5 meters, but laminated wood offers better control over the blade stiffness and it also limits shrinkage and warpage. Steel is too heavy for a blade material and, while aluminum is lighter, it is costly and still experiences metal fatigue. Fiberglass, or glass reinforced plastics, and related plastic compounds are strong and relatively inexpensive. It has good fatigue characteristics and is able to be manufactured using a variety of techniques.

A common design method for micro wind turbines is the blade element and momentum theory. Linearizing the blades results in only a small loss of power as 70% of power extracted from the wind by the rotor is produced in the outer halves of the blades.

Efficiency of the blades at a small radius is low because local tip speed ratio is quite small, while efficiency at the blade tips is also low due to tip losses [Tokuyama *et al* 2002].

The dependency of the power coefficient, on the tip speed ratio becomes smaller as the solidity increases. Also, Reynolds' Number increases and rotational velocity increases as solidity increases. The effect of the decrease in rotational velocity is less then the effect of the increase in blade chord length. A solidity of 0.5 is recommended for micro wind turbines having a diameter less than 80 cm operating in low wind speed regions [Tokuyama *et al* 2002].

Three aspects of the hub are considered important: i) how the blade is attached, ii) whether the pitch is fixed or variable and iii) whether or not the attachment is hinged. Nearly all SWT blades are cantilevered out from the hub. Struts can reduce bending stress on the root of the blade where it attaches to the hub, however they also increase drag. They have been known to work well on upwind machines, but fail if the rotor does not stay upwind [Gipe 2004]. No wind turbine using teetering hubs has proven commercially successful.

2.6.7. Robustness

There is no foolproof way to evaluate robustness of SWT designs. In general, heavier SWTs (reference to mass relative to swept area) have proven to be more rugged and dependable than lightweight machines. Unfortunately the heavier machines usually cost more and may be less sensitive to low wind conditions.

2.7. Harsh Environments

In the context of this thesis harsh environments are considered to be those regions that experience any combination of ice accumulation, extremely low temperatures, and strong turbulent winds. A detailed discussion of these three parameters follows.

2.7.1. Precipitation and Icing

Atmospheric icing can be divided into three categories: i) in-cloud icing ii) precipitation icing and iii) frost.

2.7.1.1. In-Cloud Icing

In-cloud icing occurs when supercooled water droplets from low lying clouds or fog, which have been found to exist at temperatures as low as -35^{o}C, freeze upon impact with

a surface that allows the formation of ice (conductor). This type of icing can be further categorized into rime icing and glaze icing.

Rime icing, Figure 2.13, occurs when the thermal energy of supercooled droplets is quickly removed by wind and radiation as it hits the conductor surface, resulting in the absence of liquid water. This process is known as dry growth. Depending on site conditions soft rime or hard rime can form. Soft rime generally occurs when there is low liquid water content in the air and water droplet size is small. The density of soft rime is relatively low due to large air bubbles that have been trapped during the freezing process. Hard rime occurs when there is high liquid water content in the air and water droplets are of a medium size. The density of hard rime is higher than that of soft rime due to smaller gaps and better bonding.

Figure 2.13 – Rime ice formation on a rock at high elevation, Scotland

Glaze icing is formed in a similar manner to rime icing but the thermal energy is removed at a slower rate, so a portion of the droplet remains as liquid water. Due to the presence of water in its liquid state the conductor's surface temperature is always 0^{o}C. Glaze icing is characterized by a solid covering of clear ice with a low amount of trapped air. Its density is near that of pure ice and is more difficult to remove from a structure than rime.

Increases in altitude also contribute to the amount of icing experienced. On the Finish coast, atmospheric icing is five times as frequent at 100 m above ground as at 50 m [Laakso *et al* 2003].

2.7.1.2. Precipitation Icing

Precipitation icing occurs when precipitation, either wet snow or freezing rain, freezes after striking the conductor surface. Wet snow can stick to a conductor if its surface is between 0^{o}C and 3^{o}C as the liquid water allows snow crystals to bind together when they come in contact with the conductor. Generally there is a low bonding strength while forming, but it can become quite strong and hard if the temperature drops below 0^{o}C.

Freezing rain occurs when the air temperature is below 0^{o}C while rain is falling. This happens when the liquid precipitation starts in warm air but goes through a layer of cold air nearer to the earth and becomes supercooled. It is considered to be freezing rain if droplets are greater than 0.5 mm in diameter and between 2.5 mm and 7.6 mm per hour

can fall. Freezing drizzle, which has fine droplets of less than 0.5 mm diameter, is also a concern. The precipitation is uniform and between 0.3 mm and 0.8 mm can generally fall in an hour. Both freezing rain and freezing drizzle are associated with glaze ice accretions.

2.7.1.3. Frost

Frost occurs when the conductor's surface temperature is lower than the dew point of air. Water vapor deposited on the surface freezes into small ice crystals. Compared to in-cloud and precipitation icing the effects of frost are considered to be relatively insignificant and will not be discussed here.

2.7.2. Low Temperatures

Low temperatures affect performance characteristics of glass fibers, plastics, metals, lubricants and all other manufacturing materials. Ultimately every piece of the system is at risk if not previously tested for ductility at extreme temperatures. Even insulated wires are prone to fracture under extreme temperatures.

Japanese research stations in the Antarctic have experienced several WECS failures as a result of the low temperatures including sticking of the rotor shaft due to the hardening of

the lubricants within the bearings, mechanical component failures and shortened generator life [Kimura et al 1991].

Another consideration when operating in cold climates is the increase in air density. An ideal gas approximation shows that air is 26.7% more dense at -30^{o}C then it is at 35^{o}C [Laakso *et al* 2005]. Due to this density increase, it's not uncommon for turbines to produce 20% over their rated capacity, where they run the risk of overheating.

2.7.3. Strong Turbulent Winds

Complex terrain affects the nature of the wind and can create turbulent conditions. Turbulence can be defined as the deviation of the instantaneous wind speed from the mean wind speed over some time period [Rohatgi 1996]. There are speed-up regions as the terrain changes its slope and large vertical components of wind velocity can be expected near cliffs and ridges. Topography can also significantly modify the local turbulence characteristics so that standard turbine models are no longer applicable [Botta et al 1998].

Strong gusting winds create high stresses on the turbine rotor and especially on the overspeed control. The effect of turbulence on wind turbines is important as gusts cause random, fluctuating loads and stresses on the entire structure. Fluctuation in power output and structural fatigue life must be considered during design [Rohatgi 1996].

The mean horizontal wind speed at the earth's surface is zero and it increases with altitude while contained in the atmospheric boundary layer. Wind shear is the variation of wind speed with altitude, which is also known as the vertical wind profile. On a large scale, this is governed by the vertical temperature distribution, resulting from irradiative heating or cooling of the earth's surface and convective mixing of air adjacent to the surface [Rohatgi 1996]. Wind shear commonly associates wind speed increases with altitude increases but there are exceptions where the opposite is true, as in some mountain passes in California. Temperature profiles are roughly represented in Figure 2.14.

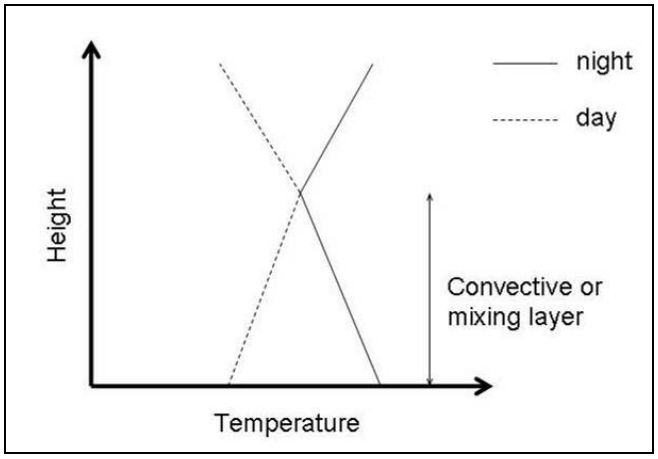

Figure 2.14 – Atmospheric temperature profiles

At altitudes of 10 000 meters the effect of the earth's surface are negligible and then wind is determined by large scale pressure patterns [Rohatgi 1996].

2.7.4. Harsh Environment Applications

As of March 2005 there was over 500 MW of wind capacity installed in cold climates in Scandinavia, North America, Europe and Asia. The economics of theses sites that are usually in higher latitudes or elevations is improving with time compared to coastal and lowland projects [Laakso *et al* 2005]. [Tammelin et al 1997] predict that by 2010, 20% of installed global capacity will operate in cold climates. Figure 2.15 gives a rough outline of harsh environment locations throughout the globe.

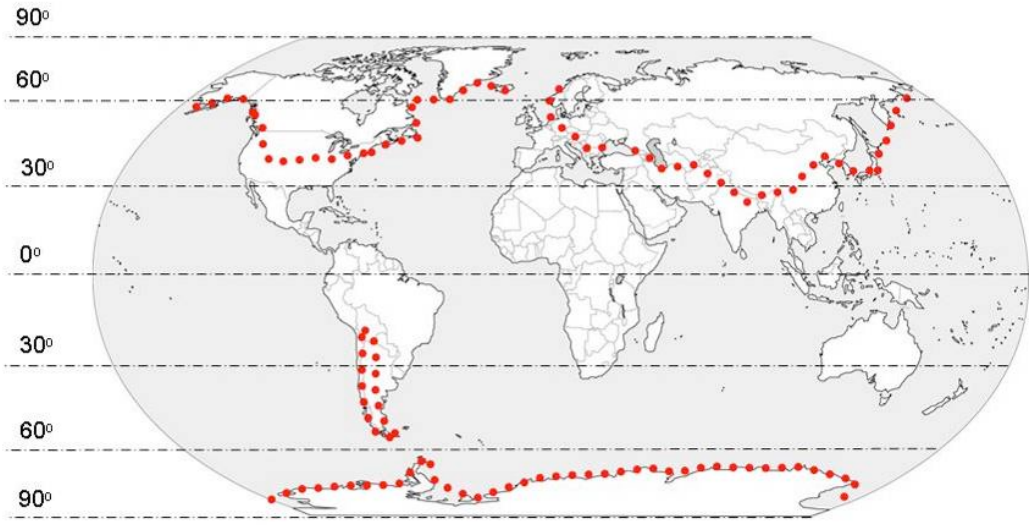

Figure 2.15 – Global harsh environment regions outlined by dotted line

2.7.4.1. Scandinavia

Scandinavia, in northern Europe, experiences occasional icing and temperatures below -20°C on the coasts and severe icing and frequent extreme temperatures in high

elevations. Nearly every site in Finland reports downtime due to icing or low temperatures during the winter, even though all installed turbines use arctic modifications. Cold easterlies off the unfrozen Baltic Sea create severe icing over large areas of Sweden. Sweden has a national database of operational problems from cold climates, with 92 impact reports between 2000 and 2002 resulting in over 8000 hours in missed production. However, several Finish farms experience just over 90% technical availability, which is just shy of the operator's 95% goals [Aarnio and Partonen 2000].

2.7.4.2. Central Europe

The effects of harsh environments on wind turbines occur in a much larger area in central Europe than initially expected, where lower temperatures and greater icing accumulation occur more frequently in mountainous regions. In Switzerland light icing occurs in elevations between 1300 and 2000 meters, while heavy icing occurs at elevations greater than 2000 meters. Swiss alpine sites experience a lower temperature and increased turbulence that accompany extreme gusts [Schaffner 2002]. In the 1980's Italian residents and farmers of isolated mountainous regions (elevation greater than 600 meters) began installing SWTs [Gaudiosi et al 1984].

2.7.4.3. North America

Sites in central North America experience low temperatures but also low icing due to their low humidity. On the eastern coast icing is more frequent, especially in low elevation mountain ridges. The arctic coast of the continent can experience high levels of rime icing depending on the elevation. Aside from some immediate coastal areas, every site in Canada will experience temperatures below -20^{o}C. There are occurrences of in cloud icing on coastal mountains while freezing precipitation is frequent in central and eastern locations.

In the Yukon Territories of Canada at elevations of 4000 to 6000 feet, rime icing can occur from 800 to 1200 hours per year (approximately 30 to 50 days). The most severe icing occurred between October and December [Maissan 2001].

2.7.4.4. Asia

Asia experiences low temperatures but has low humidity resulting in limited icing occurrences. SWTs are in wide spread use among nomadic people in Mongolia and provinces in Northern China.

2.7.4.5. Antarctica

Some of the harshest and most isolated environments on earth are located in Antarctica. Many research stations have been using wind turbines to help offset the astronomical price of transporting diesel fuel to onsite generators for nearly 20 years [Kimura et al 1991].

2.7.5. Micro-Climates

Micro-climates that experience harsh environmental conditions exist all over the world [Laakso *et al* 2005]. In micro-climates, designers and developers should pay particular attention to environmental impacts of turbine installation. Some of these may include land area and use, visual impact, acoustics, bird strike, electromagnetic interference and sustainability [Twidell 1998].

2.7.5.1. Mountainous Regions

Wind speed may double near the summit of a long ridge lying across the wind's path, but this only occurs at the top third of a gradual slope. The wind resource at the base of the ridge would be significantly decreased. The same terrain features that enhance the wind speed also create turbulence. Compared with plain winds, mountainous winds such as those found in the Torngat Mountains of Labrador in Figure 2.16, are extremely gusty

with high shear. Three of the six Bell-Aliant sites studied in this thesis are either part of or adjacent to the Torngat Mountain Range. As such, the aerodynamic load fluctuates vigorously and affects the wind turbines structure [Ichikawa et al 2001].

Figure 2.16 – Torngat Mountains of Labrador (source:_http://atlas.nrcan.gc.ca/site/english/maps/environment/land/physio_torngat_mountains.jpg/image_view)

Mountain-valley breezes occur when the prevailing wind over a mountainous region is weak and there is marked heating and cooling, which occurs during the summer months. During the day the sun heats the floor and sides of the valley and warm air rises up the slopes and cool air is brought in from the valley. At nights, the mountains cool more quickly and the cool air heads down the slopes and through the valley [Gipe 2004]. These location specific winds can be a big attraction to developers but also a technical challenge.

Mountaintops can pierce air temperature inversions and experience the high winds that do not mix with the inverted air. These inversions are like giant lakes of stagnant air and the mountaintops can be viewed as islands on the lakes. Some mountain sites don't reach the extreme temperatures (rarely below -30^{o}C in the Yukon) of the surrounding lowlands due to temperature inversions [Maissan 2001].

Experience with wind monitoring programs in Scandinavia has shown the frequency of icing is more dependent on altitude then latitude [Laakso *et al* 2003].

2.7.5.2. Coastal Regions

Wind resources are typically high in coastal areas, where the water causes no impediment and there exists a greater temperature difference between land and water causing greater pressure differentials. The land heats and cools faster than water and, during the day, warms the air directly above it causing it to rise. The air over the cooler body of water rushes in to fill the void, resulting in a wind blowing inland during the day, while it blows in the opposite direction at night.

2.8. Isolated Small Wind Turbine Systems in Harsh Environments

National, international, professional and industrial organizations generally have best practices available for turbine manufacturing, installation and operation. Even though they seldom cover harsh environment considerations, these best practices are still a good place to start [BWEA 1994, Laakso *et al* 2005]. Most national and international standards are grossly inadequate when covering governing conditions in harsh environments [Laakso *et al* 2005]. There will never be an ideal wind turbine for every site and each system becomes a balance between various factors [Watson 1981].

2.8.1. Challenges

There are several challenges that stem from operating SWTs in harsh environments that would not generally need to be overcome at more moderate locations.

A correlation between higher wind speeds and increase LWT failure rates has been shown. The failures are more common in the generator, mechanical brake and yaw control than the rotor itself [Tavner *et al* 2006]. A challenge that stems directly from excessive winds is blade strike on the tower caused by flutter or severe coning. Generator burnout has been known to occur, especially when high winds mix with low temperatures producing a fast moving high-density body of air.

Icing is a danger as it creates aerodynamic imbalances on the rotor, which lead to increased fatigue and thrown ice. The economic risks include an increased capital cost for harsh environment modifications, increased downtime, decreased production, increased fatigue that can lead to premature failure, and increased maintenance costs [Laakso et al 2005].

Ice build up increases drag and decreases lift resulting in loss of power production. Table 2.3 below shows a rule of thumb for production losses due to icing. Specific values are more difficult to produce, as many parameters can be difficult to obtain. It should be noted that downtime is higher in remote sites [Laakso *et al* 2005, Tammelin et al 1997].

Table 2.2 – Rule of Thumb Production Loss Due to Icing

Frequency of Icing (days/year)	Annual Energy Loss (%)
< 1	Insignificant
1 – 10	Small
10 – 30	5 – 15%
30 – 60	15 – 25%
> 60	> 25%

In LWTs the gearbox and mechanical drives such as a variable pitch or yaw drive are most affected by cold temperatures [Laakso *et al* 2005]. Snow and moisture in the nacelle, freezing and damaging internal components should be avoided in both SWTs and LWTs to protect internal controls and mechanics.

While lightning is less common in regions that are exposed to harsh conditions, lightning strikes can still cause catastrophic failure in SWTs [Watson 1981]. Strike potential should be considered along with any mitigating technology if warranted by the risk.

According to [Bass and Weis 1981] system failures can be attributed to six basic causes: i) Inadequate design, ii) improper manufacturing, iii) inadequate quality control, iv) improper installation, v) improper maintenance and vi) inadequate instructions.

2.8.2. Operational Experience

Even slight icing can significantly decrease electrical production [Rong 1991], while heavy icing can stop a turbine completely. Glaze icing has caused overproduction, which shortens a turbine's life, due to delayed stall on passive pitch controlled turbines. Structural loads, caused by either aerodynamic or mass induced forces, increase with increased icing accumulation. Uneven icing, which can be exaggerated by ice shedding, causes even further loading and safety risks [Laakso *et al* 2003].

Low temperatures affect fiberglass, plastics, steel, lubricants, wires and most other manufacturing materials. Standard oil viscosity increases as temperature decreases, which can delay wind turbine startup and damage internals. Every piece of equipment must be assessed for flexibility and usability at extreme temperatures.

Manufacturers say that even wind turbines with cold weather packages should be stopped at temperatures below -30^{o}C. This is due in part to the increased air density that may cause damage to the turbine. Air density increases can result in generator overheating and gearbox and braking damage [Laakso *et al* 2003].

Experience with a 150 kW turbine in the Yukon has shown that the following were successful in harsh environments: winch up tower, low temperature steel, synthetic lubrications and internal heating systems controlled by thermostats. Some challenges that they experienced include the need for fully heated instrumentation (such as anemometers) and also keeping the blade heating strips, similar to one's illustrated in Figure 2.17, on all winter as opposed to being activated by an ice detector. The heating strips on the blades leading edge required about 0.5 W/in^{2}. When the six-inch wide heating strips were replaced with 12 inch ones, no specific production improvements were noticed. Icing build up was most significant on the leading edges and further out from the blade root. A noticeable improvement in production was found after 'painting' the blades with a black coloured low adhesion coating (*StaClean*). One-piece blades work better than two-piece blades and pitch regulation will enable the turbine to have a decent output under icing conditions [Maissan 2001].

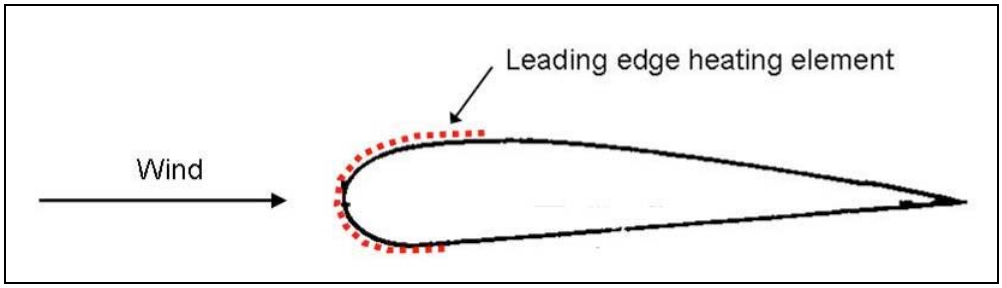

Figure 2.17 – Wind turbine blade profile with heating element

Cold weather packages largely mitigated many issues in Manitoba wind farms. All wind turbines have operating and standstill minimum temperatures and the use of cold weather packages typically drop both by 10^{o}C (to -30 and -40^{o}C respectively). A cold weather package can run 2.5 to 5% of the wind turbine's capital cost. Reduced give, or embrittlement, in steel components at lower temperatures can not only lead to steel failure but also increased stresses in other components, such as the blades, and induce micro-cracking [Manitoba Hydro 2004].

The lower temperature limit of a wind turbine is often governed by the qualities of steel and welding used [Laakso *et al* 2005].

2.8.3. Technical Mitigations for SWT Operation in Harsh Environments

There are two fundamental options when deciding on technical mitigations of ice accumulation. The first is a de-icing system that removes ice build up once it has occurred, while the other is an anti-icing system that prohibits the initial ice build up.

Anti-icing systems typically require 6 to 12% of the rated power capacity for turbines ranging from 1 kW to 220 kW in high icing environments, while de-icing systems would require more than the rated capacity [Laakso *et al* 2004].

Active protection is usually based on thermal systems many of which were developed in the mid 1990's [Laakso *et al* 2004]. On LWTs blade heating is the most common and proven method. This can range from heat tracing on the leading edge of the blades to carbon heating elements attached to the outer surface of the blade. In heavy icing conditions it is more effective to leave the heating elements on full time rather than trying to use them only during icing occurrences. Similarly some systems circulate hot air through the interior of the blade, which has been effective for light icing situations. Pneumatic systems, with inflatable membranes to literally blast the ice off the blade, have been found to be a relatively inexpensive way to combat heavy ice accumulation, however, there are inherent difficulties in pneumatic or chemical systems as experienced by the aircraft industry. Their operational experience on wind turbines is limited [Laakso *et al* 2003].

Passive ice protection can include black blades, such as those found on the Whisper 100 shown in Figure 2.18, and stick free surfaces to help prevent accumulation and ease shedding, however coatings and special ice phobic materials are not sufficient to prevent icing unless there is good exposure to sunlight, temperatures near zero and only light

icing [Tammelin et al 1998]. One suggestion is to use flexible blades that would help shed any ice as they flex but there is no published information on this.

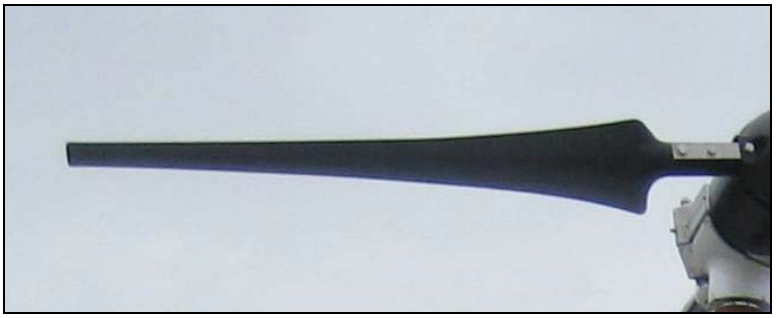

Figure 2.18 – Whisper 100 black blade

Other technical solutions include low temperature synthetic grease and oil and sealing of specific components. Extremely low temperatures have a great affect on a material's mechanical properties, unfortunately, there is little information about the properties of materials and lubricants with respect to wind turbines available. Most of the information is found in field reports [Laakso *et al* 2003]. Synthetic lubricants rated for low temperatures have been shown to be effective. Internal heating elements used to protect control electronics against moisture and condensation have also been used to some success.

Manufacturers usually offer a cold weather package. Testing in the National Wind Technology Center in the United States examined cyclic loading of wind turbine blade roots at ambient and cold temperatures (ranging down to -45 and -51 ^{o}C). Using 4140 steel root studs, a vinyl ester / E-glass laminate with an epoxy annulus to pot the root stud

inserts into the fiberglass, it was shown that each of the cold temperature tests exceeded the life of the ambient temperature [Laakso *et al* 2003].

Overspeed can be suppressed by pitch control but experience has shown this alone to be insufficient in mountainous areas and difficulties arise. A solution is to employ an electric load brake control for SWTs that connects immediately when a rotor revolution sensor detects increasing acceleration, giving pitching time to respond, at which time the load brake is disconnected [Ichikawa *et al* 2001].

3. Statistical Analysis

3.1. Introduction

Bell-Aliant, a regional telecommunications provider, operates 30 hilltop microwave relay stations throughout Labrador. As presented in the timeline in Figure 3.1, these relay stations were originally powered solely by continuously running diesel generators, with industrial scale battery banks put into use shortly thereafter. Arrays of photovoltaic cells were introduced to all feasible sites in the early 1990's.

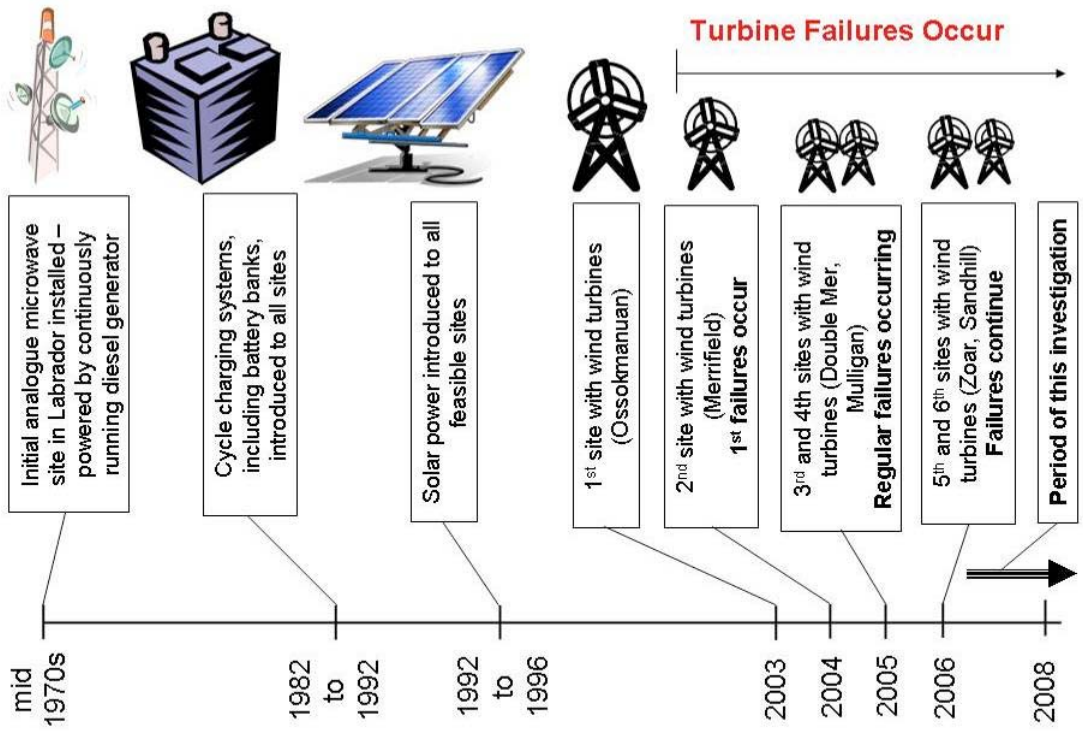

Figure 3.1 – Timeline for installations at Bell-Aliant sites in Labrador

In 2003 Bell-Aliant initiated their wind power program. Starting with just three turbines at a single site, within three years they expanded to six sites, which have complete wind-solar-diesel hybrid systems. There are 37 turbines in total throughout the six sites, all of which are Southwest Windpower's Whisper 100 model (WH100), shown in Figure 3.2.

Figure 3.2 – Southwest Windpower's Whisper 100

The motives for introducing wind power at these off-grid sites are: i) the prospect of improving battery life by reducing deep cycling that occurs at night [Spiers 1995] and ii) the high cost and environmental risk of traditional diesel, which has to be brought to each site via helicopter. The increase in availability and decrease in cost of micro wind energy conversion systems that has occurred over the past decade have facilitated this transition.

Broadly speaking, the prevailing conditions at these six sites are severe. Temperatures often fall below -30^{o}C and there are frequent strong and turbulent winds, in excess of 150 km/hour. Atmospheric icing, such as rime or glaze icing, is prevalent during the year, except for a few short summer months. At some of the Bell-Aliant operated sites over two meters of rime icing can accumulate on the communication tower [Bruneau 2006]. These meteorological conditions create challenges for the effective operation of micro turbines.

It is important to be reminded that these hilltop sites, an example of which is shown in Figure 3.3, were not selected for optimal wind or solar power production but for optimal microwave transmission. Each of the six sites in question have a small wind farm, a photovoltaic array, a microwave relay tower, and one or two diesel generators and a battery bank stored indoors with the switchgear and electronics.

Figure 3.3 – Mulligan, one of Bell-Aliant's hilltop telecommunication sites

3.2. Objective and Hypothesis

There have been several mechanical failures of turbines at these six sites leading to an increase in costly maintenance trips. The main objective of this statistical analysis is to objectively identify the factors contributing to the risk of failure and develop a quantitative tool for evaluating site suitability for new installations. The analysis is confined to Labrador and the evaluation is based upon turbine output records at unmanned sites.

The hypothesis is that the regressions will show that for specific ranges of prevailing meteorological conditions in combination with specific site characteristics, turbines will fail, often catastrophically, and therefore these conditions should be avoided or mitigated. Present practice is somewhat ad hoc and assessments for site suitability for WECS are highly subjective. Thus the intended result of this work is to improve reliability and confidence in decision making.

This work aims to give Bell-Aliant a rational basis for continuing or discontinuing their wind program as well as give direction for new, industry relevant, research. Overall, for proposed installations, Bell-Aliant would like to improve power production, increase the longevity of the turbines and reduce maintenance requirements.

3.3. Data Assembly

Data describing a wide range of meteorological and geographic conditions for six sites over a 7-month operation record was collected and tabulated. A 14-month operation record became available later in the program providing for a broader investigation. For each timeframe a multi-variable regression analysis was undertaken to isolate and quantify the influence of any or all variables on the dependent variable, machine production. More specifically, the dependent variable is the daily cumulative power output for each unit (available in Appendix A), which is assumed to reflect turbine status, though visual confirmation was not possible. From the existing records it was necessary to define a machine failure as production stoppage over several days that could not be explained by low winds, maintenance visits or diesel generator starts, which override the wind turbine power production. Daily production data was analyzed in conjunction with recorded maintenance history and anecdotal operation data from Bell-Aliant engineers.

Some failures could be attributed to severe icing, causing a temporary stoppage of the rotor, while others were of a catastrophic nature, requiring the replacement of the entire unit. The most common catastrophic failure occurred during excessive winds and is manifested in the fracture and parting of the nacelle, which leads to the rotor and generator falling ten meters to the ground. The causes and nature of this failure mechanism is discussed in depth in *Chapter 4*.

3.4. Preliminary Statistical Analysis

Bell-Aliant's most comprehensive monitoring system was implemented near the end of October 2006 and a preliminary analysis was conducted at the beginning of June 2007. This was undertaken in order to give some initial direction for further analysis in the research program. Minitab 14 was used for all statistical analyses as it is able to perform a wide range of statistical operations, is readily available and user friendly.

3.4.1. Parameters

The following were examined as control parameters for the preliminary analysis: The daily power output of each turbine; geographical information about each hilltop site; meteorological history of each site; Bell-Aliant maintenance history and; Bell-Aliant operational history.

Due to the large amount of data within each of the above categories several simplifications were made:

1. The failure rate was taken as the dependent variable and was defined as the average number of failures per turbine per site, over the time period in question (seven months in this case). This was done to ensure that sites with three turbines had the same influence on the final results as sites with eight turbines. Also, as there was an innately high cross-correlation between dependent variables (i.e. for

each individual site all of the independent parameters were the same, even though the frequency of each turbine's failure was not) individual turbines could not be singled out.

2. The extremes of regional weather data were considered as opposed to a day-by-day analysis due to the inconsistencies in the availability of certain data for each site.
3. The meteorological data for each site was also extrapolated from nearby airports, which were typically located within 50 km of each site.

The control parameter values, presented in Table 3.1, were taken from geographical information and measured meteorological data. Specific geographical parameters included elevation in meters, latitude in degrees, proximity to the ocean in kilometers and degree of surrounding area covered by water; assigned a dimensionless factor between one and ten based on the percentage of surrounding surface area covered by water. Measured meteorological data included minimum regional temperatures in Kelvin, maximum wind gust speeds in kilometers per hour and maximum daily precipitation levels in millimeters.

Variables such as latitude, elevation and distance to major sources of water were included in the study as they may represent varying meteorological conditions that could not be captured using *in situ* measurements or site specific raw data, which was limited.

Table 3.1 – Site Specific Parameter and Average Failure Information for Preliminary Analysis

Parameter	Units	Labrador Sites with Wind Turbines					
		Double Mer	**Flower Bay**	**Mulligan**	**Zoar**	**Sand Hill**	**Ossok-manuan**
Average Failures	*over 7 months*	*9*	*7.17*	*5.2*	*8.33*	*5.25*	*5*
Elevation	m	717	415	357	322	631	620
Latitude	Degrees	54.2167	55.8194	53.8617	56.1931	53.2392	53.4961
Distance to Water	See above	6	0	4	0	6	4
Distance to Ocean	km	135	15	160	5	50	420
Regional Max Gust	km/hr	96	107	85	109	83	69.5
Regional Min Temp	K	247.9	249.3	246.6	248.6	251.2	241.7
Regional Max Precip	mm	18.8	15.6	22	43.2	59.4	24.6

The data spanned a seven-month period stretching from October 28th, 2006 to June 6th, 2007, which was the range of available, consistent and relatively complete data sets at the time of analysis.

3.4.2. Correlations

A primary statistical analysis was completed by determining the individual correlations between factors and the response variable. The results are displayed in Table 3.2.

Table 3.2 – Individual Variable Correlations for Preliminary Analysis

Factor correlated with Failure Rate	r	p-value
Latitude	+ 0.663	0.151
Elevation	- 0.005	0.992
Distance to Water	- 0.286	0.582
Distance to Ocean	- 0.491	0.323
Regional Max Gust Speed	+ 0.789	0.062
Regional Max Precipitation	+ 0.330	0.552
Regional Min Temperature	- 0.215	0.682

Figure 3.4 reflects the relative importance of individual variables on the failure rate.

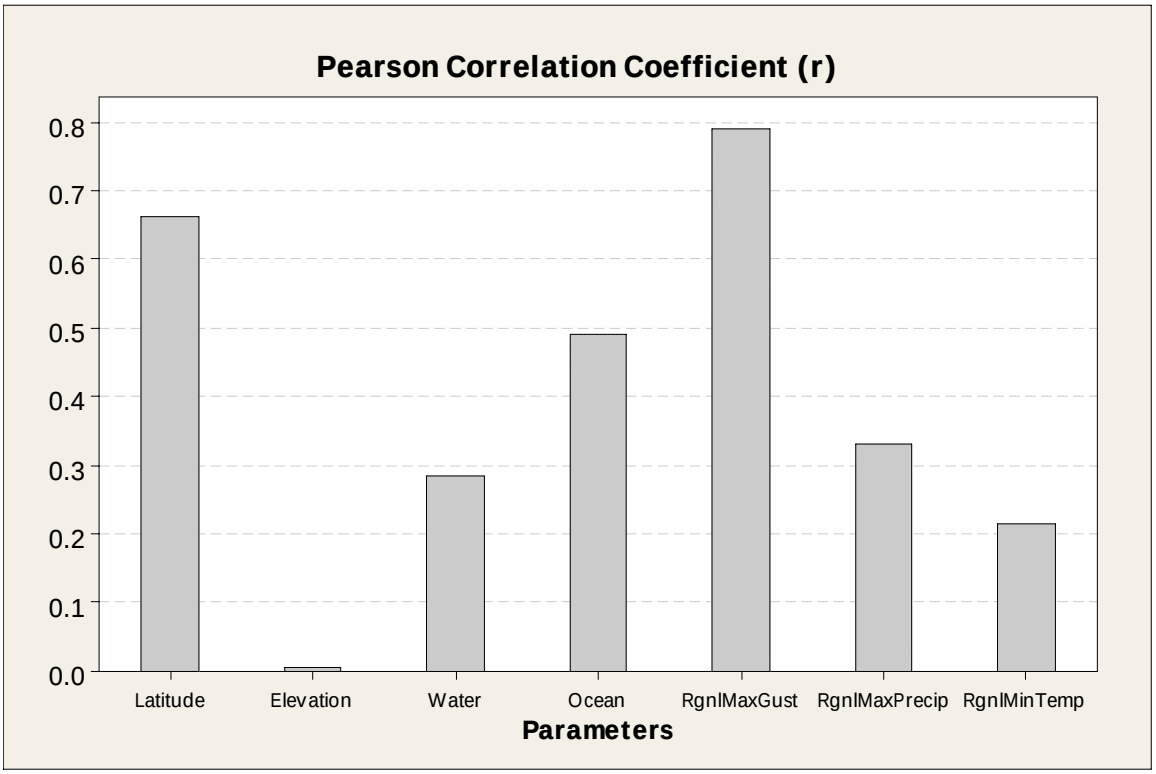

Figure 3.4 – Correlation strength of independent variables for preliminary analysis

The Pearson Coefficient, r, is a common measure of correlation between two variables, with a value of 0 indicating no correlation and values of +1 and -1 indicating perfect

positive and negative correlations respectively. The p-value displays the probability that the correlation value was due to chance and needs to be below 0.05 (5%) to be considered statistically significant [Allen 2006].

Regional Max Gust Speed is most highly correlated with failure, with a 6.2% chance that the correlation is due to random noise. While this is a relatively strong correlation, it does not fully represent all of the turbine failures that occur. However, if one were to check only a single variable for the suitability of a site, the max gust speed would be the best option.

3.4.3. Regressional Analysis of Site Parameters

As there are only six sites with independent data sets, the regression model is statistically constrained to four independent variables. Of all the regression models found several were statistically significant. However only one model met the other main criteria for validity: a high predictive R^2 value, relatively low cross-correlation between independent variables and, the appearance of being based in reality.

The regression Equation 3.1, with units as shown, was produced using multivariable regressional analysis in Minitab 14.

$$\#F = +3.31 * L + 1.07 * D_W - 0.113 * T_{\min} + 0.00173 * E_L - 150 \qquad [3.1]$$

where,

#F = Number of Average Failures over 7 month period

L = Latitude

D_W = Distance to Water

T_{min} = Minimum Regional Temperature

E_L = Elevation

Figure 3.5 is a graphical representation of the relative importance of independent variables. This tells us that Latitude has the largest influence on failure rate, followed by the Distance to Water, Min Regional Temperature and Elevation.

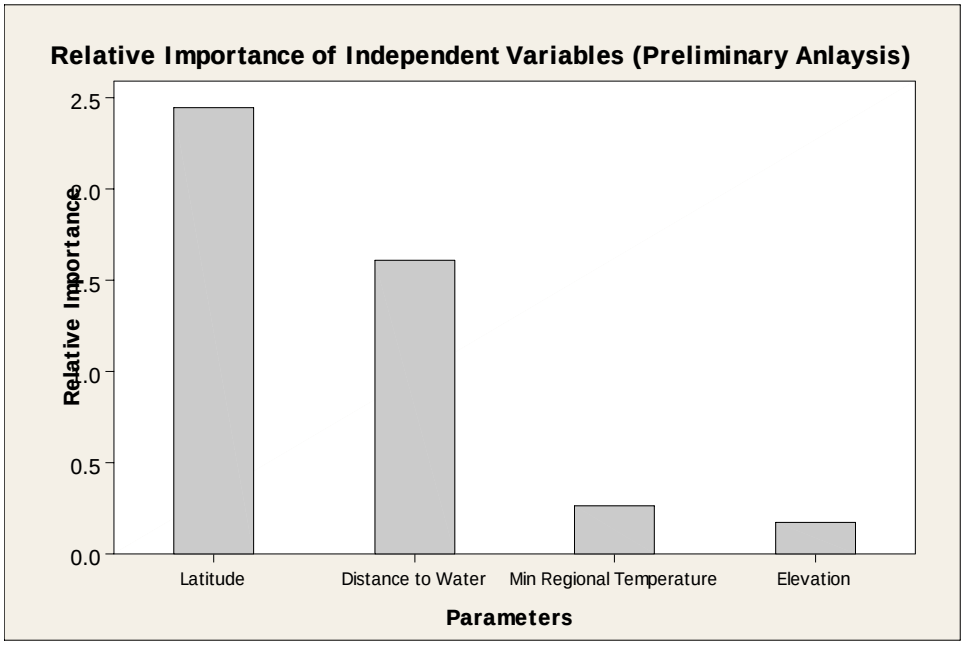

Figure 3.5 – Relative importance of independent variables for preliminary analysis

Equation 3.1 tells us that the failure rate increases with higher latitudes, greater distance from water sources, lower regional temperatures and higher altitudes. The predictive R^2 value for this model was 99.99% with a p-value of 0.002. Predictive R^2 refers to the data fit and stability (i.e. if any five data points were used to predict the sixth, the results would correlate with an R^2 value of 99.99%).

As with any statistical analysis, this model illustrates what is happening but is unable to give us any indication as to why it is happening. Even though the predictive R^2 and p-values are high, this model is limited in its predictive ability. This is due to the low number of data points used in the analysis (six data values for responses, one average for each site).

3.5. Extended Statistical Analysis

Due to the low number of data points available, the utility of the preliminary analysis results is somewhat uncertain and so an extended, fourteen month statistical analysis was undertaken. This was in an effort to clarify the results found in the preliminary analysis using expanded meteorological and operational data, as it became available.

3.5.1. Parameters

Updated versions of the control parameter values from the seven-month analyses, with the same units, are presented in Table 3.3 along with North American Regional Reanalysis (NARR) data [Mesinger *et al* 2006]. From the NARR data, selected parameters (*NARR acronym*, units) include specific humidity (*spfh10m*, kg/kg), temperature (*tmp10m*, K), wind speed (*ugrd10m* and *vgrd10m*, m/s), precipitation (*apcpsfc*, kg/m^2), low-level cloud cover (*lcdclcl*, %), surface pressure (*pressfc*, Pa) and turbulent kinetic energy (*tkehlev1*, J/kg). It is important to note that 'wind speed' used in this study represents the maximum of three-hour averages throughout the 18 month time frame and not simply average wind speed values.

The data spanned a 14-month period stretching from October 28th, 2006 to December 28th, 2007, which was selected for the availability and consistency of both dependent and independent variables. Statistical summaries of the meteorological and NARR data were included in order to allow straightforward comparison of each parameter, while 34 of the installed turbines provided useful production data for inclusion in the study.

Table 3.3 – Site Specific Parameter and Average Failure Information for Extended Analysis

Parameter	Units	Labrador Sites with Wind Turbines					
		Double Mer	**Flower Bay**	**Mulligan**	**Zoar**	**Sand Hill**	**Ossok-manuan**
Average Failures	*over 14 months*	*16.6*	*10.7*	*8.6*	*10.3*	*12.1*	*9*
Elevation	m	717	415	357	322	631	620
Latitude	Degrees	54.2167	55.8194	53.8617	56.1931	53.2392	53.4961
Distance to Water	See above	6	0	4	0	6	4
Distance to Ocean	km	135	15	160	5	50	420
Average Humidity	kg/kg	0.00342	0.00326	0.00352	0.00326	0.00374	0.00343
Minimum Temperature	K	242.19	243.36	240.21	242.81	244.5	239.04
Max 3-hr Average Wind Speed	m/s	17.13	15.93	13.54	14.82	17.03	14.88
Total Precipitation	Kg/m^2	3252	5374	7492	8043	6597	3697
Average Low Level Cloud Cover	%	53.84	51.3	57.68	53.24	52.84	57.16
Atmospheric Pressure	Pa	97056	97946	994400	100013	97930	94114
Turbulent Kinetic Energy	J/kg	10.57	9.36	7	8.6	10.76	7.73
Regional Max Gust Speed	km/hr	134.5	152	117	95	120	69.5
Regional Min Temperature	K	242.85	245.65	240.05	242.55	245.45	235
Regional Max Precipitation	mm	30.45	22.1	38.8	43.2	59.4	33.1

3.5.2. Correlations

The correlations between average turbine failure rate and individual independent variables are given in Table 3.4.

Table 3.4 – Independent Variable Correlations for Extended Analysis

Parameter	r	p
Latitude	-0.054	0.919
Elevation	0.661	0.153
Distance to Water	0.458	0.361
Distance to Ocean	-0.261	0.617
Humidity	0.087	0.87
Temperature	0.438	0.385
Max 3-hr Wind Speed	**0.831**	**0.04**
Precipitation	-0.506	0.306
Low Level Cloud Cover	-0.444	0.377
Atmospheric Pressure	-0.438	0.385
Turbulent Kinetic Energy	**0.825**	**0.043**
Regional Max Gust Speed	0.48	0.335
Regional Max Precipitation	0.445	0.376
Regional Min Temperature	-0.051	0.924

It is evident that there are two strong and statistically significant correlations shown in bold in Table 3.4; they are wind speed and turbulent kinetic energy. These correlations are represented graphically in Figures 3.6, 3.7 and 3.8. Elevation also has a relatively strong correlation with turbine failure.

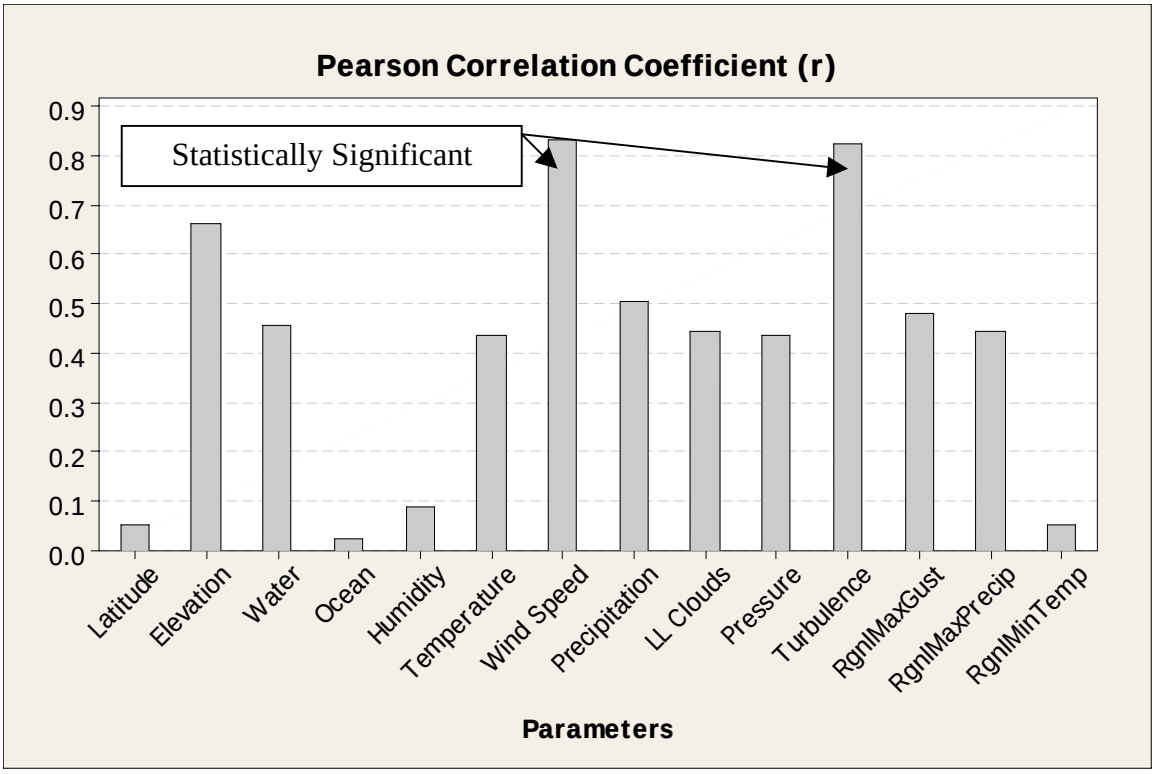

Figure 3.6 – Correlation strength of independent variables for extended analysis

Figure 3.6 shows the correlation strength of individual variables with failure rate. Figures 3.7 and 3.8 show how the failure rate varied with maximum 3-hour wind speed and turbulent kinetic energy respectively.

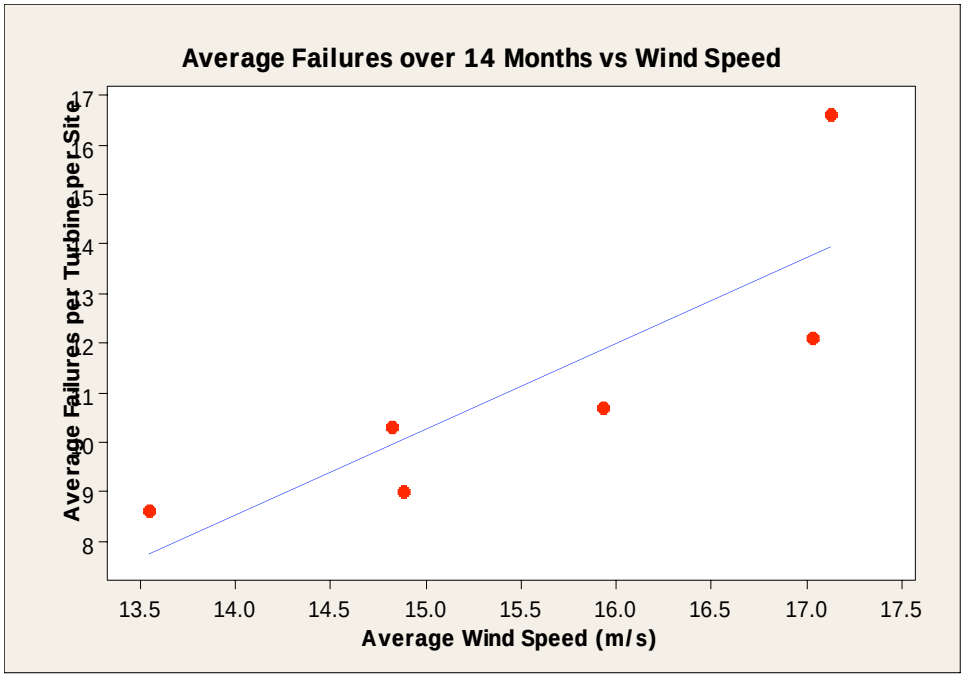

Figure 3.7 – Scatterplot of average turbine failure vs. max 3-hr average wind speed

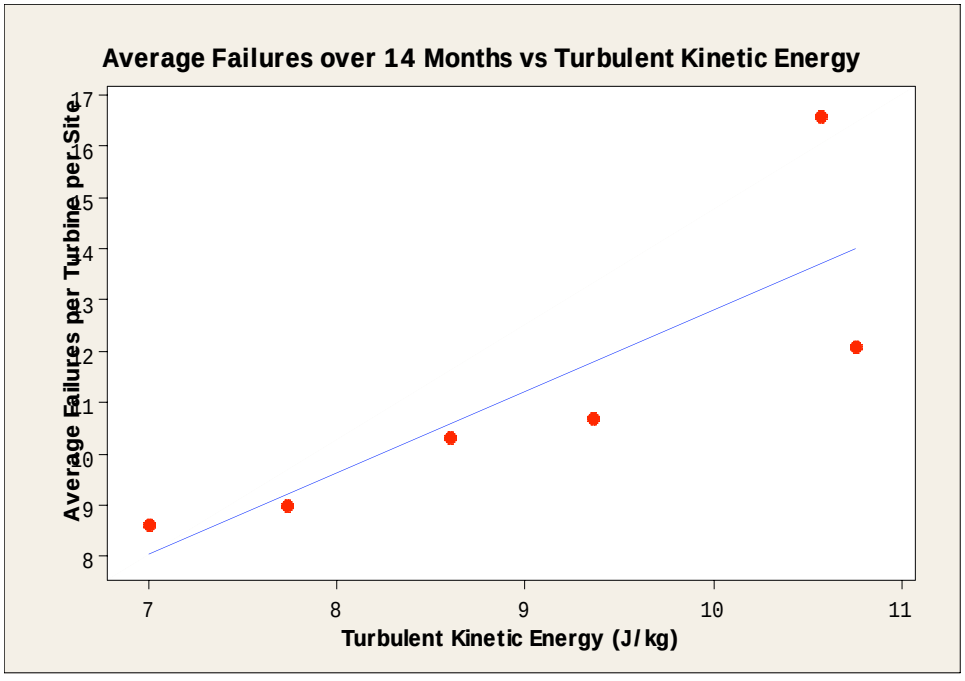

Figure 3.8 – Scatterplot of average turbine failure vs. turbulent kinetic energy

3.5.3. Regressional Analysis of Site Parameters

As there are only six sites, corresponding to each of the six data points, the regression model is statistically constrained to four independent variables, similar to the preliminary statistical analysis. However, due to the large array of dependent variables with which to work, many more models needed to be explored in order to determine which was the most suitable. Of the many regression models developed only three were determined to be statistically significant. Of these three, only one met the two other statistical criteria for validity, which are a high predictive R^2 value and relatively low cross-correlation between independent variables. The regression Equation 3.3 is shown below. The predictive R^2 and p-value for this equation are respectively 99.26% and 0.007.

$$\#F = +0.0560 * E_L - 0.0384 * D_O - 3.95 * V_W - 10479 * H + 85.1 \qquad [3.2]$$

where,

#F = Number of Average Failures over 14 month period

E_L = Elevation (m)

D_O = Distance to Ocean (km)

V_W = Average Wind Speed (m/s)

H = Specific Humidity (kg/kg)

Equation 3.3 means that failures increase with increasing elevation, decreasing distance to the ocean, decreasing wind speed and decreasing humidity. Figure 3.9 is a graphical

representation of the relative importance of independent variables. This tells us that Elevation has the highest influence on failure rate, followed by Distance to the Ocean, Wind Speed and Humidity.

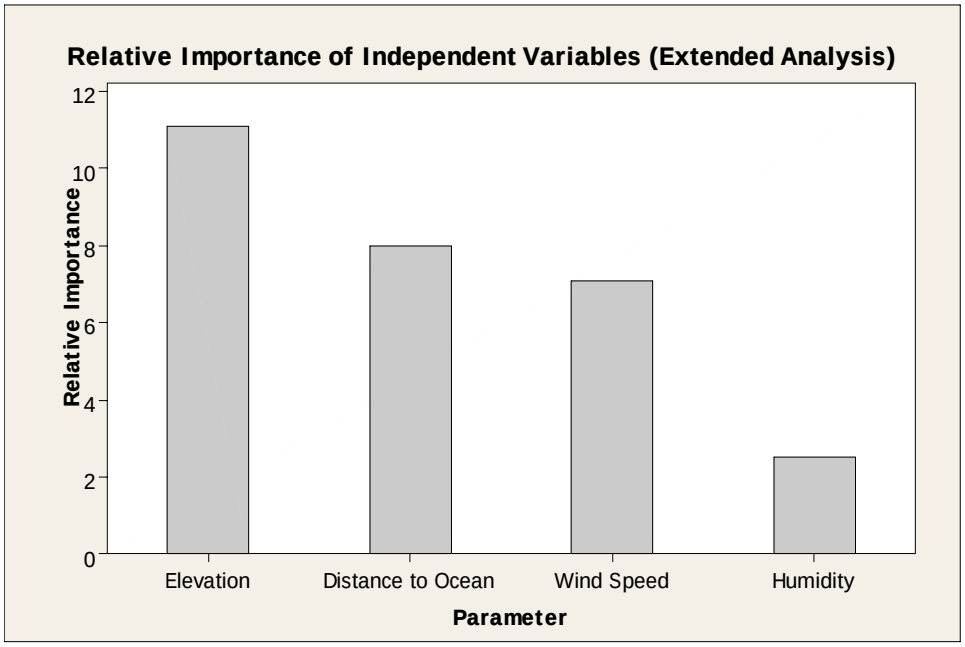

Figure 3.9 – Relative importance of independent variables for extended analysis

3.6. Discussion of Results

Although the extended analyses model fits each of the statistical requirements for validity it does not reflect realistic relationships. One can see from Equation 3.2 that wind speed appears to have a negative effect on failure rate, in the sense that as wind speed increases, failure rate decreases. This result is counter-intuitive and contradicts the correlation of wind speed to turbine failure, which is strongly and significantly positive.

To illustrate the point consider two extreme, although unlikely, situations. First of all, if there were a mean wind speed of zero there would be no turbine failures as defined above. However, if there were an extreme arbitrary mean wind speed of 500 km/hr almost nothing would be able to survive. As such, the author deduced that the above model is not an accurate representation of factors contributing to turbine failure.

In order to produce a model that is valid both statistically and in reality, improved data collection procedures and extended time frames are required.

3.7. Recommendations for Data Collection

In an ideal situation, a continuous record of site-specific meteorological conditions, continuous visual records, and turbine specific data loggers would produce the most useful and relevant information for regression. More feasible data collection recommendations are outlined below.

The collection of site-specific wind speed and direction throughout the year would be an asset. Current wind speed data is only an approximation of the actual conditions at the hilltop sites. The ‘wind speed’ independent variable (NARR data) is an approximate average covering a 32 kilometer square [Mesinger *et al* 2006], based on meteorological model output. The ‘maximum wind gust speed’ is taken directly from airports, typically within 50 kilometers of respective sites. As each of these sites sits on a hilltop, one can

assume that local topography plays an important role in mean wind speed and gust strength. A similar argument can be made for local temperature measurements.

A record of the location of each turbine within each site would also be useful. As turbines at any single site fail on different occasions, applying the same control parameters to each will always result in error within a statistical model. Locations relative to the edge of a steep incline and to prevailing wind direction as well as its position within the array are all potentially important considerations.

Similar meteorological stations and local situational data should also be collected and examined for sites under consideration for turbine implementation.

Detailed records of field modifications performed on specific turbines should be kept. Other maintenance records of each turbine repaired or replaced, including date, thorough photographic evidence and a note of possible weather conditions at the time of failure would provide further insight.

Consistent and reliable daily power production and diesel start data would help reduce uncertainty in the analysis. Clear and reliable daily power production data is critical to developing a useful model as it is used to determine the only dependent variable in the study: turbine failure.

3.8. Conclusions from Parametric Regression Analysis

There are strong correlations indicating that higher wind speed and turbulent kinetic energy in the atmosphere have a detrimental effect to the operation of micro wind turbines at Bell-Aliant's Labrador sites. However these parameters do not fully explain all of the turbine failures. A multi-variable regression analysis produced a model that, while statistically valid, was inconclusive.

A list of parameters required for an effective and useful regression analysis have been identified. These include site-specific meteorological data, individual turbine locations relative to the array and surrounding topography, detailed maintenance records and reliable, consistent power production data. The author believes that the stated objective of developing a quantitative tool for evaluating site suitability will be achieved once relevant data has been captured.

This chapter has provided a better understanding of the significant environmental factors that contribute to failures at a given site. The focus of the next chapter is a detailed examination of the most frequently occurring catastrophic failure mechanism. The objective of this is to find the root cause of the failures and thus direct subsequent work to be used as a guide for mitigating change and improving performance.

4. Turbine Failure Analysis

4.1. Introduction

Through personal communication with Bell-Aliant service technicians it is known from routine maintenance visits that ice build-up has often caused a decrease or halt in electrical production of the turbines, though a combination of the wind and solar irradiation usually free the rotor of ice within a few days. However, there is a common structural failure of Southwest Windpower's Whisper 100 (WH100) wind turbine that is catastrophic and irreversible. Bell-Aliant made available for study five broken nacelles along with one still intact unit. The failures all appeared identical: the cast aluminum nacelle was fractured along its smallest cross section, as shown in Figure 4.1.

In this chapter the cause of the failure is explored though analysis of the surviving fragments. This approach is necessitated by the absence of any witness or video recording of failure events or simultaneous meteorological conditions.

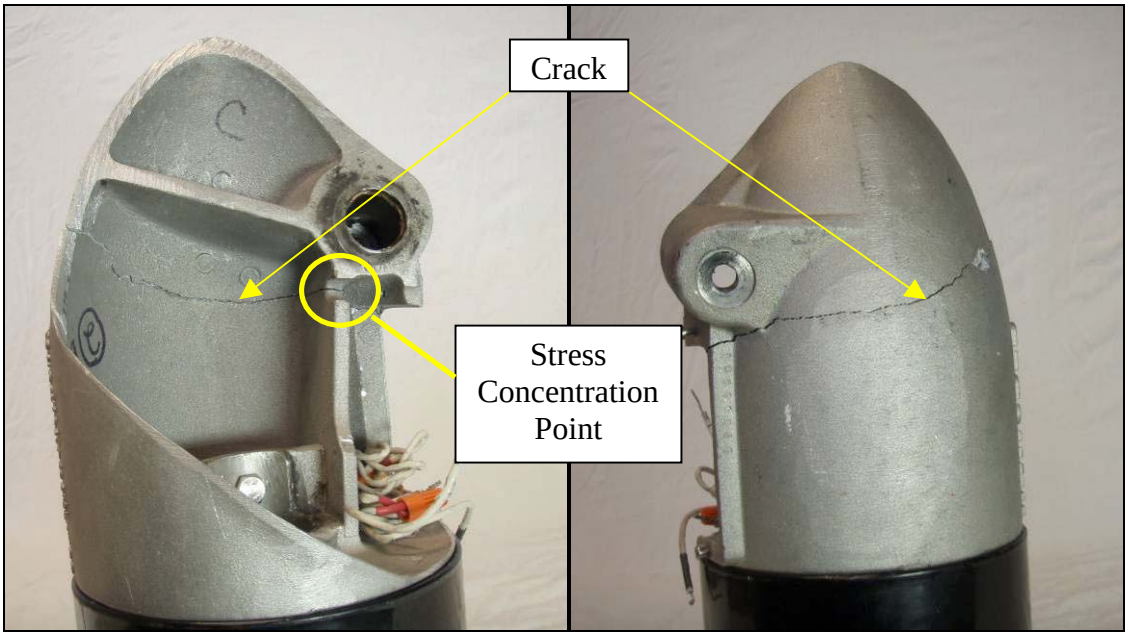

Figure 4.1 – Catastrophic cracking of the WH100 and stress concentration point

4.2. The Angled Furling Overspeed Protection Mechanism

4.2.1. Furling Motion

As discussed in Chapter 2, furling is a common overspeed protection mechanism for small turbines. The WH100 uses an angled furling mechanism shown in Figure 4.2. As the wind exerts increasing force on the turbine rotor this force is transferred to the top portion of the nacelle, which is attached to the bottom portion by means of an off-center, off-vertical pivot. If the force exceeds a certain level the top portion begins to furl, or rotate, about this pivot up to a maximum extent of approximately 65^{o}. The furling extent increases and decreases with the increasing and decreasing force of the wind respectively. At the two extremes of the furling action (full furl at 65^{o} and no furl at 0^{o}) the aluminum

casting of the top portion makes contact with square rubber stops on the bottom portion to prevent further furling or unfurling.

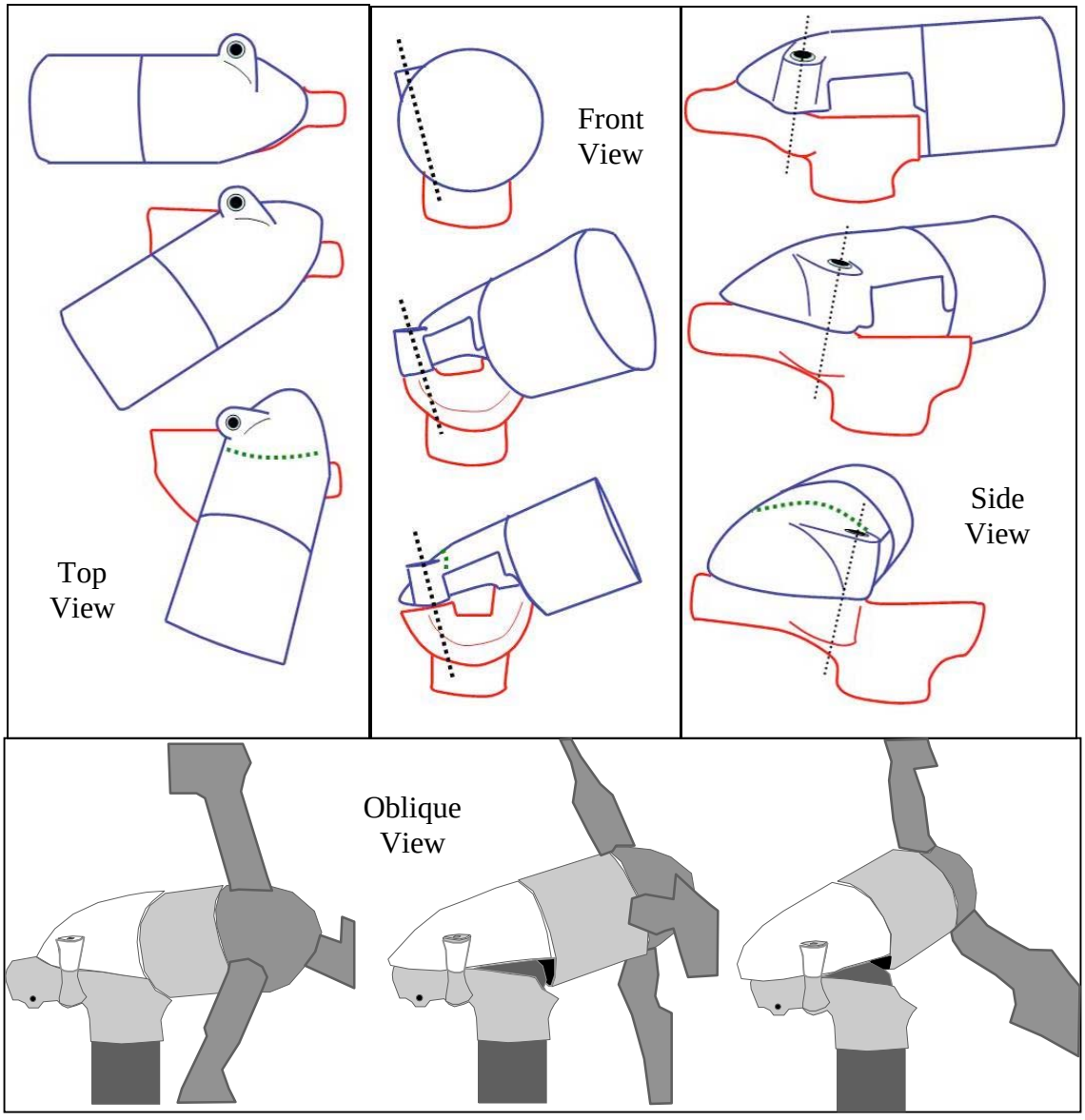

Figure 4.2 – Furling motion of the WH100

4.2.2. Points of Contact

Figure 4.3 illustrates the two points on the top (rotor) portion of the nacelle that come into contact with the rubber stops on the bottom (pole-mounted) portion – one point during the full (maximum) furling extent and one in the return (default) furling position. In both situations a stiff rubber pad on the bottom portion of the nacelle comes in contact with the painted aluminum casting on the top portion. By observation and deduction it is highly probable that fracture occurred while the split unit was in contact at one of these points, possibly when the turbine was in full furl position or in the non-furled position. Whether impact forces or quasi-steady loads were responsible is unclear.

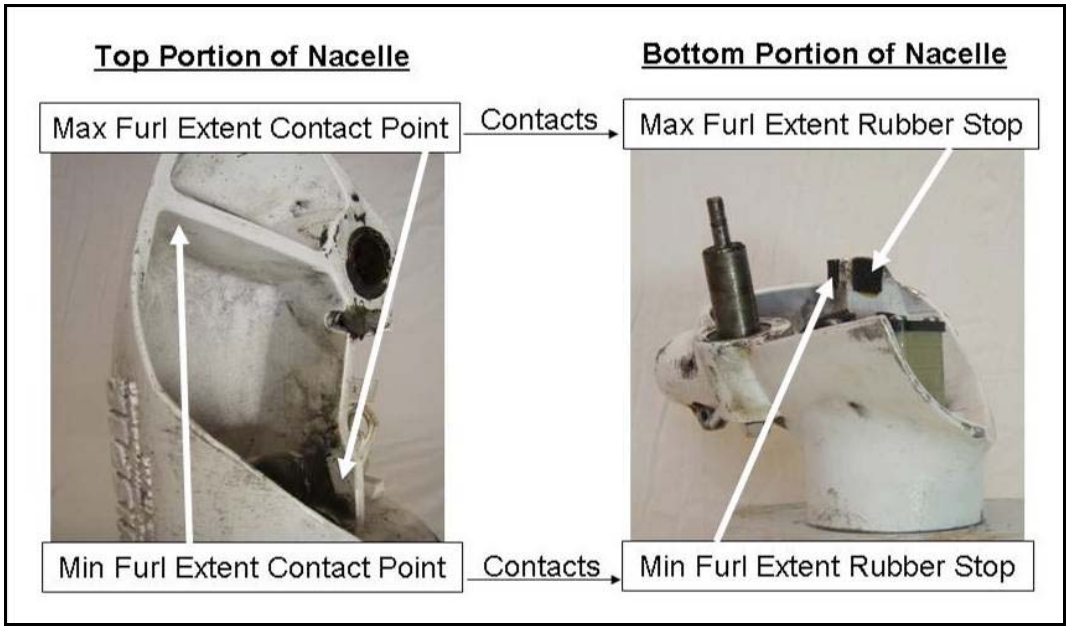

Figure 4.3 – Points of impact during furling on the nacelle

Once the catastrophic failure became commonplace, Bell-Aliant replaced the original rubber stops with ones whose elastic properties were shown to be acceptable at temperatures near -40^{o}C. This was in an effort to increase the energy absorption of the stops at low temperatures, as it was believed that the elasticity of the original stops was a major contributing factor in the failures. No significant reduction in failures was noticed.

4.3. Failure Consistency

The fracture pattern and pathway appear to be similar for the five units, as may be expected to result from common loading, fabrication and failure mechanism characteristics. The fractures were compared by three means: the first is the mass of each nacelle portion; the second method is the comparison of each turbine's fracture path; the third is the nature of the fracture surface.

The mass of the top portion of the intact nacelle (i.e. nacelle #1), visible in Figure 4.4, not including the blades, hub or connections, is 14.146 kg.

Figure 4.4 – An intact nacelle

Figure 4.5 shows the five broken nacelles available for study, with the respective masses, which are all within 5% of each other (Table 4.1). Part of the difference in mass can be accounted for the by the varying amounts of paint and grease on respective pieces while the remainder is due to the variations in the fracture line, shown in Figure 4.5. The minor differences in the fracture path and pattern are likely due to microscopic defects produced during the casting process. A less likely cause is the differences in the loading conditions at the time of failure.

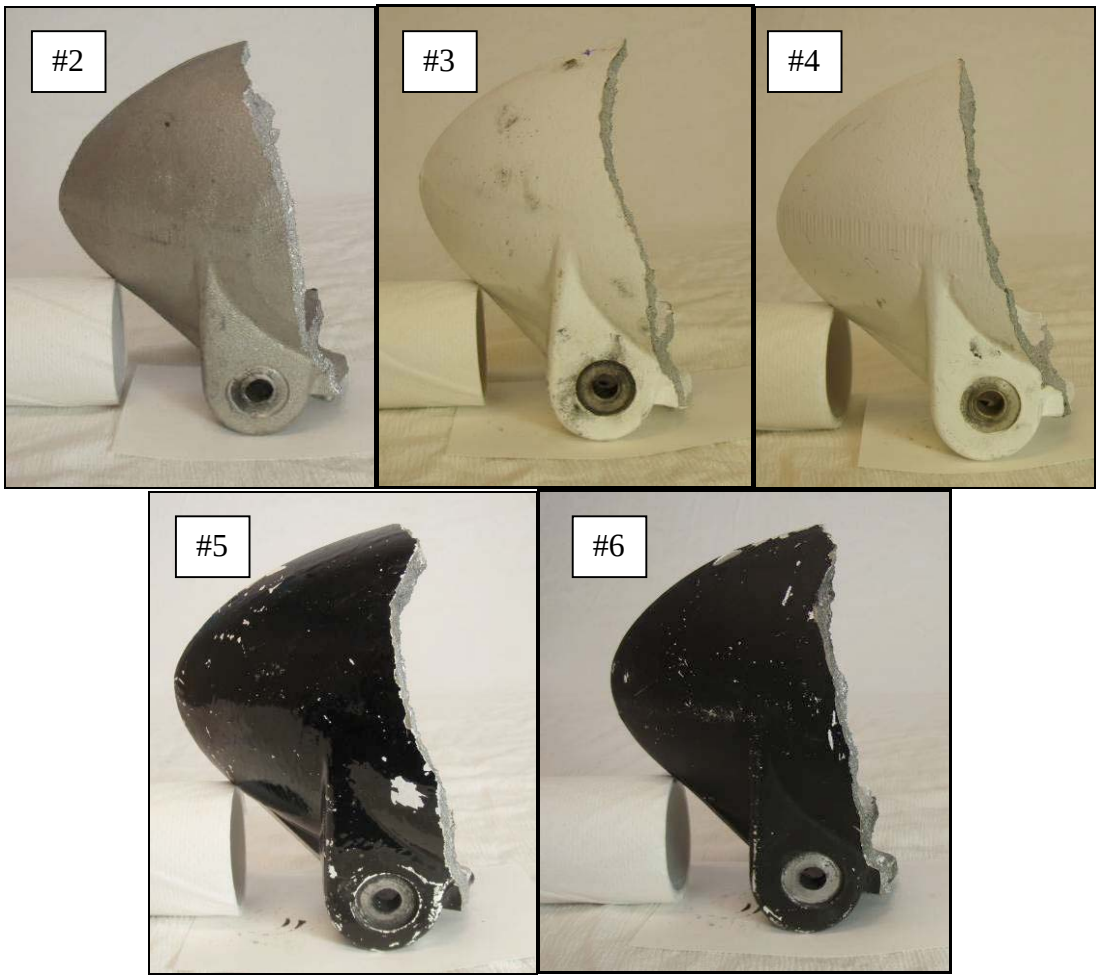

Figure 4.5 – Pieces of broken nacelles, with corresponding masses listed in Table 4.1

Table 4.1 – Nacelle Part Mass

Nacelle Number	Mass [kg]
2	0.733
3	0.723
4	0.711
5	0.742
6	0.729

Examination of the fracture surface, normal to the cast surface, reveals that each of the expected crack initiation points have a relatively even and flat surface, as indicated by the white arrow in Figure 4.6. As the paths of the fracture surfaces progress to the opposite side of the nacelles the fracture surfaces becomes less flat, often skewing to angles greater than 45^{o}, as seen in Figure 4.7, and also less consistent with each other. The cracks begin to follow the path of least resistance, unique to individual nacelles by way of unavoidable casting defects. As such, there is no indication that these five nacelles failed by different means.

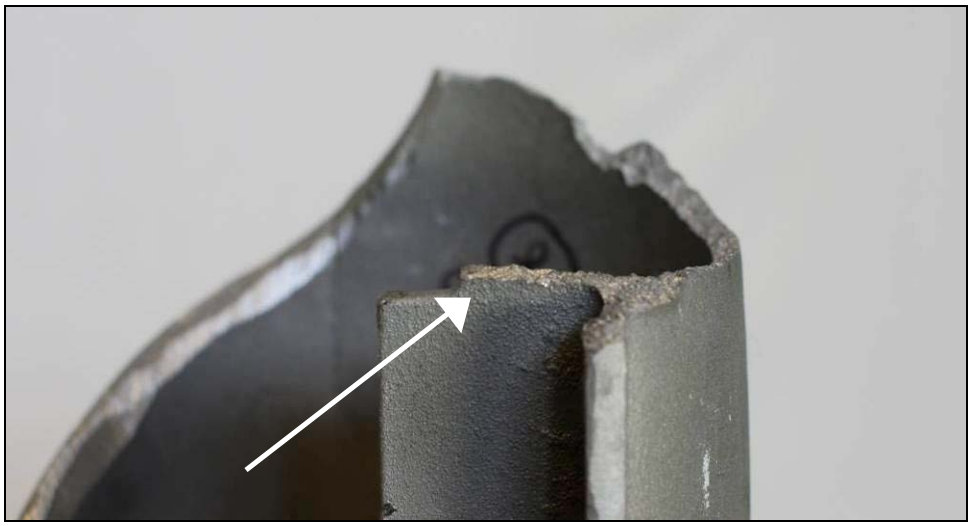

Figure 4.6 – Flat fracture surface

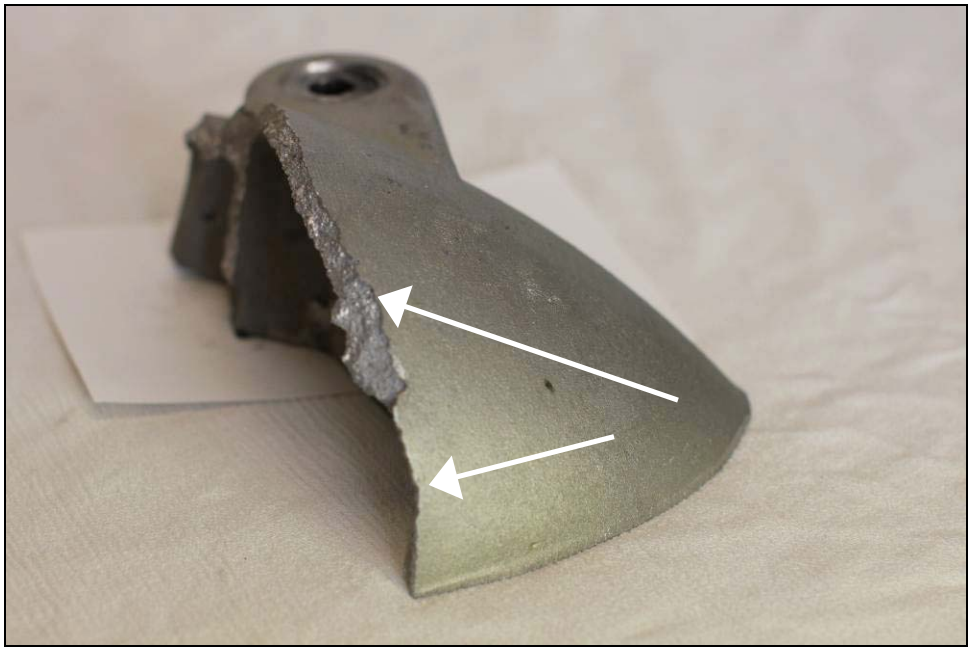

Figure 4.7 – Skewed fracture surface

4.4. Crack Initiation

There may be the tendency to think that the fracture occurred upon returning to the unfurled position due to the proximity of the impact point to the fracture line. This is unlikely as the nature of the fracture near the stress concentration point (discussed in *Section 4.4.1*) is more uniform across the five nacelles than at the opposite side of the turbine, indicating this to be the starting point, with the balance of the failure propagating from this point in a tearing and twisting motion.

The location of the furling impact point with respect to the stress concentration thus indicates the likely scenarios: a strong gust causes the turbine to furl at a high speed

causing an impact strong enough to initiate a crack, or, excessive winds on the machine while in the fully furled position create stresses beyond the resistance limits.

4.4.1. Nacelle Design

A notch in the casting introduced by the manufacturer for wire clearance is the site of all crack initiation, as identified in Figure 4.1 and Figure 4.8. This notch was introduced into the nacelle design when the WH100 was modified to include field voltage control. The notch is the pathway for the wires to access the electrical connections that lead down the tower.

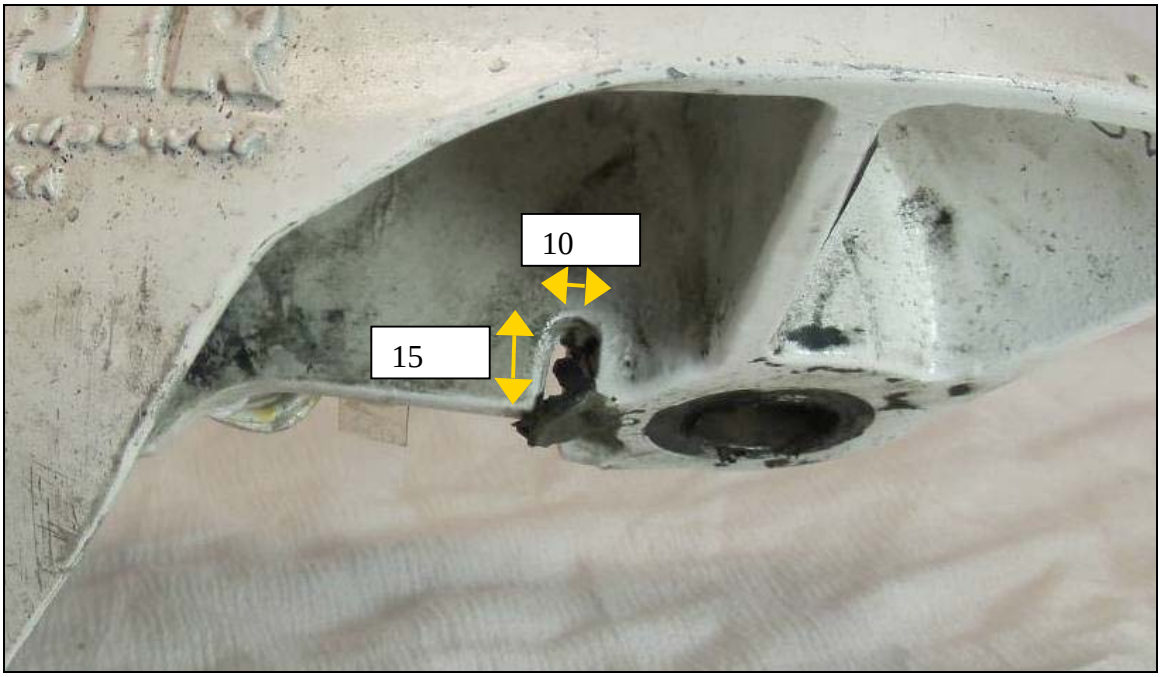

Figure 4.8 – Close up of the notch of an intact WH100 nacelle

This notch was examined to determine the potential for stress concentration according to Equation 4.1.

$$Stress.Concentration.Factor = 1 + 2\frac{a}{b} \qquad [4.1]$$

It can be shown that when ‘a’ is the depth of the notch (15 mm) and ‘b’ is half the width (5 mm) a stress concentration factor of ‘7’ is produced. This means that the stresses that are induced in this part of the nacelle are seven times greater, and thus seven times more prone to failure, than if the notch was absent.

4.5. Crack Propagation

Of the three nacelle bases available for study, shown in Figure 4.9, the furling rubber stops on two of the broken nacelles were missing (middle and right), while the third, belonging to an intact nacelle (left), remained firmly attached. It is possible that the force of the catastrophic furling incident caused the rubber stop to become dislodged from its position in two of the three units shown in Figure 4.9 and indicated by the arrows. Alternatively, one impact may have dislodged the rubber stop and the next significant furling occurrence could have initiated the fracture. The latter is unlikely as there are no apparent signs of impact following the removal of the stop. Thus it is believed that after the crack is initiated the heavy generator continues to pivot around the rubber stop and

the crack propagates until complete failure occurs. Described in this way it maybe said to be a flexural failure.

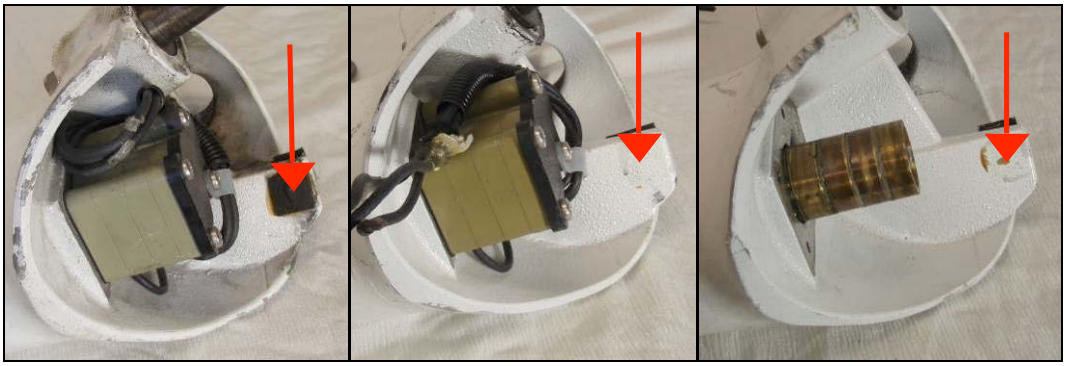

Figure 4.9 – Three nacelle bottom portions with rubber stop in place (left) and missing (middle, right)

4.6. Type of Failure

It is easily deduced from Figure 4.10, where the arrow indicates location of the notch, that the failure is flexural. As the flexural resistance of materials such as aluminum can be inferred from tensile tests, examination of the nacelle's tensile properties is important to the overall understanding of the failure.

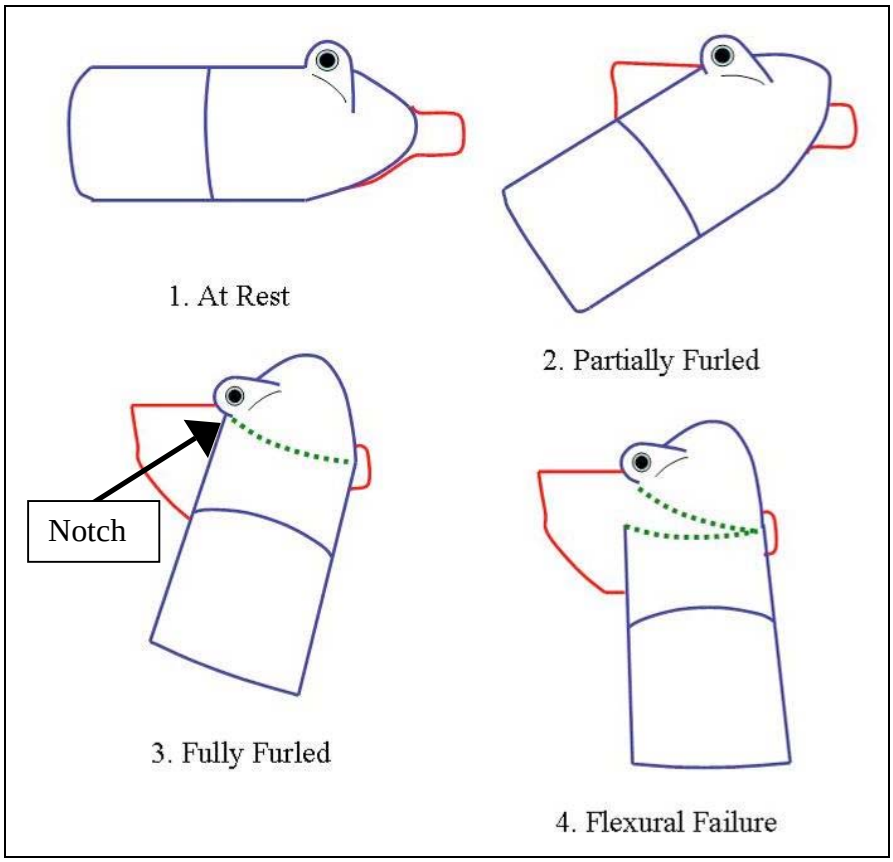

Figure 4.10 – Top view of flexural failure while furling

Tensile separation (ductile) failure is the direct separation of one plane of atoms from another that is caused by loading normal to the eventual fracture surface [Liu 2005]. During a tensile separation a plastic-deformation zone grows ahead of the crack tip if the applied load continues to increase. This leads to the formation of necking along the fracture surface, which is not apparent in the failures at hand.

4.6.1. Ductile versus Brittle Fracture

According to [Lui 2005] there are five macroscopic features of a fracture surface useful in discriminating between ductile and brittle fracture.

1. For a ductile fracture a relatively large amount of plastic deformation precedes the fracture while there is little or no visible plastic deformation visible in a brittle fracture.
2. Shear lips are usually observed at the fracture termination areas during a ductile fracture, whereas a brittle fracture surface is generally flat and perpendicular to the loading direction and to the component surface.
3. A ductile fracture surface generally appears to be fibrous or may have a matte or silky texture, as opposed to a brittle fracture surface that appears granular or crystalline and is often highly reflective. Chevron patterns may also be present in brittle fracture.
4. The cross section at a ductile fracture is usually reduced by necking
5. Crack growth is slow during ductile fracture but brittle fracture has rapid crack growth resulting in catastrophic failure.

Each of the above features indicates that the failures were brittle in nature.

Multiple cracks and separated pieces are commonly found in brittle failure, while they are less common in ductile failures, which often progress as single cracks. There were a small number of visible cracks, other than the main fracture line, present on the available

broken nacelle pieces. However, four of the five nacelles were coated in paint, which may be masking additional cracks.

4.6.1.1. Dye Penetrant Test

A dye penetrant test was conducted on the one turbine specimen that was not painted. As per Figure 4.11, both sides of the fracture were tested using *Fault-Finder*'s three step product (cleaner, penetrant and developer). Only one crack was found and can be seen in Figure 4.11. This crack was expected, as brittle failures tend to have extra cracking and separation of smaller pieces. If the two specimens below, which came from the same nacelle, are place together there are small gaps where lost fragments were likely to have been.

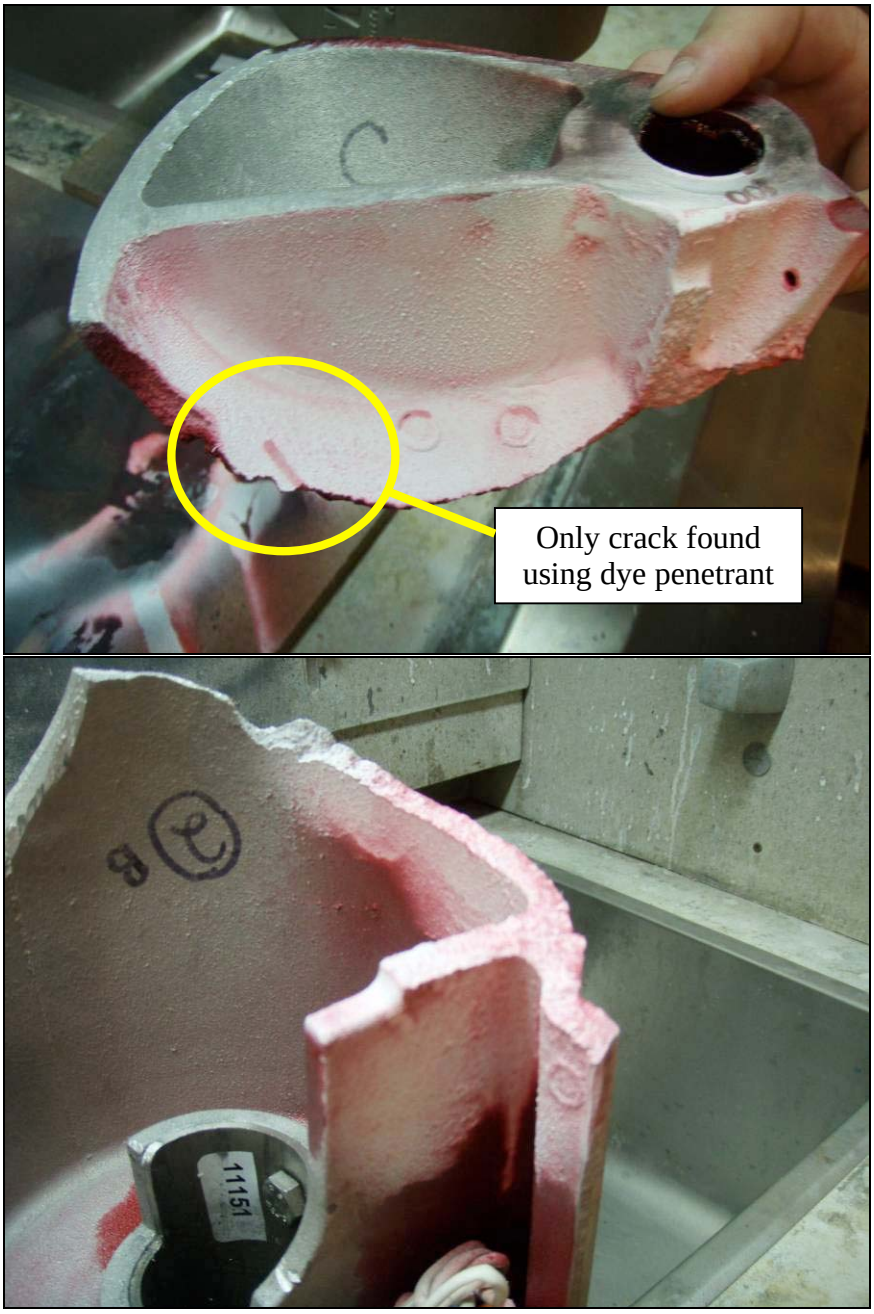

Figure 4.11 – Two halves of a fractured nacelle undergoing a dye penetrant test

While it has been determined that the nacelle experienced brittle flexural failure, the material's mechanical properties are not yet known. The following section discusses the

chemical composition of the cast aluminum and presents its theoretical mechanical properties.

4.7. Nacelle Chemical Composition

An electron microscope scan performed by Memorial University of Newfoundland technical services revealed that the chemical composition of the nacelle, found in Table 4.2, was 89.9% aluminum and 9.5% silicon, the remainder being composed of small amounts of other elements such as copper, nickel and iron. The silicon content is largely due to requirements during the casting process. This composition closely resembles the chemical composition of cast Al-380.0 [The Aluminum Association Inc. 2008]. The mechanical properties of Al-380.0 are listed in Table 4.3.

Table 4.2 – Nacelle Chemical Composition

Element	Relative Amount	Error (+/-)	Percentage
Al	145.767	3.161	89.9 %
Si	15.959	1.772	9.5 %
K	<1.610	0.805	insignificant
Ca	<1.668	0.834	insignificant
Ti	<1.887	0.943	insignificant
Fe	<2.845	1.423	insignificant
Ni	<3.884	1.942	insignificant
Cu	<4.841	2.421	2.7%

Table 4.3 – Mechanical Properties of Al-380.0

Ultimate Tensile Strength		**Yield Strength**		**Elongation**	**Young's Modulus**	
MPa	*ksi*	*MPa*	*ksi*	*%*	*GPa*	*psi*
324	47	159	23.1	3.5	71	10.3

4.8. Tensile Testing

Investigation of the material properties of the cast nacelles is needed in order to determine whether flaws or substandard materials are to blame. To accomplish this, eight tensile test specimens were machined from four of the turbines, as shown in Figure 4.12. The material adjacent to the fracture surface was sampled to ensure consistency of composition and microstructure. Tensile tests were performed on each of the specimens using the *Instron 5585h* tensile testing machine and *Bluehill*[2] analysis software (results of individual tests can be found in Appendix B).

[2]Information available at http://www.instron.us/wa/products/software/bluehill/test_methods/tensile.aspx

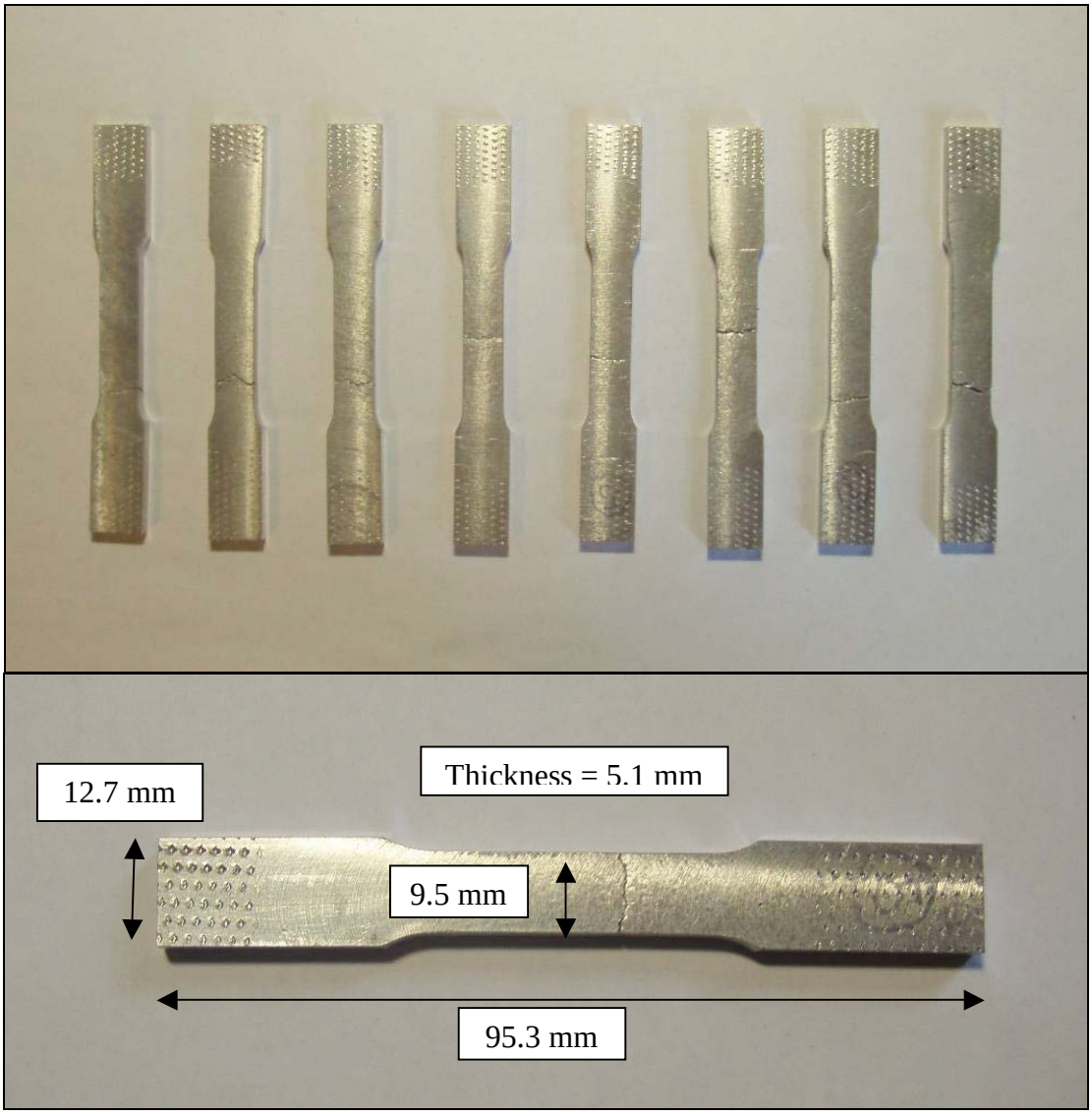

Figure 4.12 – Eight tensile test specimens after testing (above) and individual test specimen (below).

The specimens were tested at a variety of temperatures and extension rates to capture a range of operating conditions. In order to bring the test specimens down to the desired temperatures, constant temperature baths were used. A constant temperature bath along with a specimen undergoing a test can be seen in Figure 4.13.

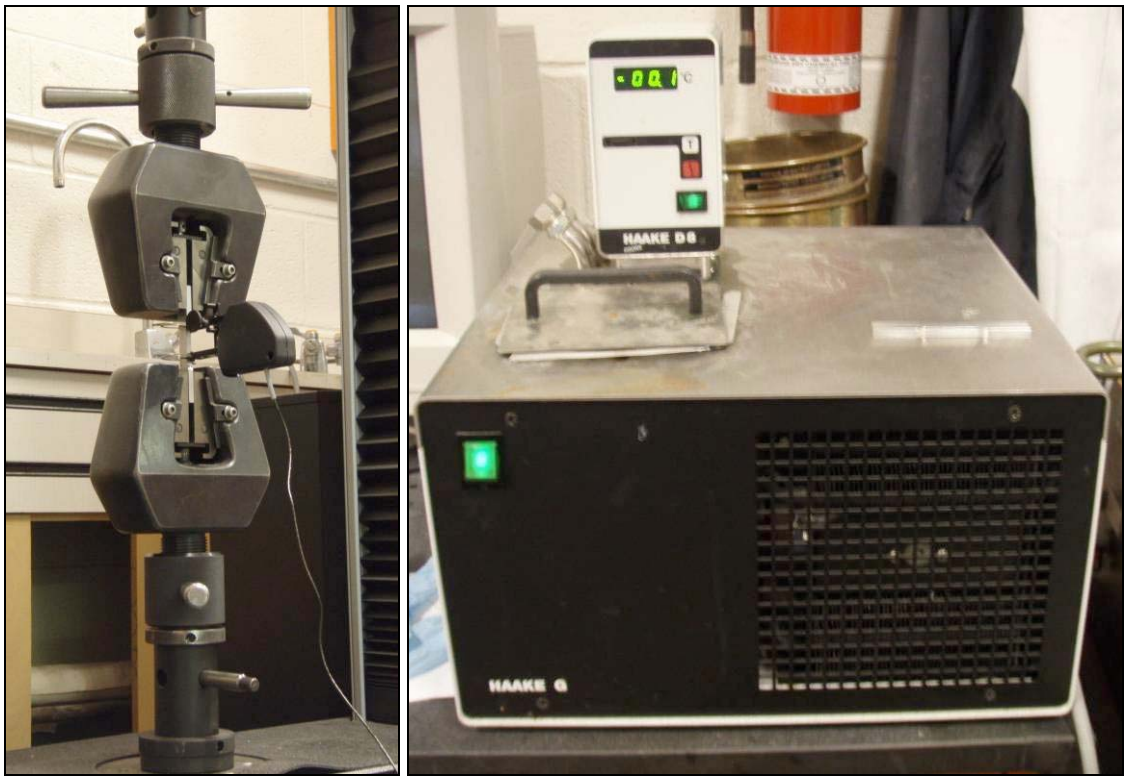

Figure 4.13 –Tensile test being performed (left) and constant temperature bath (right)

4.8.1. Tensile Testing Procedure

The eight specimens were tested in the order and according to the parameters listed on Table 4.4. A range of temperatures, from -21.0^{o}C to 23.1^{o}C, and two extension rates, 6 mm/min and 200 mm/min were used. The most probable conditions during failure were at temperatures below freezing and high wind speeds, resulting in a high 'extension rate' in the field. As such, the tensile tests employed the full range of equipment capabilities, with the constant temperature bath cooled to -21^{o}C and the extension rate maxed-out at 200 mm/min.

Table 4.4 – Tensile Test Run Details

Run No.	From Turbine	Rate (mm/min)	Temperature (^{o}C)
1	6	200	23.1
2	3	6	23.1
3	4	6	0.5
4	5	6	0.4
5	3	6	-17.3
6	4	6	-17.1
7	6	200	-0.4
8	5	200	-21.0

4.8.2. Tensile Testing Results

A summary of the results of the tensile tests can be found in Figures 4.14 and 4.15 and Table 4.5. The 'Point of Failure' in Table 4.5 refers to the maximum point before failure on the respective curves. The extension-load curve in Figures 4.14 and the stress-strain curve in Figure 4.15 both show relatively consistent failure loads and mechanical properties, regardless of loading conditions.

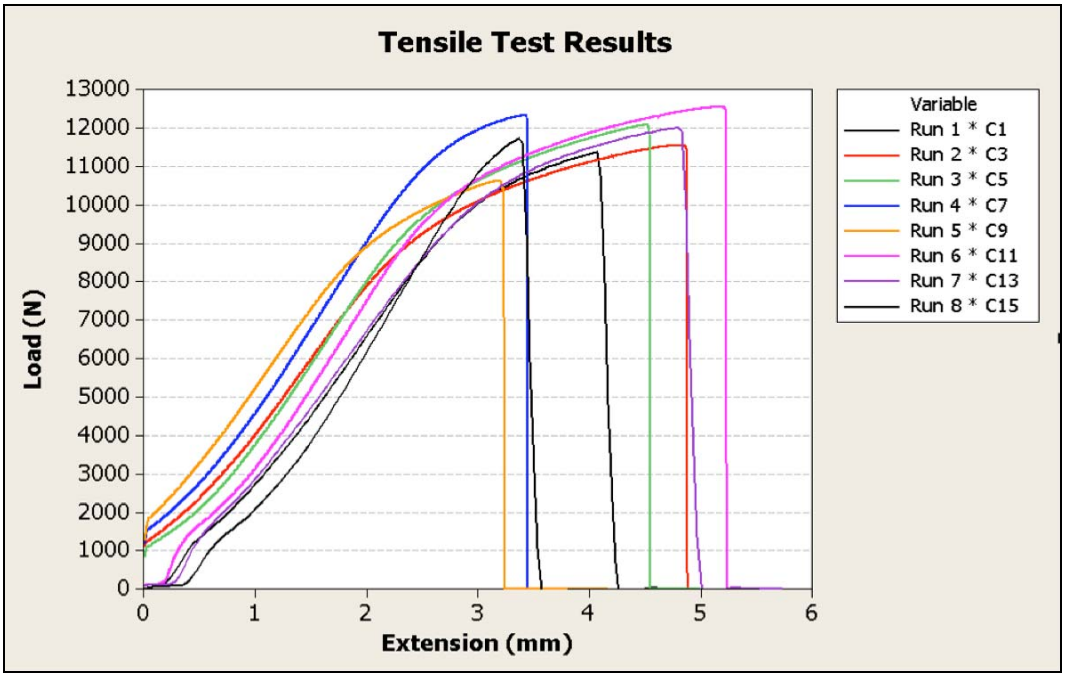

Figure 4.14 – Tensile test results

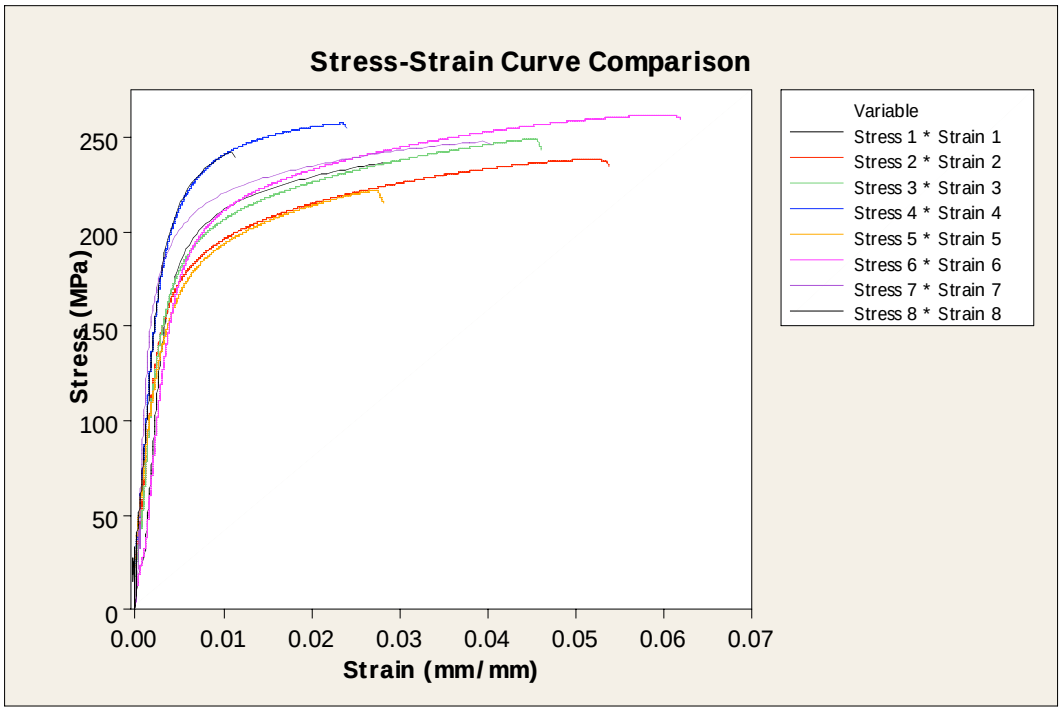

Figure 4.15 – Stress-strain curve comparison

Table 4.5 – Tensile Test Results

Run No.	Rate (mm/min)	Temp (^{o}C)	Point of Failure		Ultimate Strength (MPa)	Yield Strength (MPa)	Young's Modulus (GPa)
			Extension (mm)	Load (N)			
1	200	23.1	4.07	11 363	236	182	60.67
2	6	23.1	4.82	11 549	238	177	48.86
3	6	0.5	4.51	12 073	248	180	58.06
4	6	0.4	3.41	12 324	257	220	56.41
5	6	-17.3	3.17	10 619	222	176	41.90
6	6	-17.1	5.15	12 540	262	191	42.44
7	200	-0.4	4.80	11 999	247	190	95.00
8	200	-21.0	3.37	11 737	242	218	64.12
Average	-	-	*4.16*	*11776*	*244*	*192*	*58.43*
Std Dev	-	-	*0.767*	*608*	*12.57*	*17.69*	*16.90*

As can be seen by comparing the average values in Table 4.5 to those values in Table 4.3 the strength of the nacelle material is not appreciably different from other castings of similar composition. Also, as indicated by the standard deviation (Std Dev), each property was relatively consistent across the range of test parameters. This indicates that the cast was of consistent and acceptable quality.

Table 4.6 lists the correlations between the factors (temperature and extension rate) and the responses (extension and load at failure, ultimate strength, yield strength and Young's modulus). The top values in each cell are the Pearson Correlation Coefficients while the bottom values are the associated p-values.

Table 4.6 – Tensile Test Factor Correlations

Response\Factor	Temperature	Extension Rate	Comments
Extension at Failure	0.319 0.442	-0.089 0.834	The extension at failure was not strongly correlated with temperature or extension rate
Load at Failure	-0.092 0.829	-0.103 0.808	The load at failure was not strongly correlated with temperature or extension rate
Ultimate Strength	-0.133 0.753	-0.154 0.716	The ultimate strength was not strongly correlated with temperature or extension rate
Yield Strength	-0.386 0.345	0.230 0.583	The yield strength was not strongly correlated with temperature or extension rate
Young's Modulus	0.099 0.816	0.681 0.063	The Young's Modulus was not strongly correlated with temperature but was found to increase with extension rate

The only noteworthy correlation is that between extension rate and Young's modulus. The correlation has an r-value of 0.681 and there is a 6.8% chance that the correlation is due to random noise. This means that Young's modulus, which indicated the stiffness of the material, increases roughly with temperature.

4.8.3. Tensile Test Discussion

Both the average ultimate strength and the average yield strength of the cast aluminum tested were relatively consistent with property values for Al-380.0, as per The Aluminum Association Inc. Also, the standard deviation of each property determined by the tensile tests was acceptably low suggesting a consistent casting job. These results indicate that

casting flaws don't have a significant contribution to machine failure. The experimental setup proved to be sufficient for this examination.

4.9. Potential Failure Mechanisms

While examining the turbine's potential failure mechanisms, one must consider many interactions that either positively or negatively affect the levels of stress within the nacelle. Dynamic considerations are illustrated in Figure 4.16 and discussed below.

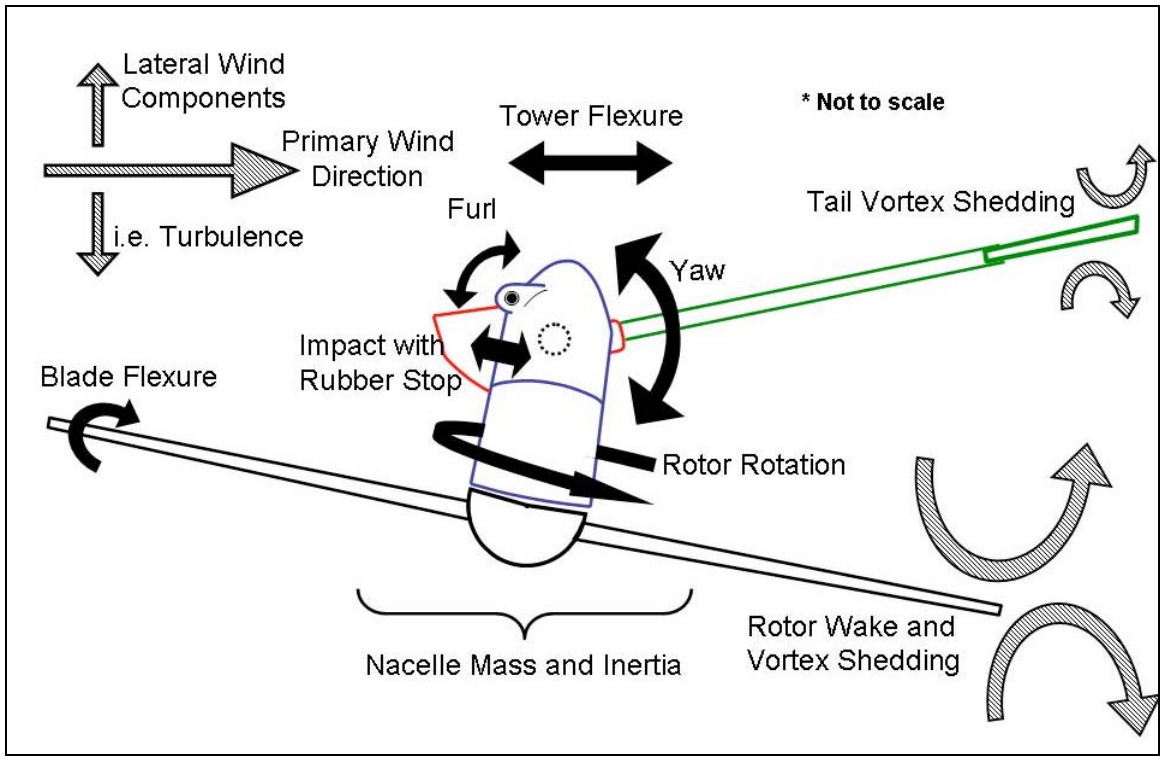

Figure 4.16 – Plan view of furled turbine with dynamic considerations

Initially, as the turbine reaches the fully furled position the impact of the top portion of the nacelle with the rubber stop mounted on the bottom portion causes the tail to yaw to the left[3]. At the instant of load application, dampening of the induced stresses may result from this turbine rotation. Tower flexure would have a similar dampening effect.

According to [Manwell et al (2006)] the Principal Theorum of the Gyroscope, based on the right hand rule and illustrated in Figure 4.17, states that "a gyroscope with an angular momentum JΩ rotates with speed ω about an axis perpendicular to Ω (precesses), then a couple, JΩω, acts on the gyroscope about an axis perpendicular to both gyroscopic axis, Ω, and the precession axis, ω." Basically this implies that the faster the rotation of the blades the more the turbine is naturally inclined to furl and yaw, which depending on direction, can either add to or subtract from this. However, if the wind gusts laterally from the right, the yaw action of the turbine (caused by the reaction of the tail to the wind) will briefly induce unfurling as the reaction time of the top portion of the nacelle is impeded by the rotors angular momentum.

[3] For discussion purposes, direction will be relative to an observer standing upwind, facing the turbine.

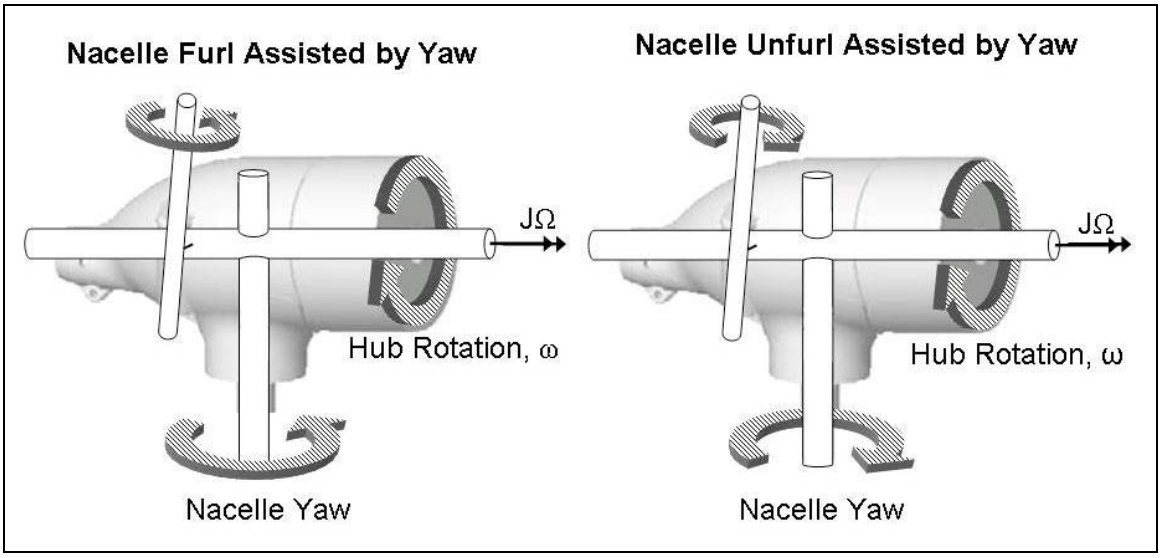

Figure 4.17 – Angular momentum during furling

Turbulence of the wind plays a large role in inducing dynamic considerations. Turbulent wind has a range of vertical and horizontal components and the typical duration of a gust ranges from 0.1 seconds to 10 seconds. This is a short enough time frame that a second wind gust can affect the state of the turbine before it has reached equilibrium with a previous gust. For example, from observation it is known that the tail, which is attached to the bottom portion of the nacelle, reacts quickly to wind gusts and turbulence while the reaction time of the top portion of the nacelle is impeded by conservation of angular momentum of the rotor. The two portions may slam together if the wind quickly changes from one direction to the other and back, which would introduce an impact load, increasing the stress in the nacelle. Also, rotor wake and vortex shedding and tower vortex shedding may compound the effects of turbulence.

Other influences that may have an impact on the state of stress within the nacelle include: the partial coning (flexure) of the blades as they are struck by the wind and the resultant decrease in swept area, the elasticity of the rubber stop (temperature dependent), and the frictional resistance of the furling and yaw pivots.

4.9.1. Quasi-Static Loading

As there are few quantifiable details known about the dynamic interactions involved in furling, a first order calculation of static loading may provide some insight into the level of influence of both static and dynamic considerations. The material strength is documented (*Section 4.8*) and the position and action of the turbine at the time of failure has been surmised (*Sections 4.4, 4.5* and *4.6*). Thus it is possible to approximate the upper-bound wind loading on the unit at the time of failure based on a quasi-static force equilibrium calculation. For this calculation it is assumed that the wind loading scenario involves the slow and steady growth in wind speed which first brings the machine to the full furl position without impact and then continues to grow until the unit fails. Dynamic interactions are omitted for the purposes of reducing this calculation to quasi-statics.

A simplified free body diagram of the unit in the furled position is shown in Figure 4.18 whereby the moment arm for the wind loading point, and rubber stop are provided. In this analysis it is further assumed that the wind load on the turbine blades creates *only* a point load on the rotor hub at the position shown as point A. This assumption is conservative as

it is probable that a moment may also be transferred to the hub at this point via the asymmetric exposure of the blades to the wind in the furl position. Acting against this conservatism however, is the action of compressive loads on the nacelle body, which serve to offset extreme fiber tensile stress under the action of flexure. These two competing mechanisms are not factored in this calculation and are thus considered to cancel, though the accuracy of this assumption is not known.

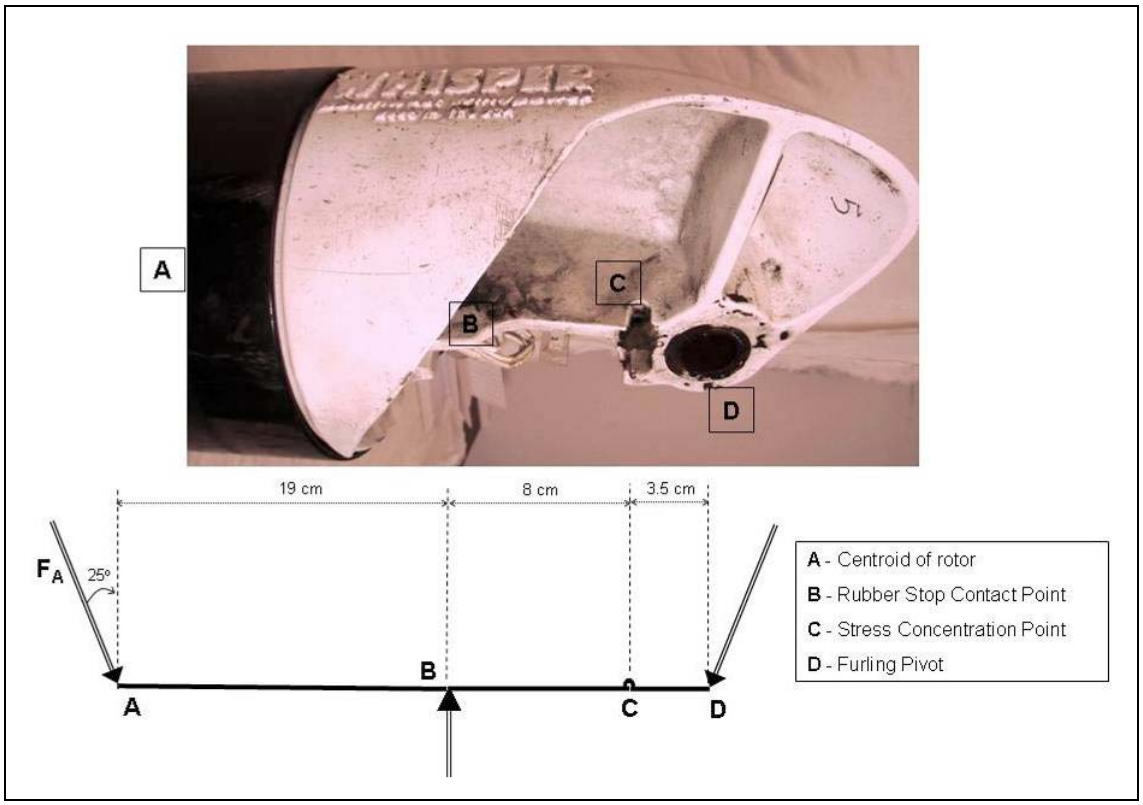

Figure 4.18 – Simplified free body diagram of static forces on nacelle

Considering the stress concentration and a moment of inertia of the failure cross section equal to 4.871×10^{-6} m^4, the wind speed that would induce a stress high enough to surpass the ultimate strength found during tensile testing (244 MPa) was found to be on the order

of 500 m/s. (The calculation is available in Appendix C.) As a result of the assumptions and simplifications made in order to perform this quasi-static calculation, the wind speed values are unrealistic representations of the failure conditions implying that dynamic effects play a significant role in the failure process.

4.9.2. Discussion

Dynamic factors, including angular momentum of the rotor, dampening effects of the tower, vortex shedding, furling rate, tail response time and the direction and strength of wind gusts, make this an intractable calculation requiring advanced modeling techniques to solve. A laboratory approach, involving destructive tests of nacelles during various furling scenarios, would likely produce the most accurate results and insight into conditions at failure.

Whether the failures occur from the impact of a full 65^{o} furl or while the turbine is already fully furled, turbulence and its induced dynamic interactions play an important role. This corresponds well to the findings of the correlational analysis undertaken in *Section 3.5.2.*

4.10. Other Factors Contributing to Failure

4.10.1. Temperature

The destructive influence of the furling impact on the turbine materials for a given wind speed will be greater as temperature decreases. Not only does the density of the air increase but all the materials involved (cast aluminum, rubber, glue, paint, etc.) lose resilience. The impact strength of non-ferrous metals increases with decreasing temperature, however ductility will decrease, increasing the likelihood of a brittle fracture. [Ross 1995]

4.10.2. Fatigue

Fatigue is caused by the application of a cyclic tensile load, [Ross 1995] as occurs during the furling process. If fatigue is a factor, a small portion of the material exceeds the ultimate tensile strength of the material causing small cracks upon each load cycle. In the failures in question, there were no striations visible, which are key indicators of fatigue induced failure and as such one can conclude that fatigue did not play a significant role.

4.11. Conclusions from Failure Analysis

The most common catastrophic failure experienced by the WH100 used by Bell-Aliant in Labrador is a brittle fracture across the smallest cross section of the nacelle. A flexural failure, the crack initiates from a single furling event causing stress to concentrate in a notch in the nacelle casting. The crack propagates immediately to the other side, separating the top portion of the nacelle into two pieces. This failure is most likely to occur at low temperatures during periods of very strong turbulent winds. As the tests conducted in *Sections 4.6.1* and *4.7* rule out a low quality cast job, it is evident the manufacturer's decision to introduce a notch in the casting was poorly advised.

4.11.1. Recommendations

The requirement to model the furling behaviour and complex fluid dynamics through and around the turbine may prevent accurate determination of wind conditions at the time of failure. This along with the consideration of the angular momentum combined with machine asymmetry makes it an exceedingly complex system [Bruneau and Roberts 2008]. Therefore, determining the instantaneous axial force, which causes the furling, would prove difficult. Finite element analyses would be useful to more accurately determine the forces required to fracture the nacelle body and what, if any, nacelle modifications maybe needed for avoiding this.

In an effort to improve the survivability of Bell-Aliant's turbines two options are considered, as identified in Figure 4.19. The first option is to strengthen the nacelle; the second option is to reduce the loads on the nacelle. Modifying the nacelle may prove difficult as it is cast as a single piece and any modifications may introduce additional stress concentrations. Also, recommended actions have to be quick and easy for technicians to apply to existing units in the field. As such, reduction of the loads on the nacelle was the only option considered in this study.

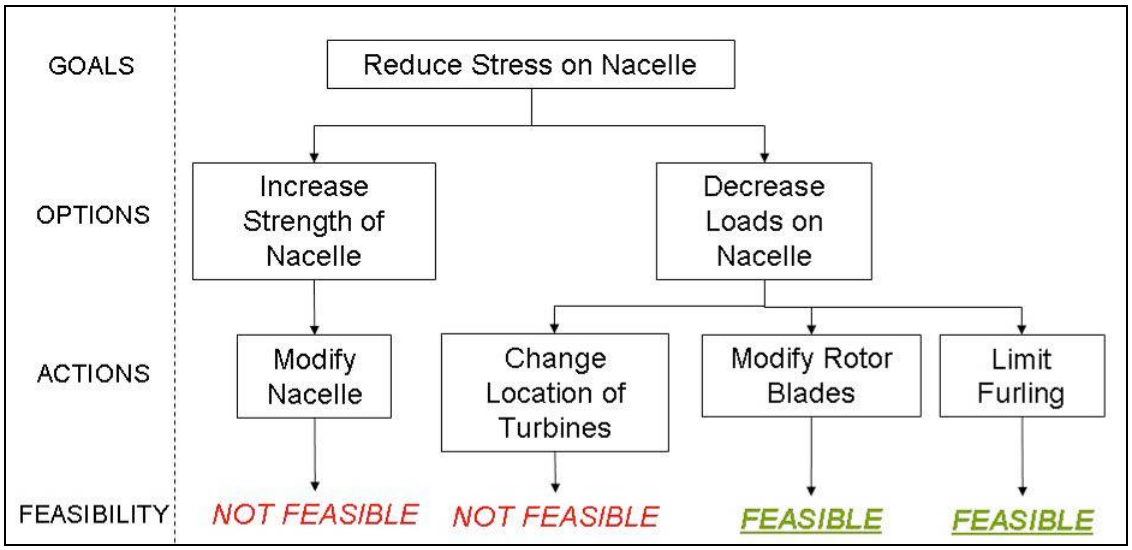

Figure 4.19 – Decision tree for reducing stress on the nacelle

While moving the turbines to a less severe environment would likely decrease the loads applied to the nacelle, it is clearly not an option in this situation. An alternative is to modify the blades in an effort to reduce the overall force transferred to the nacelle. The blades are the part of the rotor that interacts most with the wind and translates the thrust from the wind not only into rotation but also into the axial force that causes furling.

Changing blade geometry may decrease loads and change the furling characteristics and prevent, or decrease, future failures. Another concept is to limit the furling capability of the turbine. It is during the act of furling that the nacelle experiences the failure loads so a reduction, or elimination, of furling may prevent this type of failure, however the consequences of doing so include overloading the generator and possibly initiating some other type of failure. The next chapter describes a series of field experiments aimed at testing these few mitigation measures.

5. Field Trials

5.1. Introduction

Following the recommendations for reducing the nacelles stress discussed in the previous chapter, Chapter 5 presents an experimental program aimed at exploring the potential of the two mitigating actions: modifying the rotor blades and limiting the furling capabilities.

5.2. Hypothesis

These tests intend to explore the relationship between wind speed, power produced and the extent to which the unit furls. The hypothesis of the following experiment is that if the blades of Southwest Windpower's Whisper 100 (WH100) are shortened by a certain amount then the furling action may occur at a higher wind speed. This would result in less furling of the turbine in general and also a lower axial load on the turbine. Though production may be curtailed, survival may be ensured. The experiment will also assess the usefulness of limiting the turbine's furling capability.

5.3. Experimental Program

5.3.1. Concept

The goal of this experimental program was to study WH100 performance under controlled velocity conditions. Once productivity and furling characteristics of a standard, off-the-shelf unit were determined, trials were repeated with modified blades. The blades were shortened at regular intervals, effectively reducing the swept area. The hope was that this sacrifice of power production would increase survivability by changing the turbine's furling characteristics. Trials were also run when the furling mechanism itself is suppressed. The theory was that there is a point where the blades are short enough to cause furling to become a mechanical, structural or electrical liability, rather than an asset.

Blade lengths were selected based on the calculated assumption that the load reduction is proportional to swept area reduction, so that according to Equation 2.4 an approximate $1/10^{th}$ and $1/3^{rd}$ power reduction results from a 5 cm and 20 cm tip removal respectively. It is assumed that the startup speed will not be greatly affected as the startup of the turbine is dominated by the region of the blade nearest to the root. It is also assumed that if power production was decreased by greater than 33% the potential improvement in survivability would not be justified. Relevant blade lengths are shown in Figure 5.1.

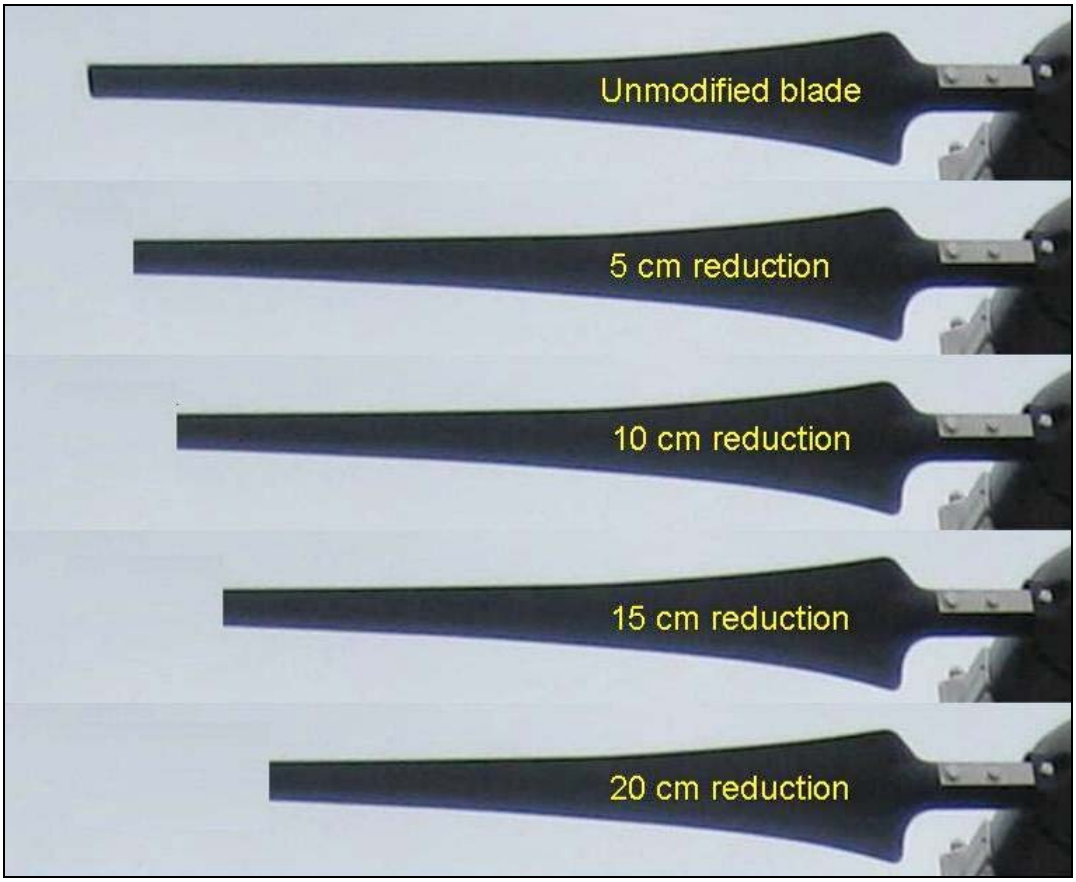

Figure 5.1 – Relevant blade lengths

Wind tunnel testing, the ideal control situation, was not possible as a tunnel of adequate size was not available for use. The most promising alternative that falls within budget constraints was a vehicle and trailer mounted system. All equipment was mounted on a trailer and in the back of a pickup truck, which was driven down a straight stretch of road under favourable conditions. Though imperfect, this approach offered huge financial and time benefits over other methods, such as conventional ambient *in-situ* testing.

5.3.2. Location

The selected location is a remote public roadway with extended flat and straight sections with no overhead obstructions, such as overpasses or transmission lines.

5.3.3. Equipment

A 7 m long and 1.5 m wide dual axis ATV trailer was selected for its large load capacity, surface area, stability, ease of mobility, availability and excellent tracking characteristics. A structural skeleton of steel beams was assembled on the trailer bed, on which most of the equipment will be installed. The turbine was mounted near the rear while the anemometer was mounted between the 1.5 and 6 times the rotor diameter (approximately 6 m or roughly 3 diameter lengths) upwind of the rotor centerline required for accurate wind readings [AWEA 2008]. Both the anemometer and the turbine were mounted on 10 ft poles in order to be above the disturbed airflow influence of the truck [Cooper 2004]. The anemometer and turbine towers have similar setups where they can be easily pivoted down for modification, maintenance and transportation.

All electrical equipment was kept in the back of the pickup truck, with a spotter, for easy access and monitoring during trials. This includes a battery bank and dump load, turbine controlled and display, anemometer display, a camera trained on turbine and a laptop. An auxiliary AC power supply was used for any external power requirements.

A configuration of the experimental setup is illustrated in Figure 5.2 and shown in Figure 5.3.

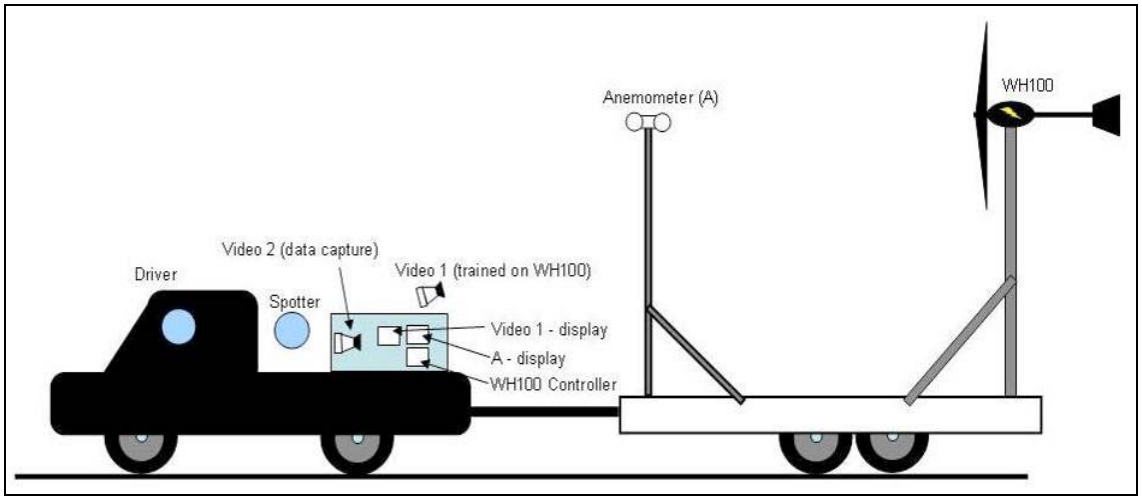

Figure 5.2 - Experimental setup illustration

Figure 5.3 - Experimental setup photograph

5.3.4. Data Acquisition

Experience in fieldwork has shown that simple and robust data acquisition systems are most suitable for consistent and reliable results, especially for the relatively simple information desired during the tests in question. The downside is low data resolution, which may result in the inability to capture higher order effects and subtleties that may be captured by a more sophisticated system.

The turbine controller display was mounted along with the anemometer display on top of the laptop screen. A live video feed from the camera trained directly on the turbine was fed into the laptop and was shown along side the other displays. A second video was taken of the entire data display setup and recorded onto a tape. This tape was then manually analyzed frame-by-frame to capture the data by transferring it to a spreadsheet. Figure 5.4 shows a screen shot of the data display setup.

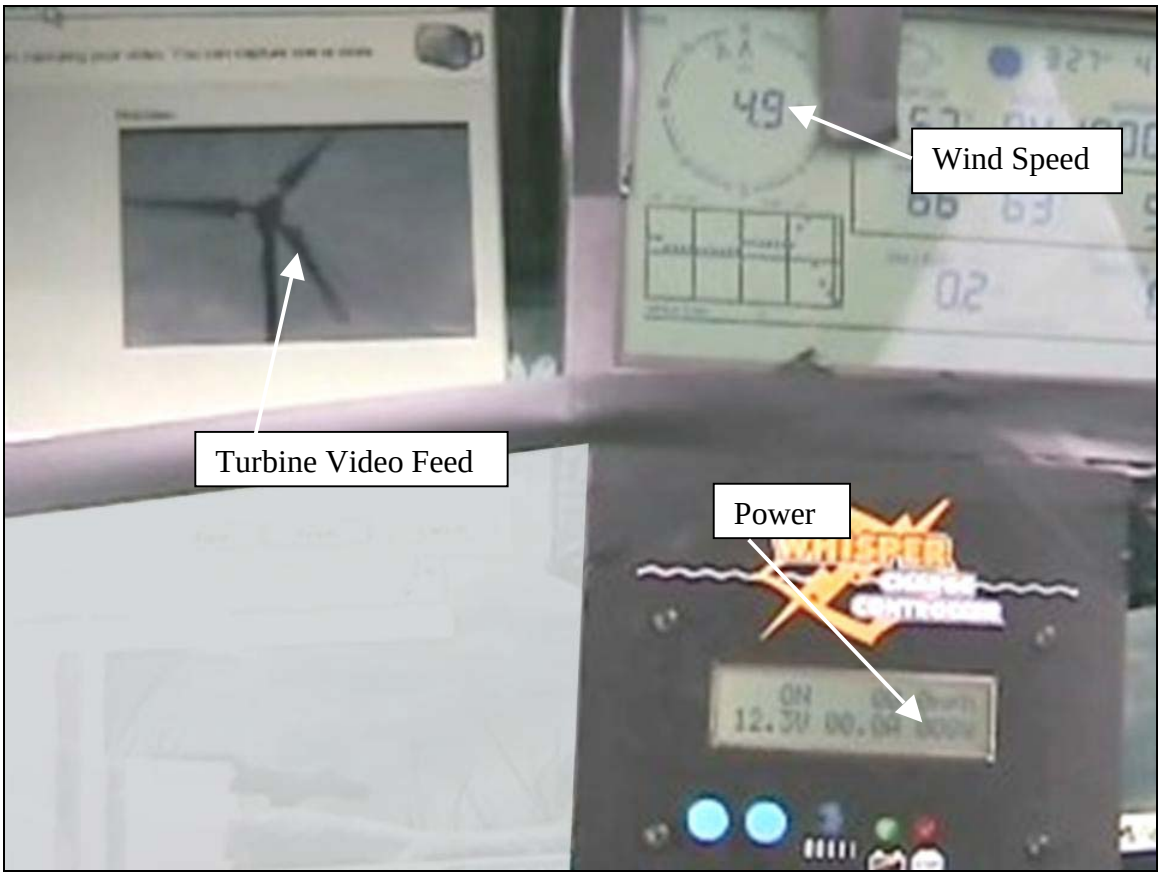

Figure 5.4 - Data display setup screenshot

5.4. Test Procedure

5.4.1. Experimental Range

The airspeed range of approximately 0 to 20 m/s is expected to encapsulate the full range of furling, from 0^{o} to approximately 65^{o} as observed by others [Davis and Hansen 2000] in Figure 5.5. Discrete values from 0 to 5 were assigned for data capture purposes to

represent the furling extent. This scale corresponds to the resolution of data capture and is represented graphically in Figure 5.6.

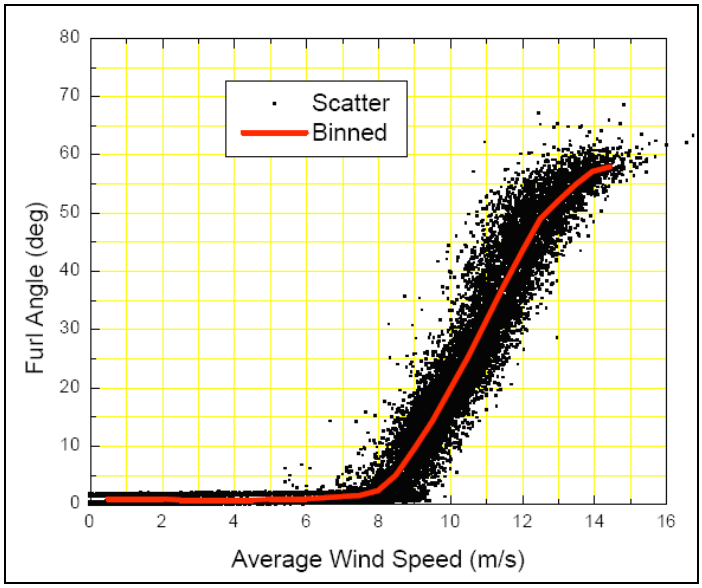

Figure 5.5 - Furl angle versus wind speed [Davis and Hansen 2000]

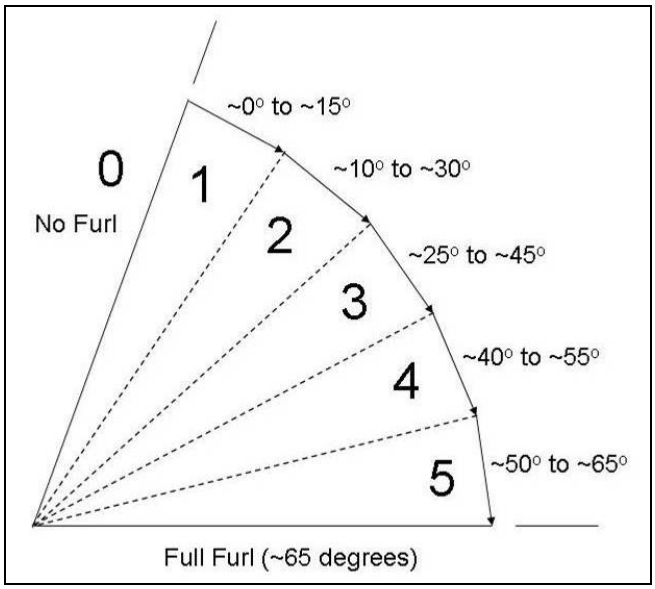

Figure 5.6 - Furl extent and corresponding angle

5.4.2. Road Tests

Days on which trials can be performed required little wind and no rain. While all of the trials where usable data was captured were performed on the same day and on the same stretch of road, several earlier road tests were performed in preparation. The first road test was to ensure the structural stability of the trailer-mounted setup, with the turbine operating a shorted-out configuration to discourage rotation.

The second road test was conduced with the turbine wired directly to a rectifier and dump load and illustrated the need for proper controls. The turbine operated in a manner similar to when it was shorted-out except that once it encountered a certain airspeed the rpm increased dramatically. This resulted in two unique power curves, one before the rpm increase and one after, and did not accurately represent the operation of the turbines at the Labrador hill top sites.

The third road test was conducted to validate the controller configuration and to perform a data acquisition test, both of which were acceptable. The fourth road test was intended to be our first trial run, however the WH100 controller failed under no-load conditions, likely due to a manufacturing defect. Once the controller could be replaced, the final road test was used to capture all of the data required for analysis.

5.4.3. Trial Runs

A full set of tests were completed with the original, unmodified blades attached then repeated with 5 cm, 10 cm, 15 cm and 20 cm removed from the blade tip. Each trial began at approximately 5 m/s and was slowly ramped up to speeds of 10 m/s, 15 m/s then 20 m/s. Table 5.1 shows the full suite of tests performed. Relatively constant wind speed was maintained through feedback from the anemometer display and communication between the spotter in the back of the truck and driver. Once tests were completed, copies of the data tape were made ready for data extraction.

Table 5.1 - Trial Runs

Blade Length	Configurations	No. of Trials
Original Length	Furling enabled	3
Shortened by 5 cm	Furling enabled	2
Shortened by 10 cm	Furling enabled	2
	Furling disabled	1
Shortened by 15 cm	Furling enabled	2
	Furling disabled	1
Shortened by 20 cm	Furling enabled,	2
	Furling disabled	1

5.5. Collected Data and Time Series

5.5.1. Data Obtained

Full data sets for the original blade length, 5 cm and 20 cm configurations were captured and analyzed. However, due to complications with the data acquisition system, data for

the 10 cm and 15 cm configuration trails was irretrievable. As the displays for the anemometer and WH100 controller are not back lit (i.e. they require an external light source to be seen) their outputs on the data capture video were not visible during the time of their runs (even though they were clearly visible in real life), as it was nearing the end of the day and the sun was setting. On the final trials, with the 20 cm shortened blades, an external lighting source was used and the data was retrievable.

5.5.2. Time Series Graphs and Discussion

Figures 5.7 to 5.14 show a time series of each respective trial run. There are a few common characteristics within the time series. One commonality is that power generally reached two peaks, one that coincided with achieving the rated wind speed of 12.5 m/s and the other as wind speeds approached 20 m/s. There was a decrease in power production after furling had reached its maximum extent, shortly after the rated wind speed. Although present across all three blade length configurations, this effect was most notable in the 20 cm configuration runs. It did not happen in Trial 2 of the 0 cm configuration due to the fact that the wind speeds never went above the turbine's rated wind speed. As expected, the power production increased more predictably with wind speed when the furling mechanism was disabled (Figure 5.14). A more detailed investigation of individual response characteristics is explored in the following sections.

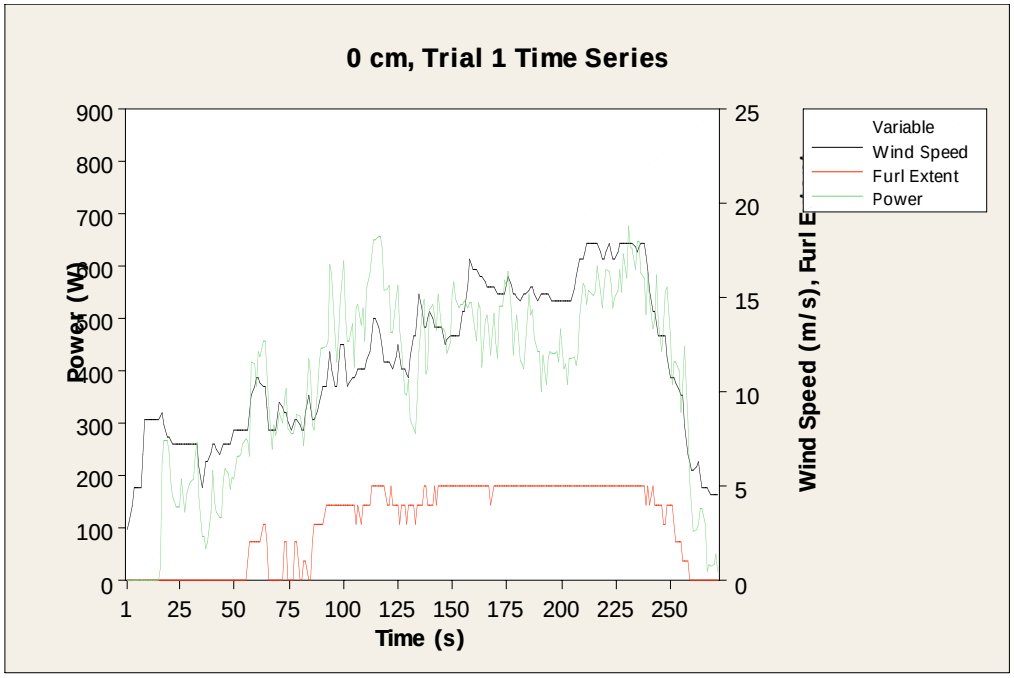

Figure 5.7 - 0 cm configuration, Trial 1 time series
(Furl Extent represented by dimensionless scale of 0 to 5 as per Figure 5.6)

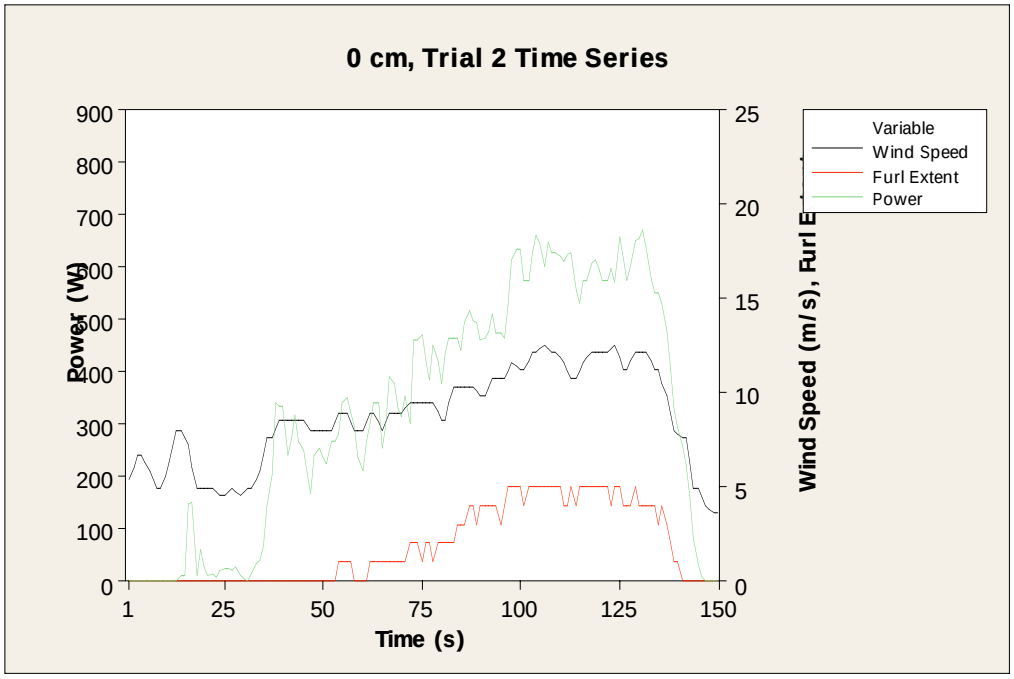

Figure 5.8 - 0 cm configuration, Trial 2 time series
(Furl Extent represented by dimensionless scale of 0 to 5 as per Figure 5.6)

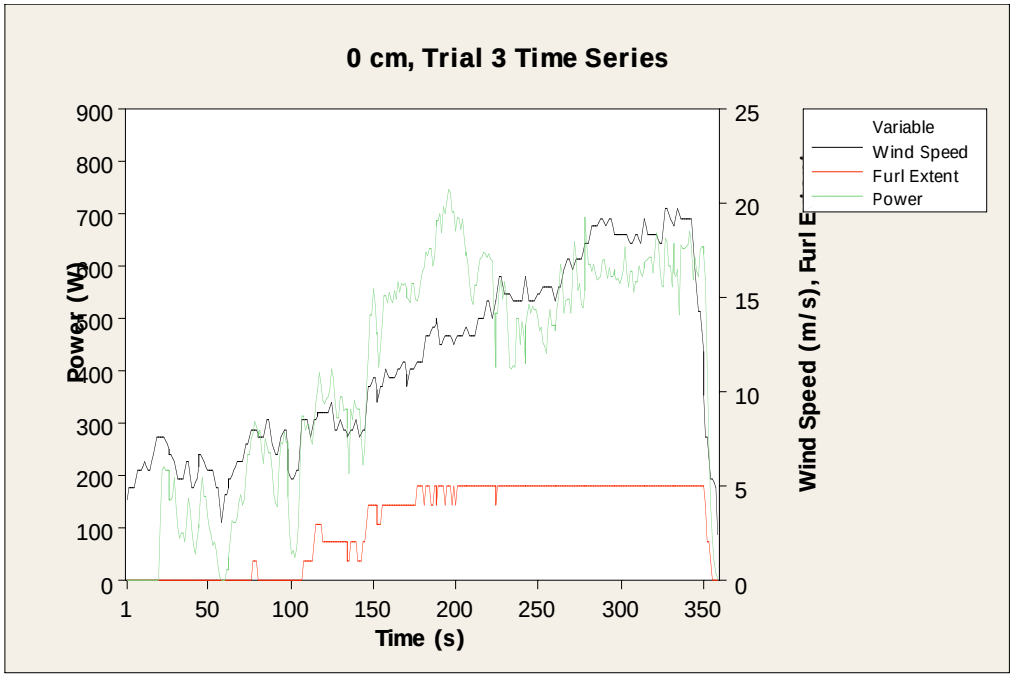

Figure 5.9 - 0 cm configuration, Trial 3 time series
(Furl Extent represented by dimensionless scale of 0 to 5 as per Figure 5.6)

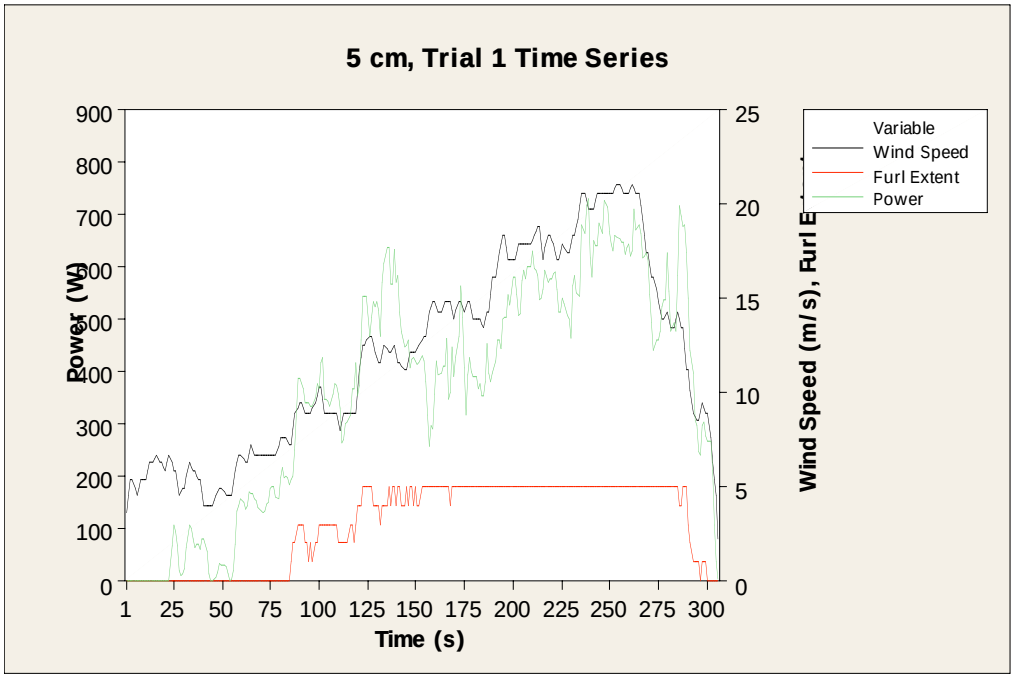

Figure 5.10 - 5 cm configuration, Trial 1 time series
(Furl Extent represented by dimensionless scale of 0 to 5 as per Figure 5.6)

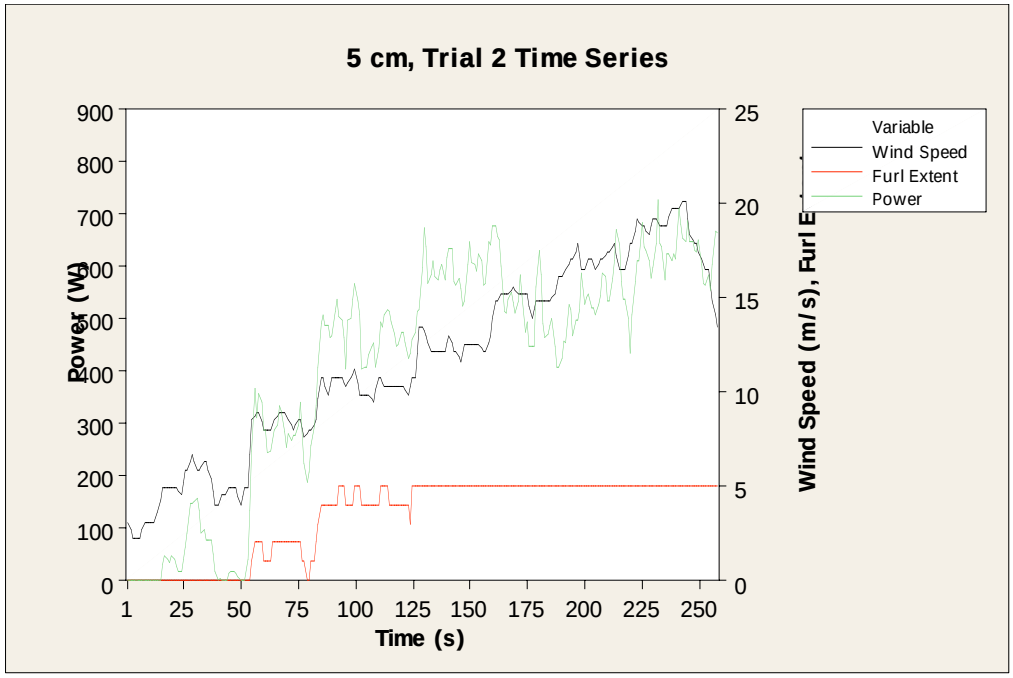

Figure 5.11 - 5 cm configuration, Trial 2 time series
(Furl Extent represented by dimensionless scale of 0 to 5 as per Figure 5.6)

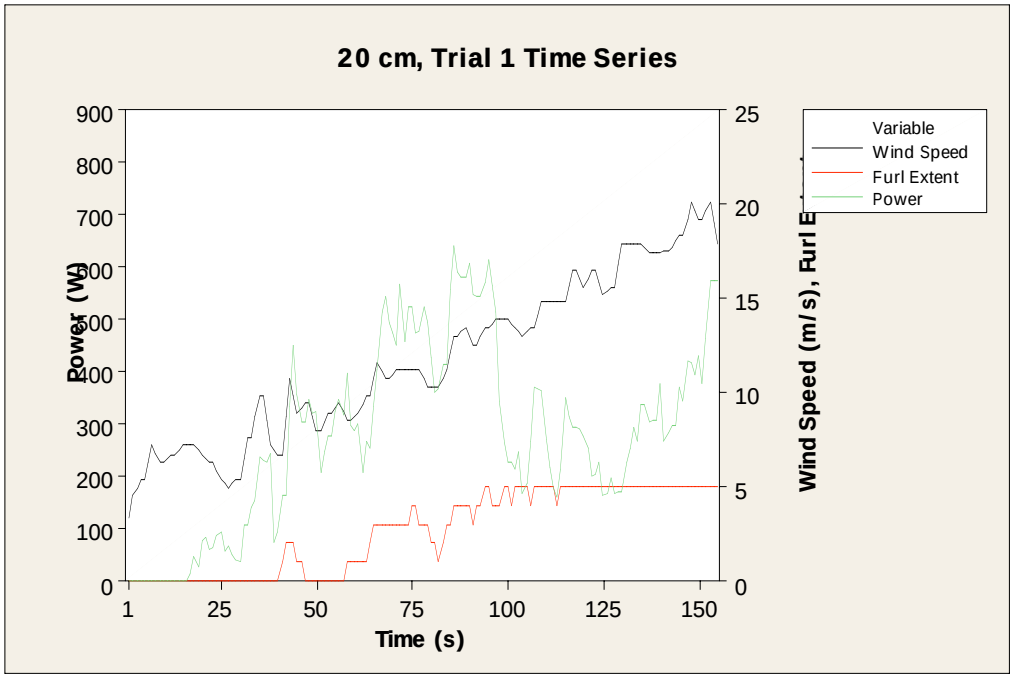

Figure 5.12 - 20 cm configuration, Trial 1 time series
(Furl Extent represented by dimensionless scale of 0 to 5 as per Figure 5.6)

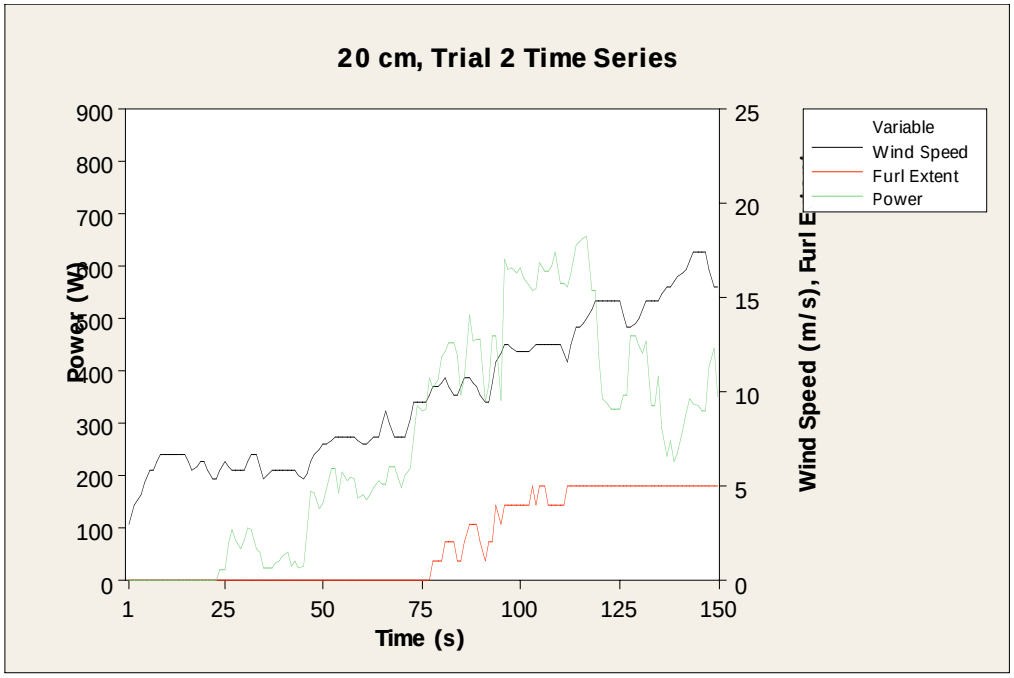

Figure 5.13 - 20 cm configuration, Trial 2 time series
(Furl Extent represented by dimensionless scale of 0 to 5 as per Figure 5.6)

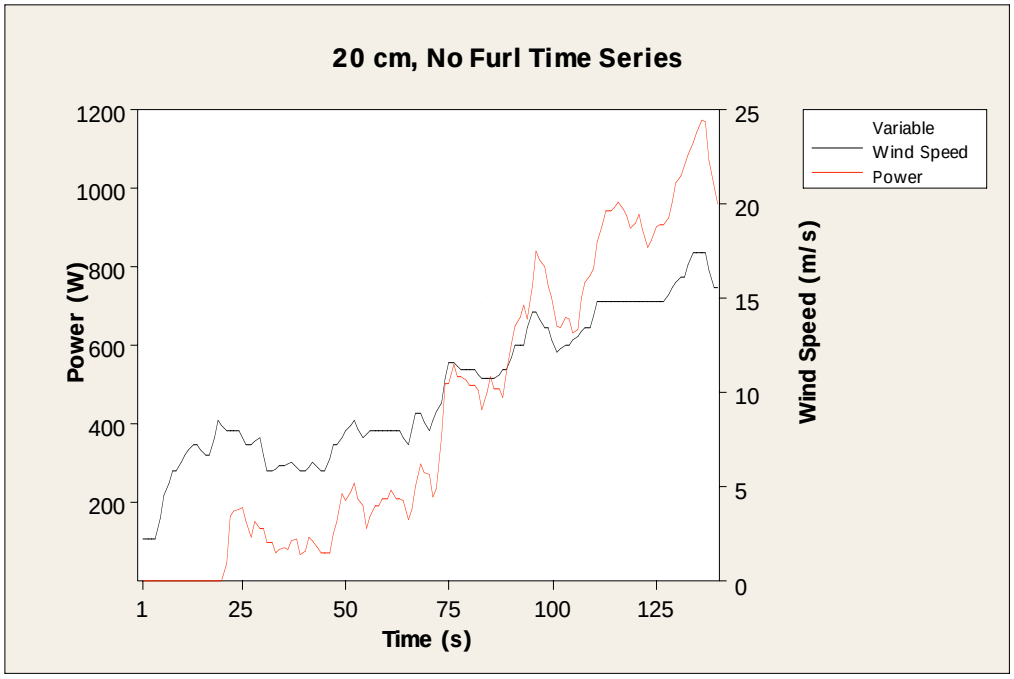

Figure 5.14 - 20 cm configuration, No Furl time series

5.6. Data Analysis

5.6.1. Power Production

Figure 5.15 shows the power curve for the WH100 as available from Southwest Windpower [Southwest Windpower 2008]. In Figures 5.16, 5.17 and 5.18, the power curves for the 0 cm, 5cm, and 20 cm configurations as obtained during the field tests are shown. A comparison of all three configurations is available in Figure 5.19.

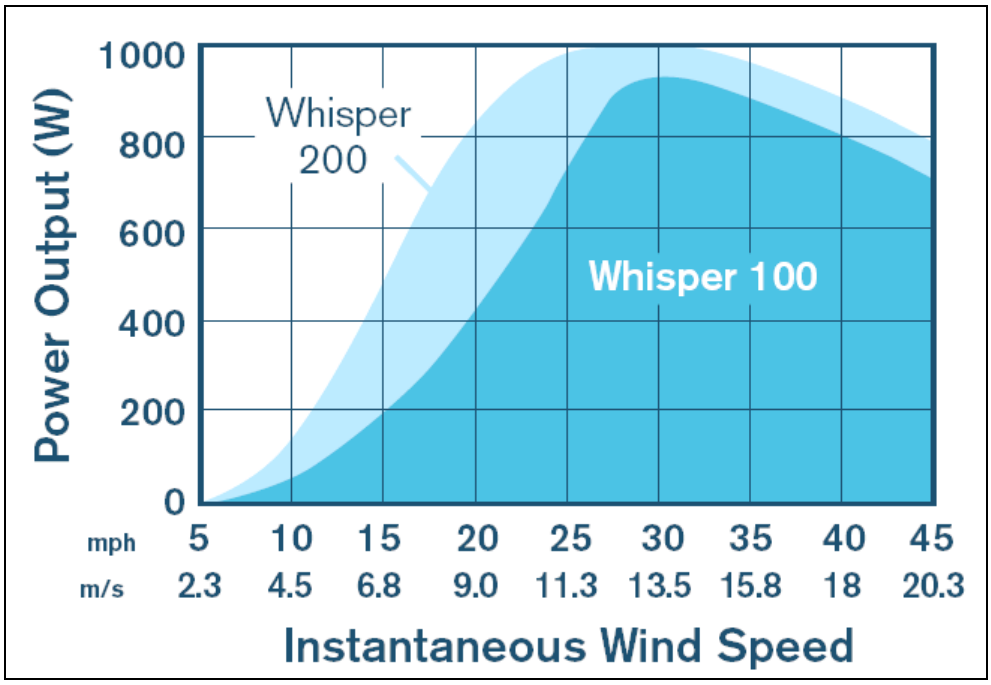

Figure 5.15 – Southwest Windpower's provided WH100 power curve

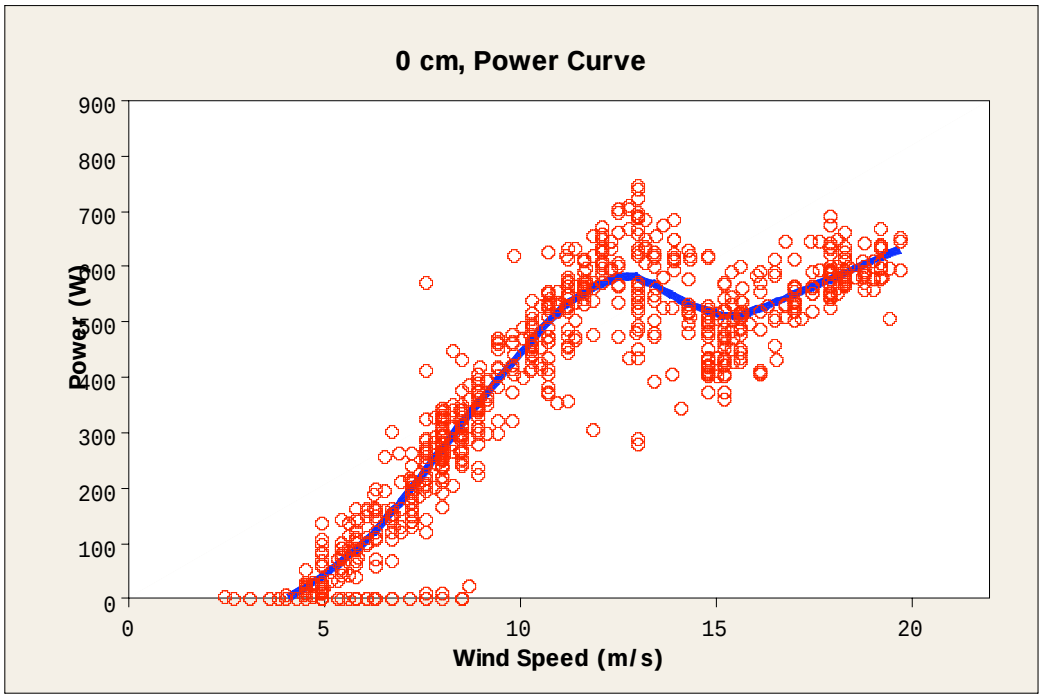

Figure 5.16 – 0 cm configuration, wind speed vs. power

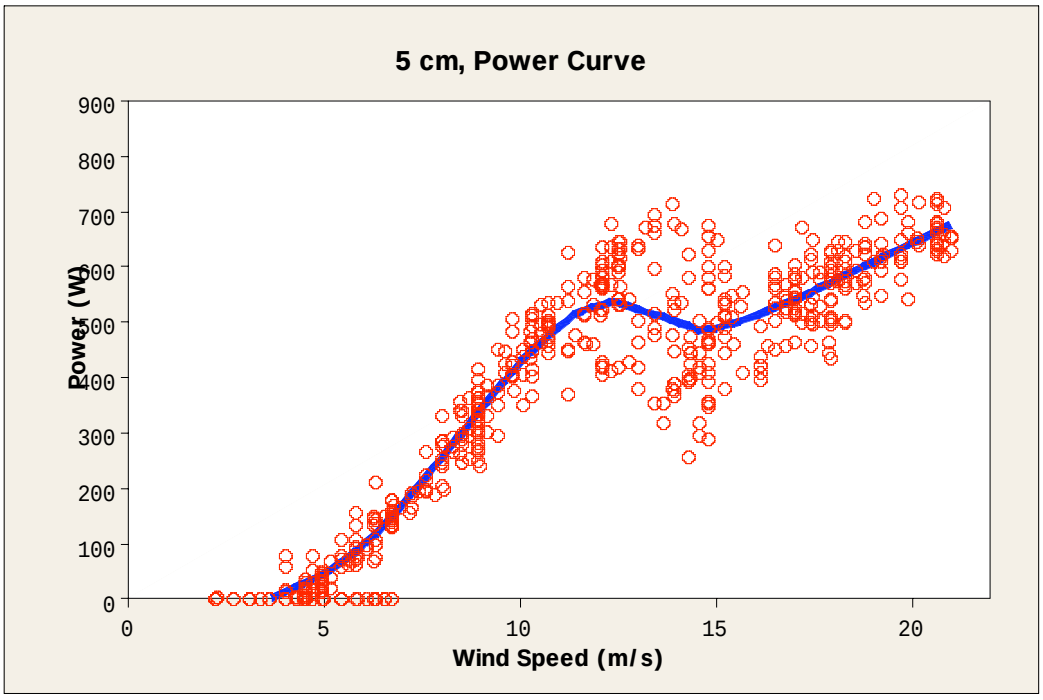

Figure 5.17 – 5 cm configuration, wind speed vs. power

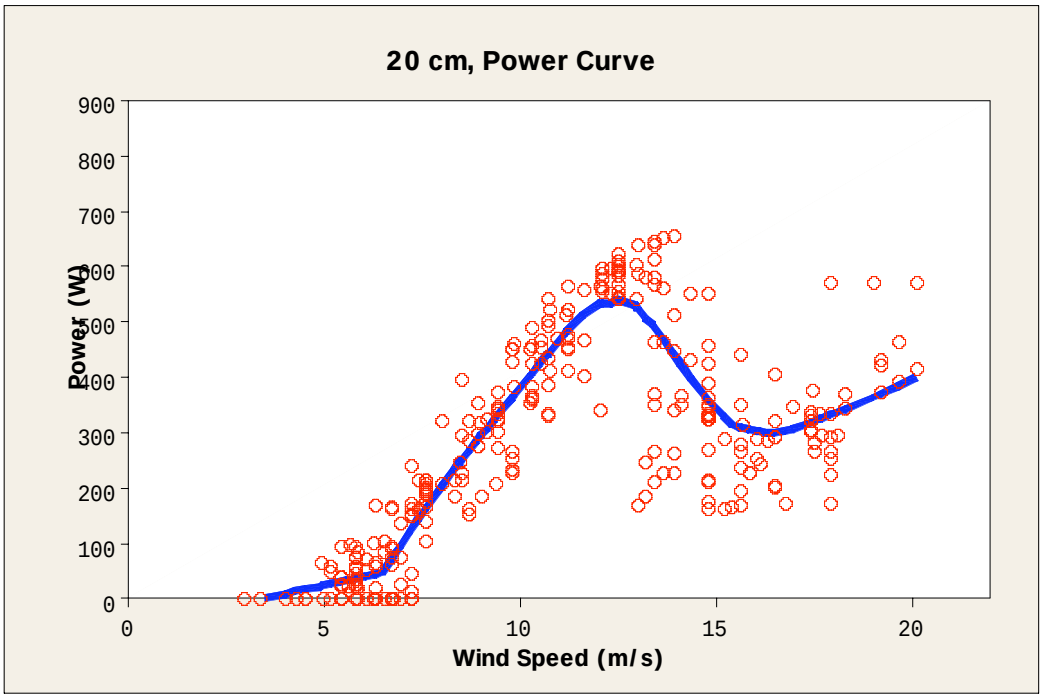

Figure 5.18 – 20 cm configuration, wind speed vs. power

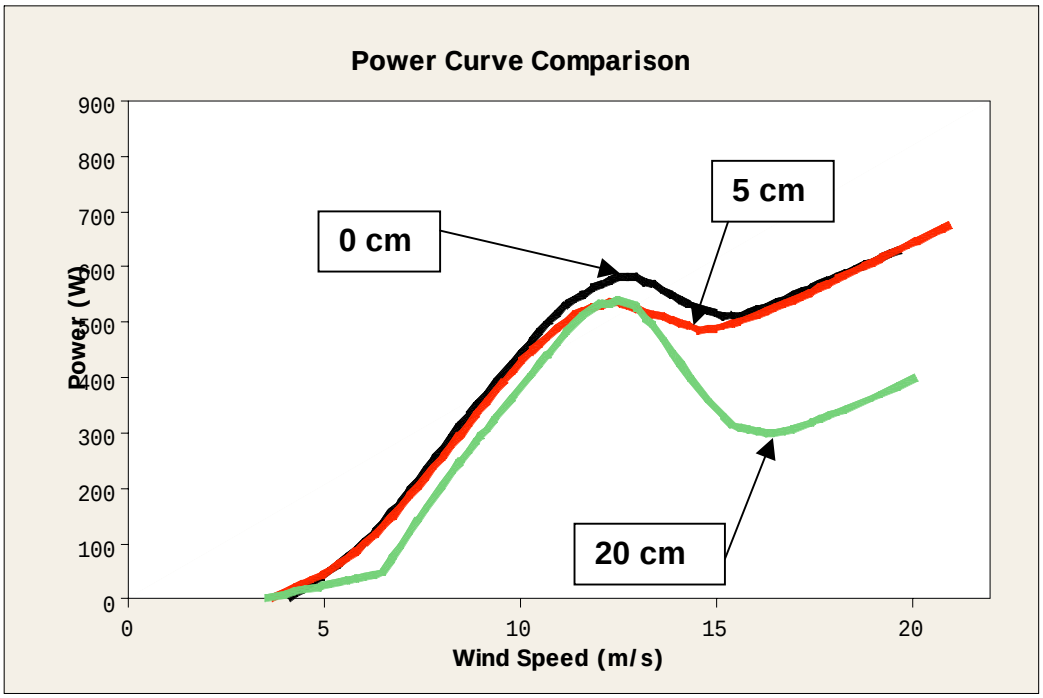

Figure 5.19 – Wind speed vs. power trend lines

As visible in the previous figure, the overall power curves tend to decrease with blade length. There is a small drop from the 0 cm to the 5 cm configurations and a notable drop when comparing them with the 20 cm configuration. While the 20 cm curve is consistently lower than the others its decrease is most significant once wind speed is past the turbine's rated speed. The rated speed, where optimal power output is typically reached, of 12.5 m/s remained roughly consistent across the three configurations.

Start up speed appears to be unaffected. This was expected as the nature of the blade taper was such that the chord length was substantially longer and the angle of attack was higher closest to the root and would operate most efficiently at lower, or start up, wind speeds. As such, reducing the blade length by cutting off the ends would have a limited effect on the start up speed.

5.6.2. Theoretical vs. Actual Power Production

Figure 5.20 below shows the power curve for the 20 cm configuration during the trials where furling was disabled as well as those when it was enabled. As one can see the power curve produced from a 'No Furl' condition rapidly exceeded the 900 W rated power of the WH100 at approximately 15 m/s, producing roughly three times the power as when furling was enabled.

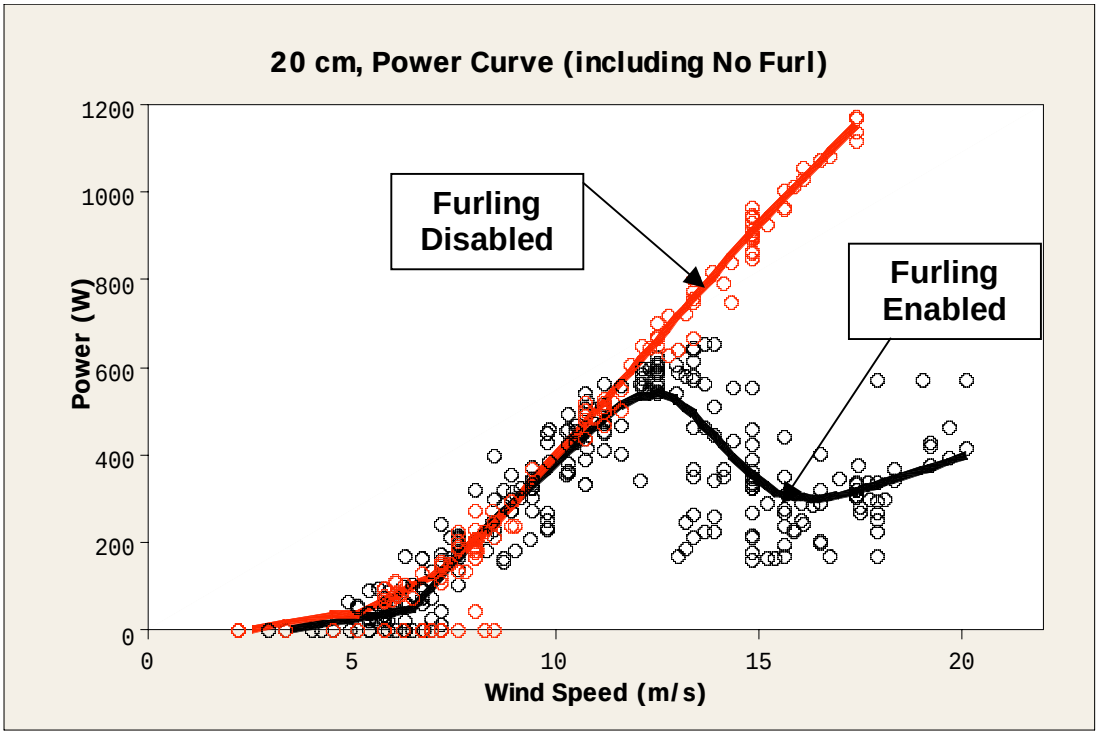

Figure 5.20 – 20 cm configuration (including No Furl), wind speed vs. power

Figure 5.21 highlights the difference between the 'No Furl' power curve and the theoretical maximum power curve. Applying Equation 2.4 gives the total available power in the wind (top curve) and according to Betz's Law, no more than 59.26% of the energy from the wind can be extracted by a turbine (the middle curve). Assuming the density of air during the day of the trials was 1.225 kg/m^3, the WH100 maintained an average efficiency of 24.6%[4], which is comparable with industry norms of 30-40%. Unfortunately Southwest Windpower does not provide an efficiency value for the WH100. Figure 5.22 compares the efficiency and power production as they related to wind speed.

[4] It is important to keep in mind that 24.6% is the efficiency of a system with modified blades and furling disabled.

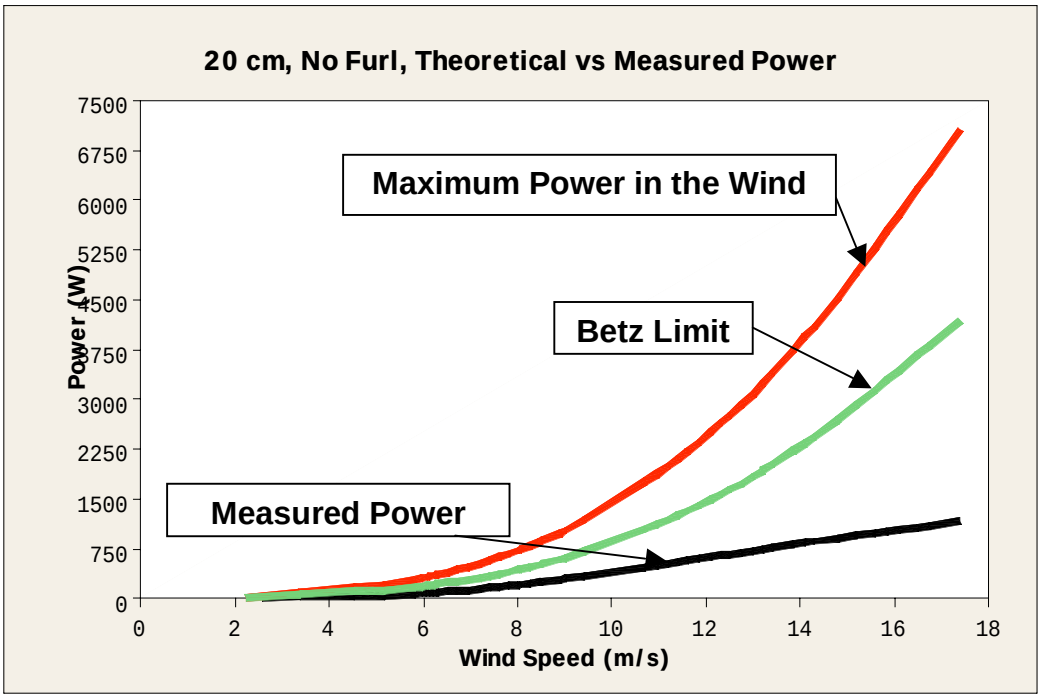

Figure 5.21 – Theoretical vs. actual power production, 20 cm configuration, No Furl

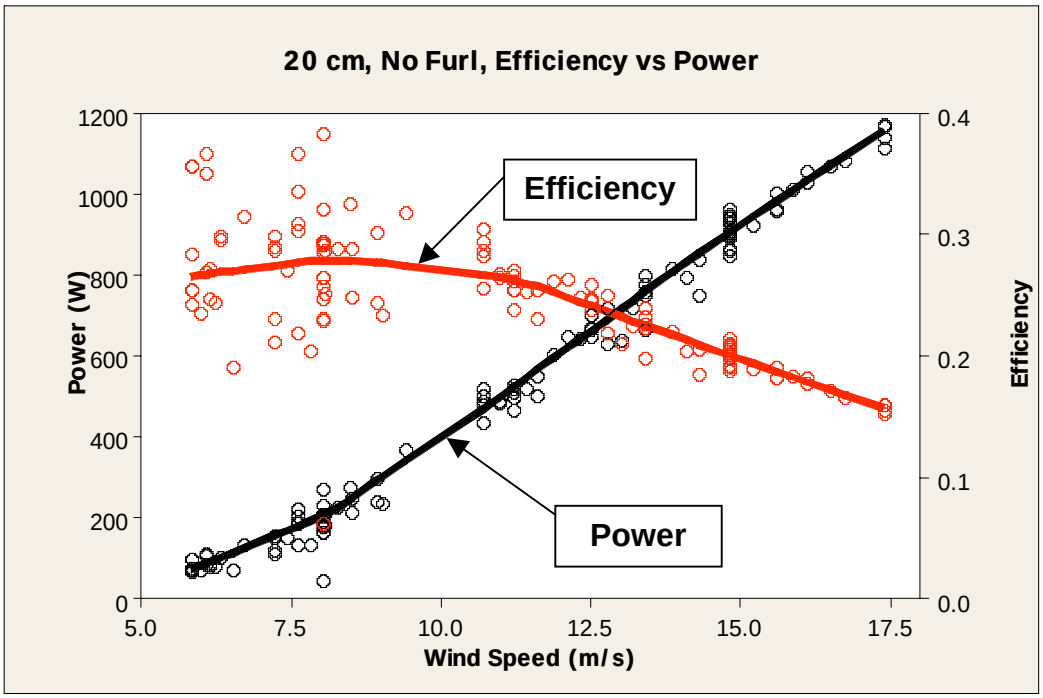

Figure 5.22 – Efficiency vs. power, 20 cm configuration, No Furl

5.6.3. Furl Extent

In Figures 5.23, 5.24 and 5.25, the furl extent curves for the 0 cm, 5cm, and 20 cm configurations as obtained during the field tests are shown. A comparison of all three configurations is available in Figure 5.26.

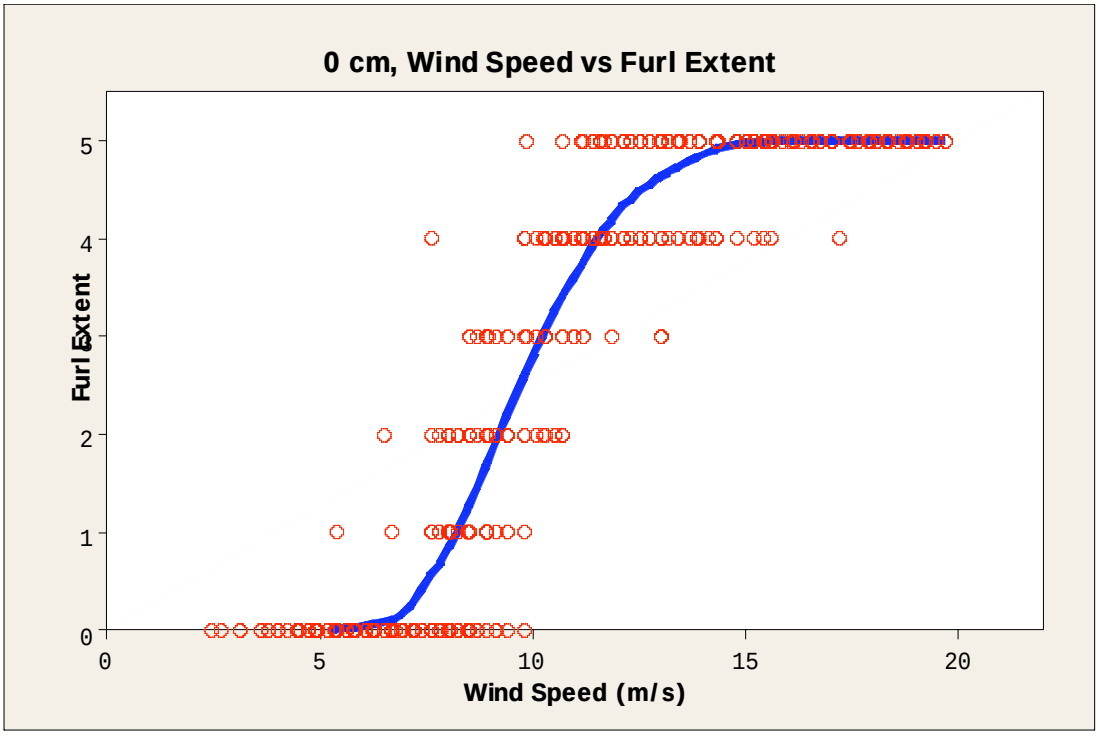

Figure 5.23 - 0 cm configuration, wind speed vs. furl extent
(Furl Extent represented by dimensionless scale of 0 to 5 as per Figure 5.6)

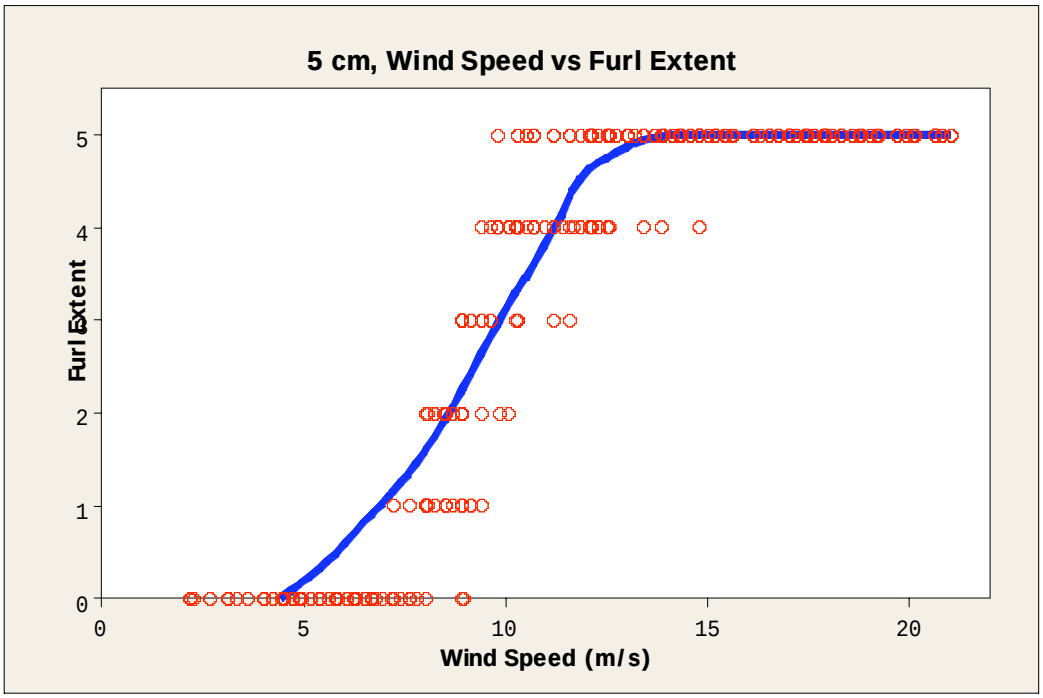

Figure 5.24 - 5 cm configuration, wind speed vs. furl extent
(Furl Extent represented by dimensionless scale of 0 to 5 as per Figure 5.6)

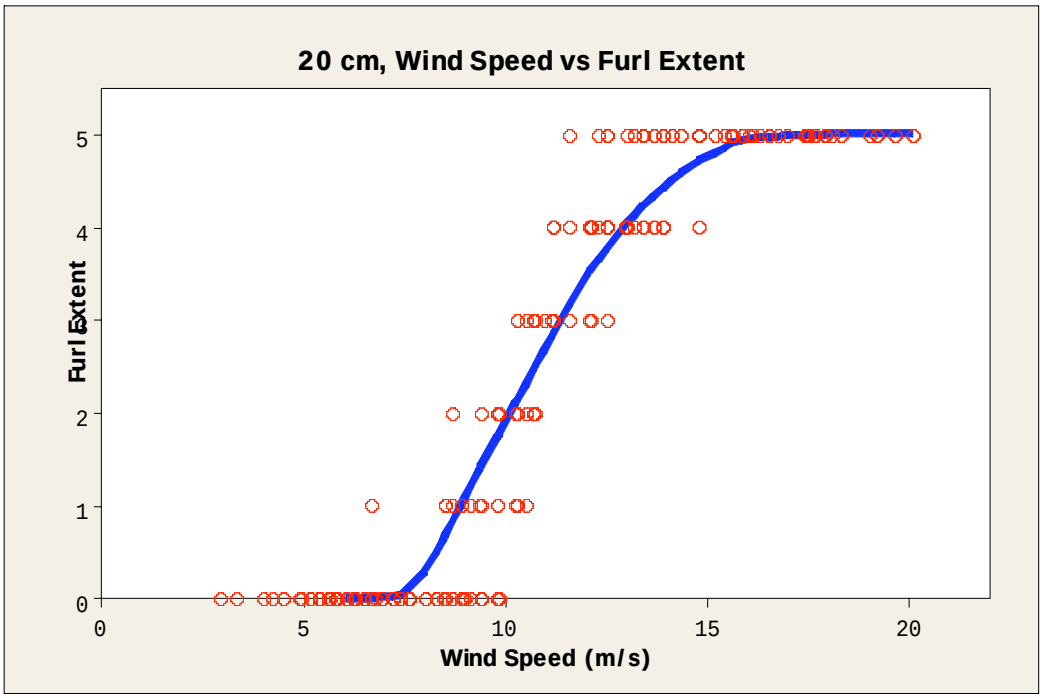

Figure 5.25 - 20 cm configuration, wind speed vs. furl extent
(Furl Extent represented by dimensionless scale of 0 to 5 as per Figure 5.6)

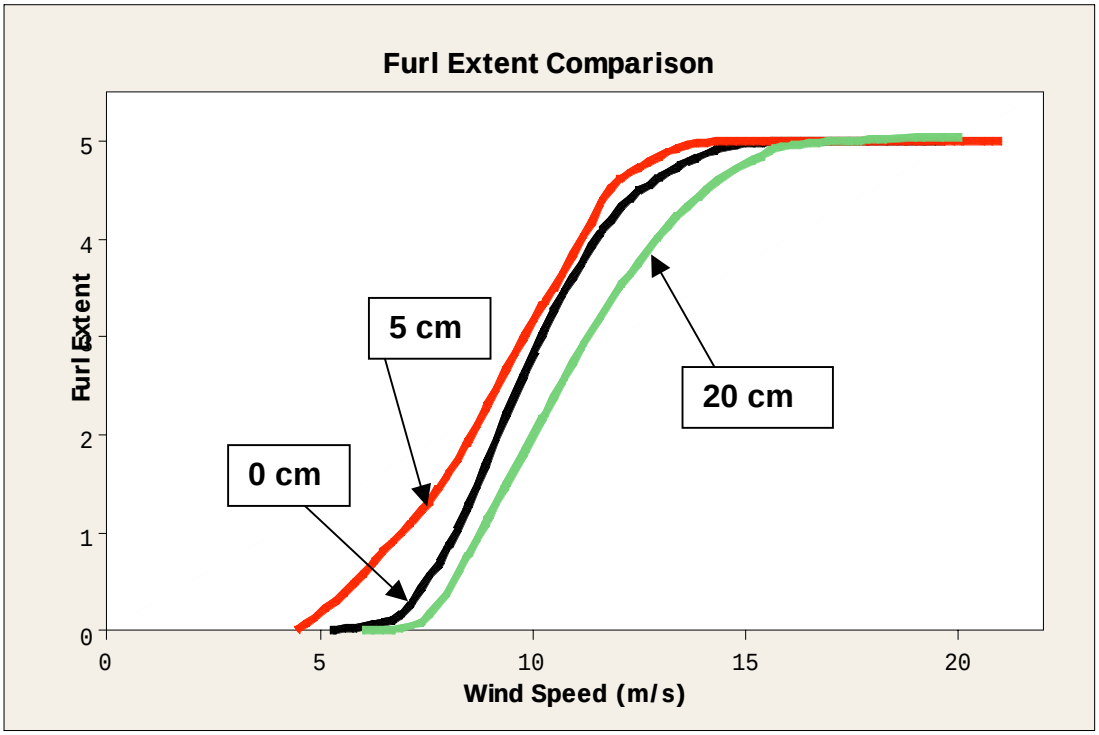

Figure 5.26 - Wind speed vs. furl extent trend lines
(Furl Extent represented by dimensionless scale of 0 to 5 as per Figure 5.6)

The previous figure shows that furling occurred at the lowest wind speeds while using the 5 cm configuration and not with the unmodified 0 cm configuration, as one would expect. The 20 cm configuration did result in delaying the furling effect, by roughly 2 m/s from the 5 cm configuration.

The 5 cm configuration started furling at slightly less than 5 m/s while the 0 cm and 20 cm configurations began at around 6 m/s and 7.5 m/s respectively. This curious result may be a function of the competing mechanisms relating to driving force and preventative force. In other words, the reduced axial force caused by blade shortening

may initially be less than the reduction of angular momentum that encourages furling. This relationship appears to change in a non-linear fashion as the blades are shortened further.

5.7. Assessment of Experiment

5.7.1. Setup

The experimental concept has proven sound. The truck and trailer setup was shown to be an effective and convenient test apparatus. The support frame mounted on the trailer is adaptable and can be used for testing a variety of other small turbines, the skeleton frame was securely built and the turbine mount can be easily replaced with one of a different diameter for minimal cost. One consideration for future tests would be to include the cost of fuel for the truck in the project budget.

The biggest area for improvement is the data acquisition setup. The anemometer updated the displayed wind speed every 2 seconds, and was on a 2 second delay, for which compensation was needed in the analysis. One recommendation would be to use an anemometer compatible with the WH100 controller board, which would then display the wind speed in the same manner as the power output, which is once a second.

Transferring information from the data capture video to a spreadsheet was a tedious and time consuming process, as it required going through nearly and hour of video frame-by-frame. A power output display and anemometer with data logger capability would be greatly advantageous when analyzing data.

If the same displays (or similar) are used it would be useful to have a powerful external light source to compensate for the diminishing light near the end of the day. It would also be prudent to view the data capture video on the laptop at regular intervals. Special attention should be made to avoid any data masking reflections in any of the data displays or video display.

If improved resolution on the furling angle is required then gradations with an indicator stick should be marked on the underside of the turbine. A video camera can be trained on these gradations to capture the more accurate furling extent. This video would need to be synchronized with the data capture video.

5.7.2. Procedure

The trials were completed by trying to maintain a steady wind speed, then increasing it to another and maintaining it and so on. A more accurate representation of steady state responses might be found by very slowly ramping up to maximum wind speed and then

very slowly back down to zero. There was some scatter caused by the momentum of the blades and time delay in reacting to the change in wind speed.

Bumpy portions in the road, due to construction, caused the trailer to bounce that caused slight variations in the furling mechanisms. If possible, use only pristine roadways.

Another factor worth examination is the effect of sudden wind gusts on the furling mechanism. This could be achieved using a simple pulley system with a rope loosely attached at one end to a turbine blade, effectively eliminating rotation while ramping up to speed. Once the desired wind speed is reached, the spotter could pull the rope to reactivate the turbine.

5.8. Conclusions

While there wasn't an appreciable difference in the wind speeds at which furling occurred from the 0 cm to the 20 cm configuration, there was a significant decrease in electrical power production. One can then conclude that these modifications are not suitable for producing the desired increase in survivability.

6. Conclusions and Recommendations

This work covered a range of investigation into the failure and survivability of the WH100 at hilltop locations in Labrador.

A statistical analysis of site-specific parameters indicated the best indicators of turbine failure potential at a given site were found to be wind speed and turbulence. A strong and significant positive correlation was found between turbine failure and these factors. A regression analysis failed to produce a useful predictive model and recommendations were made to Bell-Aliant for a more specific data collection program, which has already begun. Once relevant data has been captured, the stated objective of developing a quantitative tool for evaluating site suitability can be achieved.

A brittle, flexural failure of the nacelle was found to be the most common catastrophic failure experienced by the WH100. The crack initiates from a single furling occurrence causing stress to concentrate in a notch designed into the cast nacelle. The crack propagates immediately to the other side, separating the top portion of the nacelle into two pieces. This failure is most likely to occur at low temperatures during periods of very strong steady winds, or extremely gusty winds.

In an attempt to mitigate the above failure, a test program was undertaken, whereby the effect of modifying blade length on the turbine's response characteristics was

investigated. While there wasn't an appreciable difference in the wind speeds at which furling occurred over the experimental range, there was a notable decrease in electrical power production. One can then conclude that these modifications were not suitable for producing the desired increase in survivability, while maintaining strong power production.

The successful field tests were sufficient to prove that the experimental concept is sound.

6.1. Attributes of a Robust Small Turbine

If one was to look for a small robust turbine to operate in a harsh isolated environment there are several design elements that are important for survivability. From information found in the literature review, observations made and insights had during this research the following characteristics should be considered in the design or purchase of such a turbine. All components, and the system as a whole, should be tested in cold temperatures, possibly with simulated icing conditions, to ensure a high probability of successful operation. A summary of this section can be found in Table 6.1.

Winch up towers, made from low temperature steel with hot dip galvanized bolts have been shown to work well. All electrical wires and connections should have a good low temperature rating and should remain ductile in the lowest operating ranges. The generator should have the permanent magnets placed on the rotating external casing

(rotor) as opposed to the internal stator to help keep them in place during operation. There should be an automatic shutdown (and subsequent startup) built into the system controls, for when certain wind speeds and temperatures are exceeded. Use synthetic lubricants if needed.

The turbine itself should have a higher than industry average mass per swept area. This additional bulk should come partly from the robust nacelle design, which should be made of low temperature steel, cast aluminum or a metal of similar mechanical properties, and should be thoroughly examined, perhaps using finite element techniques, to ensure minimal stress concentrations.

If the turbine has an upwind orientation then furling is the recommended overspeed protection, and the tail vane should have a long tail and small fin to keep yaw rate to a minimum. If a downwind orientation is selected the overspeed protection should include coning of the rotor, aided by hinged connections.

The blades should be made from glass or carbon reinforced plastic or wood laminate with polyurethane tape for leading edge protection. There should be minimal taper on the blades and blade thickness should not increase substantially as it approaches the root. Blade flutter should be avoided and a tip speed ratio of five (optimal) or lower should be reached at the rated speed. A black, low adhesion coating should be used on the blades (and possibly the nacelle), such as *StaClean*.

Table 6.1 – Attributes of a Robust Small Turbine

Component	Characteristics
General	- All components tested in low temperatures - Have higher than average mass per swept area
Tower	- Winch up - Made from low temperature steel, with hot dip galvanized bolts
Generator	- Permanent magnets placed on rotating exterior casing
Other Electrical Components	- Good low temperature ratings - Remain relatively ductile in low temperatures
Controls	- Automatic shutdown if certain wind speeds or temperatures are exceeded
Nacelle	- Robust design - Low temperature steel, aluminum, or similar - Minimal stress concentrations - Possibly use black, low adhesion coating
Overspeed Protection	- Furling (upwind rotor) - Rotor coning (downwind rotor), with hinged connections
Tail	- Long tail, small fin
Blades	- Made from glass or carbon reinforced plastic, or wood laminate with polyurethane tape on leading edge - Minimal taper - Thickness should not increase substantially as it approaches the root - Avoid blade flutter - Tip speed ratio of < 5 at rated speed - Black, low adhesion coating

6.2. Recommendations for Future Research

The following improved data collection should be undertaken to help improve the basis for future site selection. The collection of site-specific temperature, wind speed and direction throughout the year would be an asset. As each of these sites sits on a hilltop, one can assume that local topography plays an important role in mean wind speed and gust strength. A record of the location of each turbine within each site would also be

useful. Locations relative to the edge of a steep incline and to prevailing wind direction as well as its position within the array are all potentially important considerations. Similar meteorological stations and local situational data should also be collected and examined for sites under consideration for turbine implementation. Video surveillance, similar to security installations would be integral to determining exact conditions and turbine behaviour at failure.

Records of maintenance and field modifications of each turbine repaired or replaced, including date, thorough photographic evidence and a note of possible weather conditions at the time of failure would provide great insight. Consistent and reliable daily power production and diesel start data would help eliminate uncertainty in analysis. Clear and reliable daily power production data is critical to developing a useful model as it is used to determine the only dependent variable in the study: turbine failure.

With regard to the turbine failure analysis a finite element analysis would prove to be invaluable in determining the conditions during failure. If the results of such an analysis could be compared with real life data or an accurate furling simulation, potentially significant improvements could be made to the turbine design.

Within the experimental program, the greatest room for improvement exists within the data acquisition and capture setup. Expansion of the program is also a possibility due to the adaptable nature of the trailer-mounted apparatus. Things to be considered include a

finer resolution of furling data, body stresses within the turbine and tower, comparison of various, similar sized, turbines and the effect of strong gusts.

6.3. Recommendations for Bell-Aliant

The recommendation to Bell-Aliant is to systematically replace WH100's as they experience catastrophic failure with a turbine of comparable output and size. There are several turbines on the market, such as the Bergey XL.1, that are likely better candidates for the severe conditions at hill-top sites in Labrador. Alternatively, installing turbines of a lager rated capacity, such as the 2.5 kW Proven Energy turbine or Southwest Windpower's Skystream 3.7 (currently being tested by Bell-Aliant) should be considered for future sites.

When considering adding a wind power installation to other Labrador sites a short-term wind assessment should be made. A record of wind speeds throughout the winter season would be mode useful in indicating which sites should be avoided, having the strongest and most turbulent winds.

Once other turbines have been installed in the field and an operational history has accumulated, it may be useful to revisit some of the analysis and tests performed in this thesis to further develop a rational basis for continued and improved development.

7. References

Aarnio, E. and Partonen, S. (2000) “Operational Experience of Arctic Wind Farms” BOREAS V Conference Proceedings, Levi, Finland

Allen, T.T. (2006) “Introduction to Engineering Statistics and Six Sigma: Statistical Quality Control and Design of Experiments and Systems” Springer, London

Arifujjaman, Md. et al (2008) “Energy capture by a small wind-energy conversion system” Applied Energy 85, pp. 41-51

AWEA (2008) “Wind Industry Standards and Technical Information” American Wind Energy Association, available at http://www.awea.org/standards/, United States.

Bass, L. and Weis, P. (1981) “Hazards, Safety and Small Wind Energy Conversion Systems” Journal of Products Liability, Vol. 4, pp. 203-214

Bechly, M.E., Clausen, P.D., Ebert, P.R., Pemberton, A., Wood, D.H. (1996) “Field testing of a prototype 5 kW wind turbine” Proceedings of the 18th BWEA Conference, London, UK.

Bianco, G.L., Honorati, O., Mezzetti, F. (1996) “Small-Size Stand Alone Wind Energy Conversion System for Battery Charging” Proceedings of 31st Universities Power Engineering Conference, pp. 62-65, Sweden

Bota, G., Cavaliere, M., Viani, S., Pospisil, S (1998) “Effects of hostile terrains on wind turbine performances and loads : The Acqua Spruzza experience” Journal of Wind Engineering and Industrial Aerodynamics 74-76, pp 419-431.

British Wind Energy Association (1994) “Best Practice Guidelines for Wind Energy Development” BWEA, UK.

Bruneau, S. (2006) Personal communication with the author, St. John’s, Newfoundland.

Bruneau, S., Roberts, J., White, G. and Card, J. (2008) “Controlled Velocity Testing of a Micro Wind Turbine with Varying Blade Geometries” Proceedings of the Newfoundland and Labrador Electrical and Computer Engineering Conference, St. John’s, Newfoundland

Callister, W.D. (2000) “Materials Science and Engineering: An Introduction” John Wiley & Sons, Inc., Toronto, Canada.

Clausen, P.D. and Wood, D.H. (2000) “Recent Advances in Small Wind Turbine Technology” Wind Engineering Vol. 24, No. 3, pp. 189-201

Cooper, K.R. (2004) “Pickup Truck Aerodynamics – Keep Your Tailgate Up” SAE International, 2004 SAE World Congress, Michigan, United States

Davis, D., Hansen, C. (2000) “Results of the Whisper 900 Testing in Spanish Fork, Utah” Proceedings of the National Wind Technology Center Furling Workshop, United States

Ebert, P.R., Wood, D.H. (1995) “On the dynamics of tail fins and wind vanes” Journal of Wind Engineering and Industrial Aerodynamics, Vol. 56, pp 137-158

Gaudiosi, G. et al. (1984) “Wind Energy for Small Isolated Users (Piedmont – Val D’Aosta)” European Wind Energy Conference Proceedings, pp. 650-655

Giguere, P. and Selig. M.S. (1997) “Low Reynolds number airfoils for horizontal axis wind turbines” Wind Engineering, Vol 21, pp. 367-380.

Gipe, P. (2004) “Wind Power: Renewable Energy for Home, Farm, and Business” Chelsea Green Publishing Company, United States

Gipe, P. (1999) “Wind Energy Basics: A Guide to Small and Micro Wind Systems” Chelsea Green Publishing Company, United States

Hibbeler, R.C. (2003) “Mechanics of Materials, 5th Edition” Pearson Education, Inc., New Jersey, United States.

Ichikawa, Y. et al (2001) “Electric load-brake control for a small wind-turbine operating in mountainous winds” Wind Engineering Vol. 25, No. 2, pp.71-80

Kaufman, J.G. (1999) “Properties of Aluminum Alloys: Tensile, Creep, and Fatigue Data at High and Low Temperatures” ASM International, United States

Kentfield, J.A.C. (1996) “The Fundamentals of Wind-driven Water Pumpers” Gordon & Breach Science Publishers, The Netherlands.

Kimura, S., Ishizawa, K., Susuki, K. (1991) “Development and Low Temperature Test of the Generator of a Wind Turbine System for Antarctica” Wind Engineering, Vol. 15, No. 2

Laakso, T. et al (2005) “Expert Group Study on Wind Energy Projects in Cold Climates” Submitted to the Executive Committee of the International Energy Agency Programme for Research and Development on Wind Energy Conversion Systems

Laakso, T., Ronsten, G. (2004) “Operation of Blade Heating System in Different Icing Conditions” New Icetools internal project report, Finland

Laakso, T. et al (2003) “State-of-the-art of wind energy in cold climates” International Energy Agency R&D Wind Annex – Wind Energy in Cold Climates

Leuven, J.V. (1984) “The Economic Feasibility of Small-Scale Wind Energy Conversions Systems” European Wind Energy Conference Proceedings, pp. 814-819

Liu, A. (2005) “Mechanics and Mechanisms of Fracture: An Introduction” ASM International, United States.

Maissan, J.F. (2001) “Wind Power Developcment in Sub-Arctic Conditions with Severe Rime Icing” Yukon Energy Corporation, Canada

Manitoba Hydro (2004) “Clarification of Wind Turbine Cold Weather Considerations: Manitoba Hydro Summary” *Manitoba Hydro* and the Nisichawayasihk Cree Nation , Regulatory Document, Canada

Manwell, J.F. et al (2006) “Wind Energy Explained: Theory, Design and Application” John Wiley & Sons, Ltd, England

Mesinger, F. *et al* (2006) North American Regional Reanalysis. Bulletin of the American Meteorological Society, v 87, n 3, March, 2006, p 343-360.

Norton, J.H. (1982) “Small Wind Energy Conversion Systems, Application and Performance” Energy-Sources Technology Conference & Exhibition Proceedings, pp.45-50

Quaschning, V. (2005) “Understanding Renewable Energy Systems” Earthscan, United States

Roberts, J. *et al* (2007) “Performance Analysis of Off-Grid Micro Wind Energy Conversion Systems in Harsh Environments” Proceedings of Canadian Wind Energy Association National Conference, Quebec, Canada

Rohatgi, J. (1996) “An Analysis of the Influence of Atmospheric Stability on Vertical Wind Profiles – Its Influence On Wind Energy And Wind Turbines” Wind Engineering Vol. 20 No. 5, pp. 319-332

Rong, J. (1991) “Icing Effects on a Horizontal Axis Wind Turbine” Master of Engineering Thesis, Faculty of Engineering and Applied Science, Memorial University of Newfoundland, Canada

Ross, B. (1995) “Investigating Mechanical Failures: The metallurgist’s approach” Chapman and Hall, UK.

Sagrillo, P. (1995) “Apples and Oranges: An update” Home Power, Vol. 47, pp. 36-47.

Schaffner, B. (2002) “Wind Energy Site Assessment in Harsh Climatic Conditions” METEOTEST internal report, Switzerland.

Southwest Windpower (2008) “Whisper 100 Wind Turbine” available at http://www.windenergy.com/products/whisper_100.htm

Spiers, D.J. (1995) “Predicting the service lifetime of lead/acid batteries in photovoltaic systems” Journal of Power Sources, Vol. 53, pp. 245-253

Stull, R.B. (1988) “An introduction to boundary layer meteorology” Kluwer Academic Publishers, Dordrecht, The Netherlands.

Tammelin, B. et al (1997) “Wind Energy Production in Cold Climate” Proceedings of the European Wind Energy Conference, Ireland.

Tammelin, B., Holttinen, H., Morgan, C., Richet F., Seifert, K., Santti, Volund, P. (1998) "Wind Energy Production in Cold Climates" Proceedings of Boreas IV Conference, Finland.

Tavner, P. et al (2006) "Influence of Wind Speed on Wind Turbine Reliability" Wind Engineering Vol. 30, No. 1, pp.55-72

The Aluminum Association Inc. (2008) "Standards for Aluminum Sand and Permanent Mold Castings, 15th Edition" The Aluminum Association Inc., United States

Tokuyama, H. et al (2002) "Experimental Determination of Optimum Design Configuration for Micro Wind Turbines at Low Wind Speeds" Wind Engineering Vol. 26, No. 1, pp. 39-49

Twidell, J. (1998) "Fundamentals of Wind-Power Technology and Environmental Impact: An Educational Aid" Wind Engineering Vol. 22, No. 5, pp. 235-241

Walker, B. (1999) "Renewable energy in outback Australia" Proceedings of the World Renewable Energy Congress, Perth, Australia.

Watson, G.R. (1981) "Some Practical Aspects of Small Wind Energy Conversion Systems" Northumbrian Energy Workshop Ltd, England

WWEA (2008) World Wind Energy Association website available at www.wwea.com

Appendix A – Daily Cumulative Wind Turbine Power Output from Bell-Aliant

Appendix B – Stress-Strain Curves from Tensile Tests

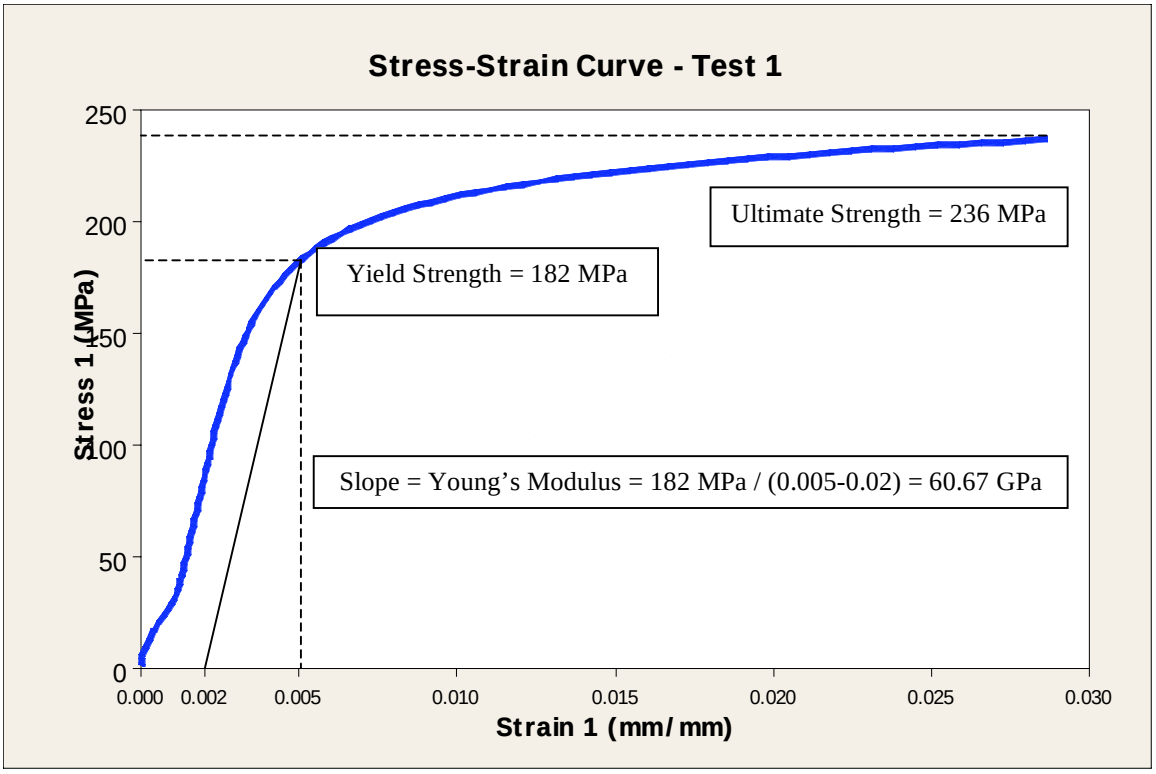
Stress-Strain Curve - Test 1
Stress 1 (MPa)
250
200
150
100
50
0
0.000
0.002
0.005
0.010
0.015
0.020
0.025
0.030
Strain 1 (mm/mm)
Ultimate Strength = 236 MPa
Yield Strength = 182 MPa
Slope = Young's Modulus = 182 MPa / (0.005-0.02) = 60.67 GPa

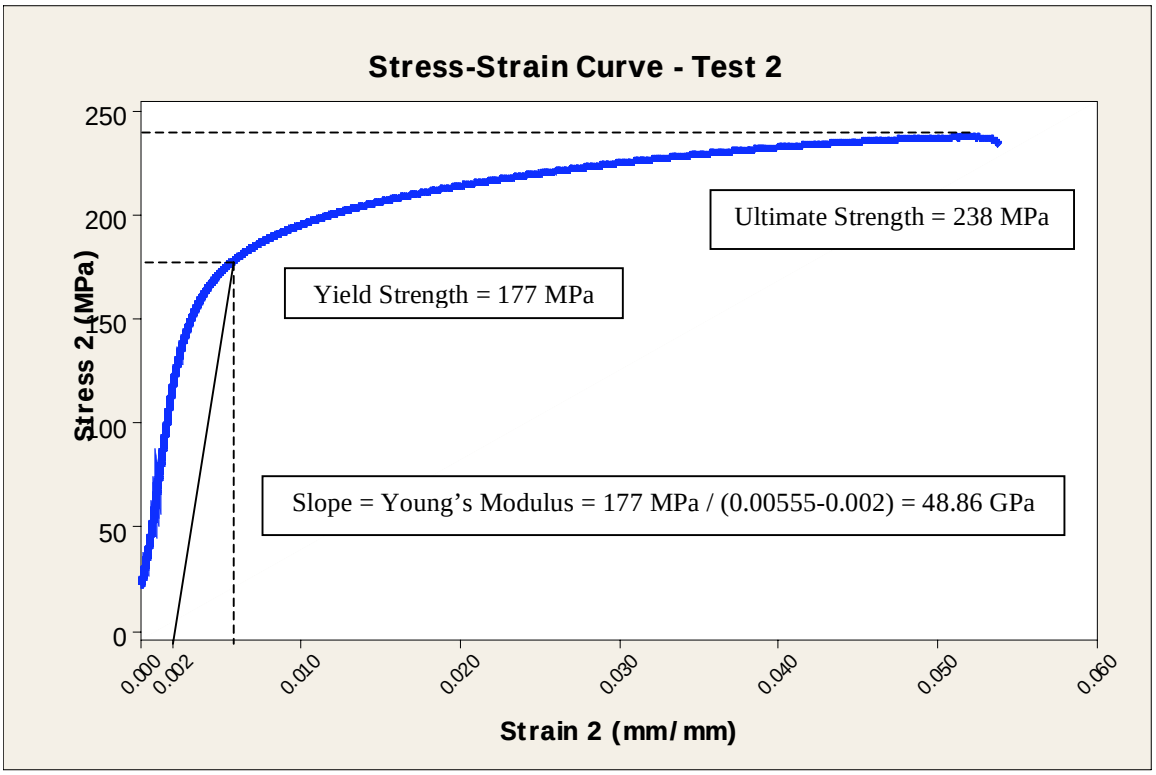
Stress-Strain Curve - Test 2
Stress 2 (MPa)
250
200
150
100
50
0
0.000
0.002
0.010
0.020
0.030
0.040
0.050
0.060
Strain 2 (mm/mm)
Ultimate Strength = 238 MPa
Yield Strength = 177 MPa
Slope = Young's Modulus = 177 MPa / (0.00555-0.002) = 48.86 GPa

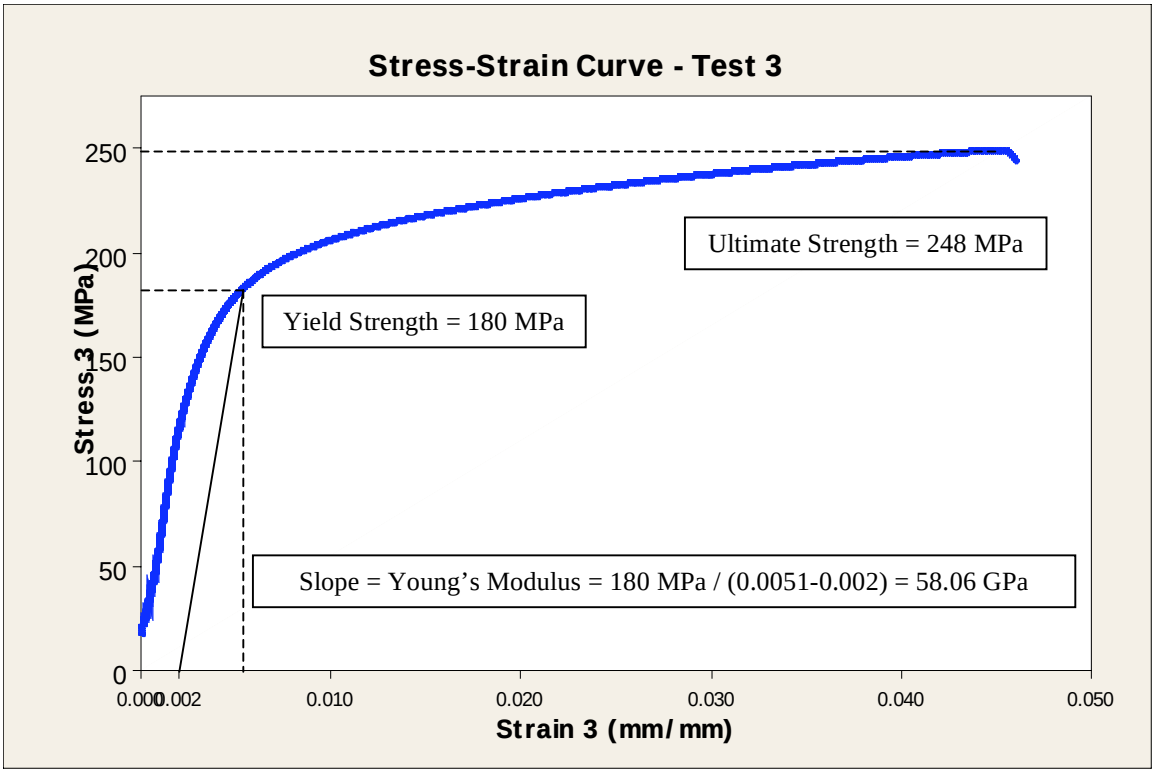
Stress-Strain Curve - Test 3
Stress_3 (MPa)
Strain 3 (mm/mm)
Ultimate Strength = 248 MPa
Yield Strength = 180 MPa
Slope = Young's Modulus = 180 MPa / (0.0051-0.002) = 58.06 GPa
0
50
100
150
200
250
0.000
0.002
0.010
0.020
0.030
0.040
0.050

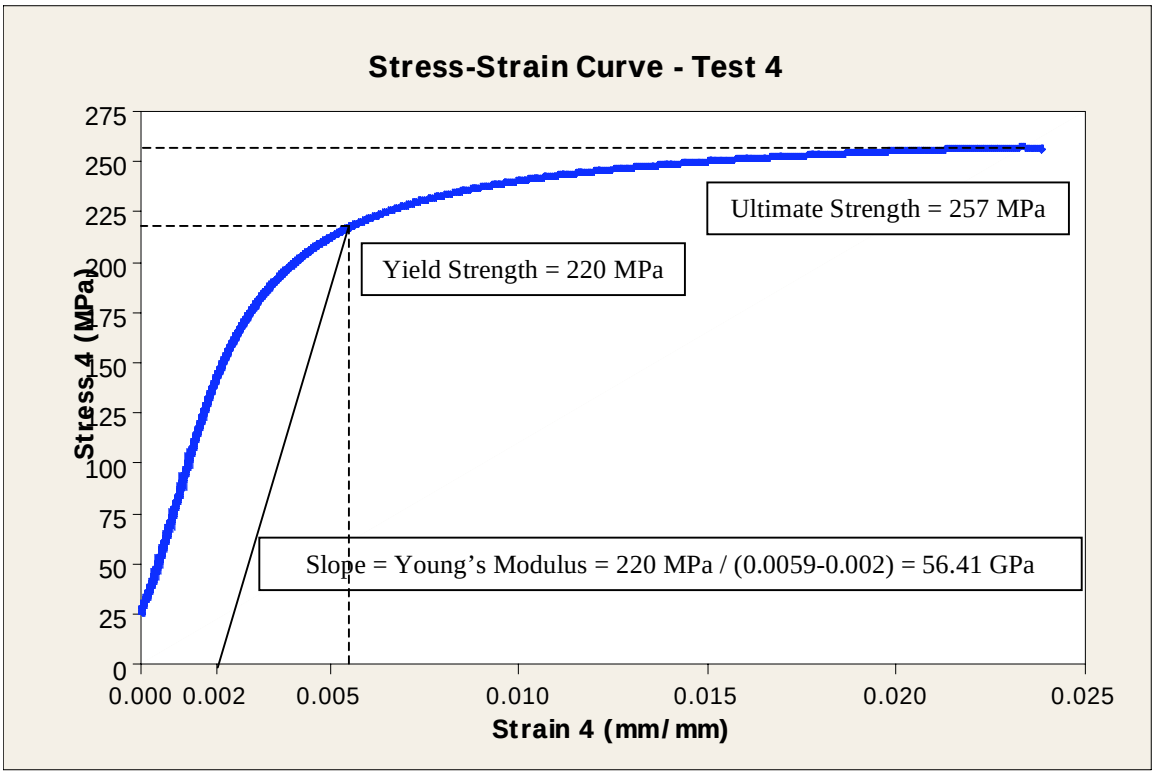
Stress-Strain Curve - Test 4
Stress_4 (MPa)
Strain 4 (mm/mm)
Ultimate Strength = 257 MPa
Yield Strength = 220 MPa
Slope = Young's Modulus = 220 MPa / (0.0059-0.002) = 56.41 GPa
0
25
50
75
100
125
150
175
200
225
250
275
0.000
0.002
0.005
0.010
0.015
0.020
0.025

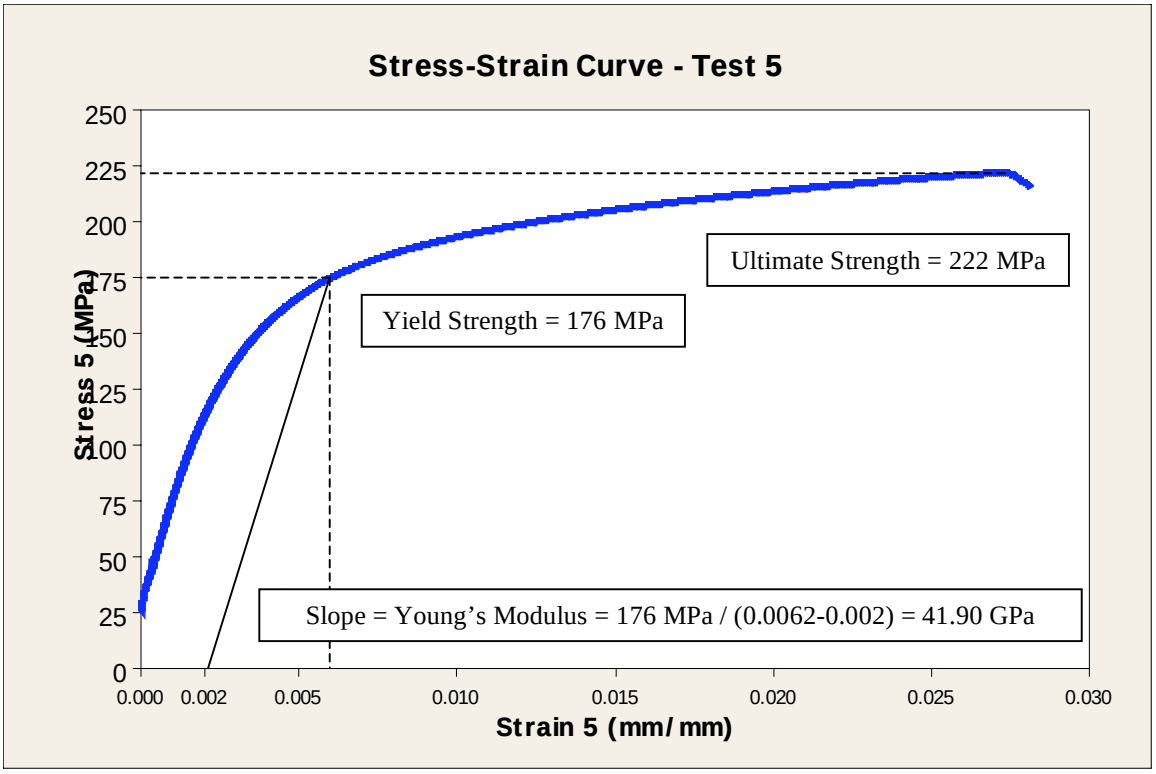
Stress-Strain Curve - Test 5
Stress 5 (MPa)
Strain 5 (mm/mm)
Ultimate Strength = 222 MPa
Yield Strength = 176 MPa
Slope = Young's Modulus = 176 MPa / (0.0062-0.002) = 41.90 GPa
0
25
50
75
100
125
150
175
200
225
250
0.000
0.002
0.005
0.010
0.015
0.020
0.025
0.030

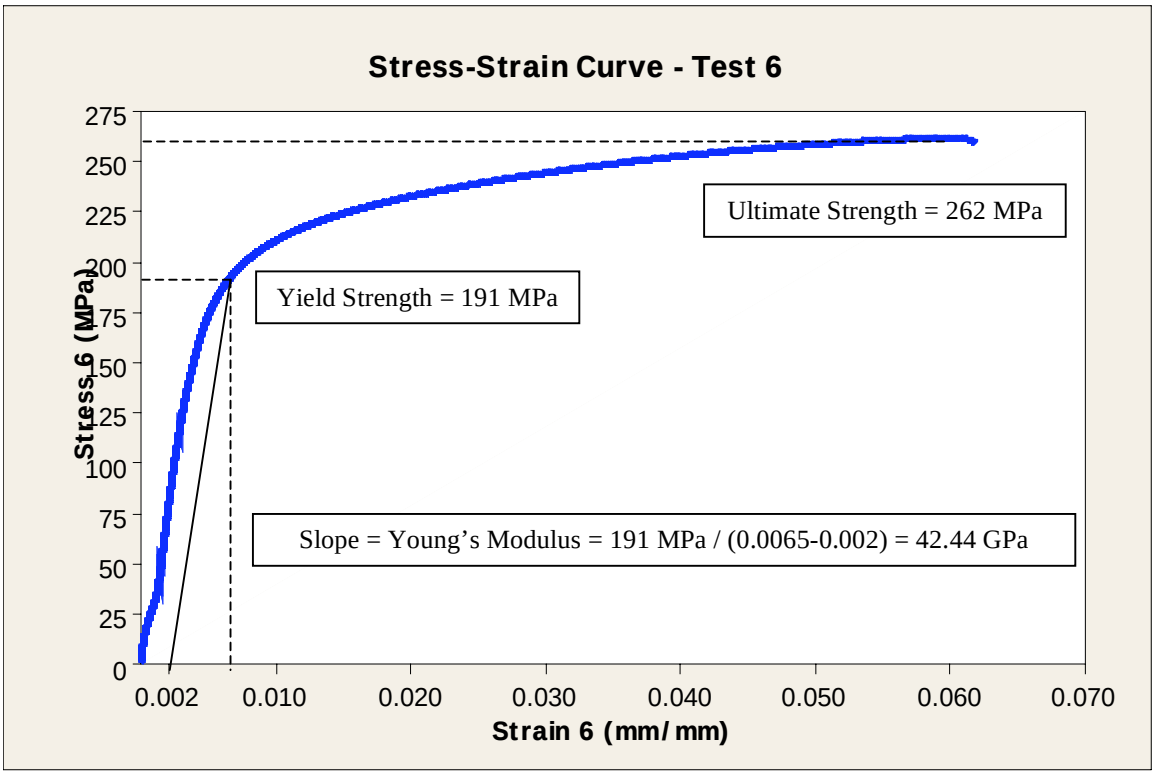
Stress-Strain Curve - Test 6
Stress 6 (MPa)
Strain 6 (mm/mm)
Ultimate Strength = 262 MPa
Yield Strength = 191 MPa
Slope = Young's Modulus = 191 MPa / (0.0065-0.002) = 42.44 GPa
0
25
50
75
100
125
150
175
200
225
250
275
0.002
0.010
0.020
0.030
0.040
0.050
0.060
0.070

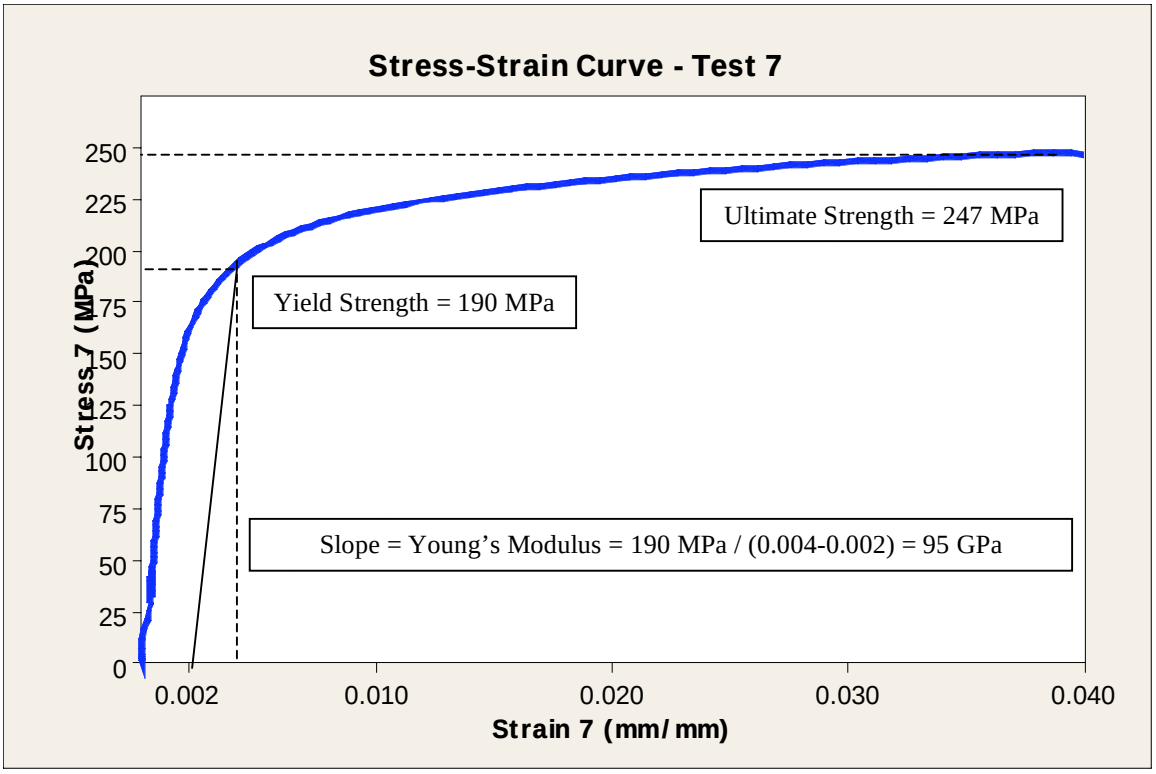
Stress-Strain Curve - Test 7
Stress_7 (MPa)
250
225
200
175
150
125
100
75
50
25
0
0.002
0.010
0.020
0.030
0.040
Strain 7 (mm/mm)
Ultimate Strength = 247 MPa
Yield Strength = 190 MPa
Slope = Young's Modulus = 190 MPa / (0.004-0.002) = 95 GPa

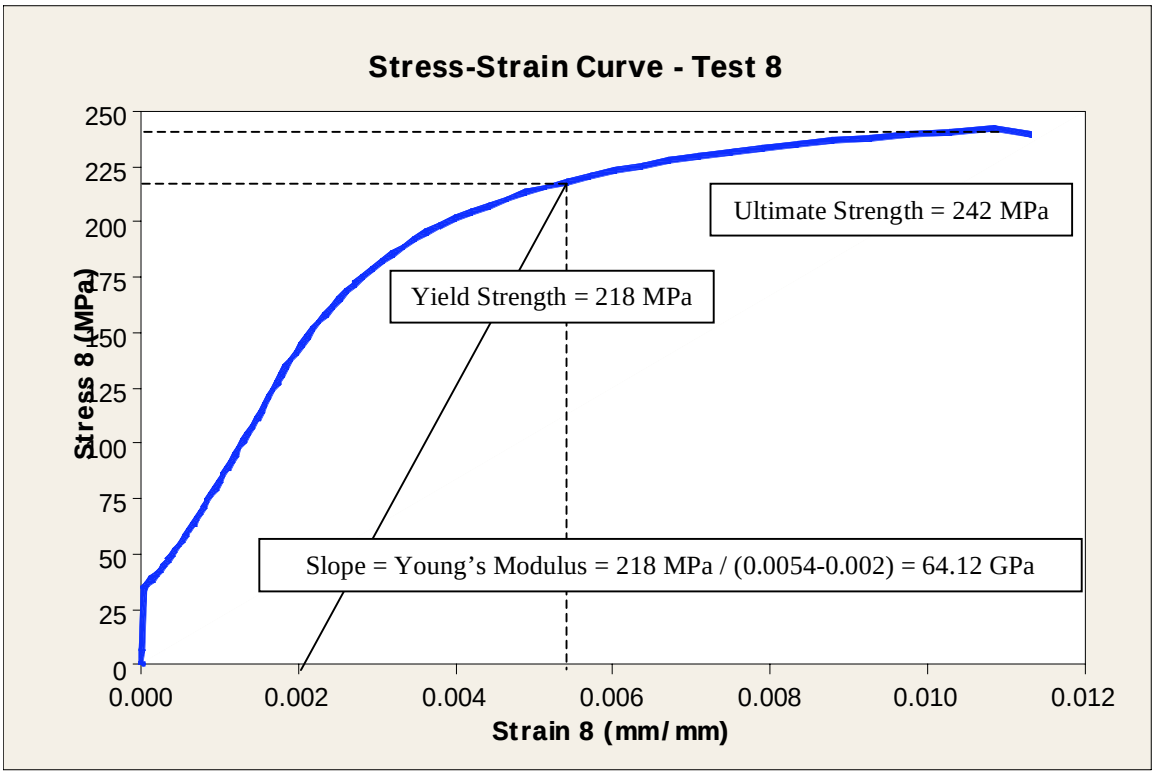
Stress-Strain Curve - Test 8
Stress 8 (MPa)
250
225
200
175
150
125
100
75
50
25
0
0.000
0.002
0.004
0.006
0.008
0.010
0.012
Strain 8 (mm/mm)
Ultimate Strength = 242 MPa
Yield Strength = 218 MPa
Slope = Young's Modulus = 218 MPa / (0.0054-0.002) = 64.12 GPa

Appendix C – Quasi-Static Calculations for Wind Speed at Failure

The expression for extreme fiber stress in an element subjected to bending is:

$$\sigma = \frac{M * y}{I} \qquad [B.1]$$

where,

σ = Normal bending stress

M = Applied moment at distance y from the neutral axis

y = Perpendicular distance to the neutral axis

$I = 4.871 \times 10^{-6}\ m^4$ = Moment of inertia about the neutral axis, calculated by discretizing the failure cross-section into rectangles and applying the parallel axis theorem

If it is assumed that the stress experienced at the notch is equivalent to the ultimate strength determined by experiment (244 MPa) then the moment required to fail the structure at point C is 55.93 kNm. By analyzing the free body diagram of Figure B.1 it can be shown that the M resulting from the above equation results from a loading at point A equivalent to 1067.21 kN.

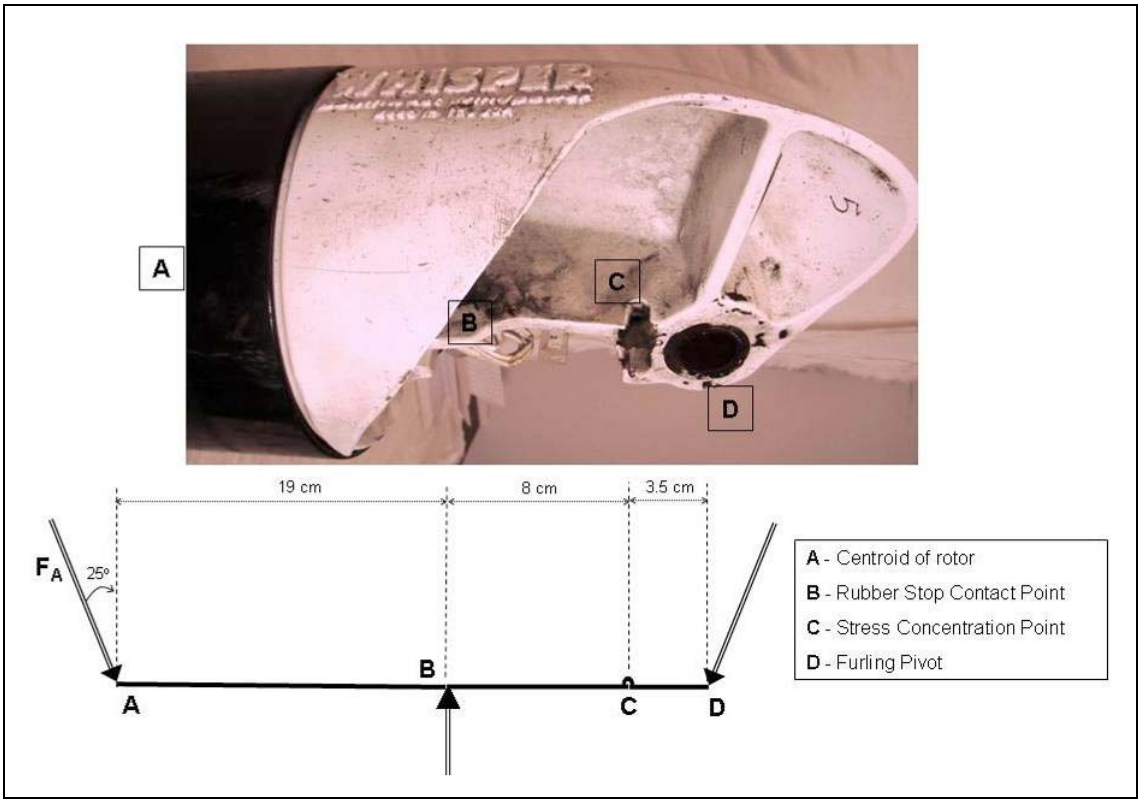

Figure B.1 – Simplified Free body diagram of static forces on nacelle

In the formula for wind forces on structures, Equation B.2, we must assign a value for C_d and A that may provide a realistic product so that the wind speed may be calculated. For this work it is assumed that the area A is equal to the projected frontal area of the now-oblique turbine "disk". Given a furl angle of 65^o, it is considered to be an ellipse with major and minor radii of 2.1 m and 0.8875 m respectively and an area = 1.4378 m^2. It will be assumed that C_d, the drag coefficient of this disk is 0.6. The continued production of near-maximum power while in the fully furled position indicates an active coefficient of this range.

$$F = \frac{1}{2}\rho * V^2 * C_d * A \qquad [B.2]$$

where,

F = Force exerted on structure = 1067.21 kN

ρ = Density of the air assumed to be 1.225 kg/m^3

V = Wind speed (m/s)

C_d = Drag coefficient of turbine rotor = 0.6

A = Area of the rotor perpendicular to wind direction = 1.4378 m^2

Thus the equation for wind force becomes F = 0.537 * V^2 and the wind speed is computed as 1409.75 m/s. If the previously discussed stress concentration factor of 7 is taken into account the normal bending stress at failure is seven times less (i.e. 244/7 = 34.86). This influence carries through to the moment-force calculation giving a loading at point A equivalent to (1067.21/7) 152.46 kN and considering the simplified equation relating force and wind speed the wind speed at failure becomes 532.8 m/s.